

**THICKENERS FOR NATURAL GAS LIQUIDS TO IMPROVE THE
PERFORMANCE IN ENHANCED OIL RECOVERY AND DRY HYDRAULIC
FRACKING**

by

Aman Kishorji Dhuwe

Bachelor in Chemical Engineering

Institute of Chemical Technology (formerly UDCT), Mumbai, India, 2013

Submitted to the Graduate Faculty of
Swanson School of Engineering in partial fulfillment
of the requirements for the degree of
Master of Science

University of Pittsburgh

2015

UNIVERSITY OF PITTSBURGH
SWANSON SCHOOL OF ENGINEERING

This thesis was presented

by

Aman K. Dhuwe

It was defended on

November 19, 2015

and approved by

Eric Beckman, Ph.D., Professor, Department of Chemical and Petroleum Engineering

Giannis Mpourmpakis, Ph.D., Professor, Department of Chemical and Petroleum Engineering

Thesis Advisor: Robert Enick, Ph.D., Professor, Department of Chemical and Petroleum
Engineering

Copyright © by Aman K. Dhuwe

2015

**THICKENERS FOR NATURAL GAS LIQUIDS TO IMPROVE THE
PERFORMANCE IN ENHANCED OIL RECOVERY AND DRY HYDRAULIC
FRACKING**

Aman K. Dhuwe, M.S.

University of Pittsburgh, 2015

Natural gas liquid (NGL), a mixture consisting primarily of ethane, propane, and butane, is an excellent enhanced oil recovery (EOR) solvent. However, NGL is typically about ten times less viscous than the crude oil within the carbonate or sandstone porous media, which causes the NGL to finger through the rock toward production wells resulting in low volumetric sweep efficiency of the NGL solvent. In this work, targeted thickeners are broadly classified into two categories, polymeric thickener and small associative molecule thickener. In either case, the resultant thickened ethane, propane or butane solution is expected to be thermodynamically stable, transparent, and capable of flowing through the pore throats (~1 micron) of sandstone or carbonate rock.

In the category of polymeric thickeners, a dilute concentration of a drag-reducing agent (DRA) poly(α -olefin) that has an average molecular weight greater than 20,000,000 was proposed as a thickener for liquid butane, liquid propane and liquid or supercritical ethane. High molecular weight polydimethyl siloxane polymer (molecular weight of ~1,000,000) and polyisobutylene (PIB) (molecular weight ~10,000,000) were also assessed as potential thickeners for NGLs. Phase behavior data (cloud points) and viscosity induced by these polymeric thickeners were obtained as

a function of temperature, pressure and concentration. Results indicate that butane is the most effective NGL component at both dissolving the polymer and expanding the polymer coils. In general, viscosity enhancement increases with decreasing temperature and increasing pressure, reflective of increased NGL solvent strength at low temperature and high pressure. Only the DRA induced significant viscosity changes for NGL at dilute polymer concentrations. To the best of my knowledge, the DRA-alkane mixture data presented in this thesis represent the most significant polymer-induced increases in viscosity reported to date for butane and propane and the first report of thickening ethane.

Three types of small associating molecule thickeners were considered; trialkyltin fluoride, aluminum di-soaps, and crosslinked phosphate esters. Phase behavior (cloud point) and viscosity data were obtained as a function of temperature, pressure and concentration. The crosslinked phosphate ester mixture was difficult to dissolve completely in NGL and induced very modest viscosity changes, especially for ethane. Hydroxyaluminum di(2-ethyl hexanoate) was insoluble in ethane, but was the best thickener for propane and butane at temperatures above 40°C. However, the hydroxyaluminum di(2-ethyl hexanoate) mixtures required heating to 100°C to attain dissolution prior to cooling to the temperature of interest. Tributyltin fluoride was a remarkable thickener for ethane, propane and butane that did not require heating for dissolution. To the best of my knowledge, these tributyltin fluoride-ethane mixture results represent the first report of thickening ethane with a small associating molecule.

TABLE OF CONTENTS

ACKNOWLEDGEMENTS	xv
1.0 INTRODUCTION	1
1.1 DENSE NGL FOR ENHANCED OIL RECOVERY	1
1.2 NGL GEL FOR DRY FRACKING	6
2.0 OBJECTIVE	8
3.0 METHODOLOGY	10
3.1 LOW PRESSURE VISCOMETRY	10
3.2 PHASE BEHAVIOR APPARATUS.....	11
3.3 HIGH PRESSURE FALLING BALL VISCOMETRY	13
4.0 POLYMERIC THICKENER.....	19
4.1 SILICONE POLYMERS.....	19
4.1.1 Ambient pressure testing.....	20
4.1.2 High pressure testing	22
4.2 HYDROCARBON POLYMER	26
4.2.1 PIB polymer.....	26

4.2.1.1	Ambient pressure testing	27
4.2.1.2	High pressure testing.....	29
4.2.2	DRA polymer.....	29
4.2.2.1	Ambient pressure testing	30
4.2.2.2	High pressure testing.....	31
5.0	SMALL ASSOCIATING MOLECULE THICKENER	39
5.1	TRIALKYL TIN FLUORIDES.....	39
5.1.1	Ambient pressure testing.....	43
5.1.2	High pressure testing	44
5.2	ALUMINUM SOAPS.....	51
5.2.1	Ambient pressure testing.....	54
5.2.2	High pressure testing	56
5.3	CROSS LINKED PHOSPHATE ESTERS (CPE)	61
5.3.1	Ambient pressure testing.....	63
5.3.2	High pressure testing	65
6.0	CONCLUSIONS.....	71
6.1	POLYMERIC THICKENERS	71
6.2	SMALL ASSOCIATIVE MOLECULE THICKENERS.....	72
BIBLIOGRAPHY		74

LIST OF TABLES

Table 1. Data on US - hydrocarbon flooding (Koottungal, 2014)	2
Table 2. High molecular weight silicone polymers	20
Table 3. Cloud point pressures of Silanol 980,000 in NGL.....	23
Table 4. Vapor pressure of light alkanes	23
Table 5. High molecular weight polyisobutylene (PIBs).....	27
Table 6. Cloud point pressure of DRA in light alkanes. DRA is part of a 1wt% DRA in 99% hexane solution except for mixtures designated as *, in which case a 2wt% DRA in hexane solution was used to prepare mixtures with NGLs.	32
Table 7. Cloud point pressure of TBTF in NGL.....	45
Table 8. Aluminum soaps	53
Table 9. Cloud point data for HADEH. In all cases the HAD2EH-alkane mixture was heated to 100oC at high pressure while being mixed, followed by cooling to the temperature listed in table.....	56
Table 10. Cloud point data for Phosphate ester (HGA-70 C6) and cross linker (HGA65). Unlike the other systems that formed transparent single phases, these CPE cloud point values correspond to the transition from a translucent phase with small suspended droplets to a completely opaque mixture.....	65

LIST OF FIGURES

Figure 1. Early breakthrough of NGL resulting in low areal and vertical sweep efficiencies	4
Figure 2. Model showing sweeping efficiency as a function of mobility ration (M)	5
Figure 3. Low pressure viscometry apparatus (Brookfield Viscometer).....	11
Figure 4. Schematic of phase behavior apparatus (Robinson Cell).....	12
Figure 5. (left and center) Close-clearance falling ball viscometer operation; (right) multiple cylinder approximation of sphere used to derive average shear rate expression based on cylindrical coordinates	14
Figure 6. Relative viscosity (viscosity of pentane solution/viscosity of pentane) associated with silicone polymers at 25oC, 1 atm, 100-375 s-1. □ Silanol; ◇ Silanol-1; Δ PDMS-2; x PDMS-1; ○ Silanol-2; + Silanol-3.....	21
Figure 7. Relative viscosity (viscosity of hexane solution/viscosity of hexane) associated with silicone polymers at 25oC, 1 atm, 100-375 s-1. □ Silanol; ◇ Silanol-1; Δ PDMS-2; x PDMS-1; ○ Silanol-2; + Silanol-3.....	21
Figure 8. Relative viscosity change in ethane by Silanol at T=25oC and average shear rate of 6000-7100 s-1. Δ 2 wt% Silanol; ○ 1 wt% Silanol.....	24
Figure 9. Relative viscosity change in propane by Silanol at T=25oC and average shear rate of 3500-7100 s-1. Δ 2 wt% Silanol; ○ 1 wt% Silanol.....	25
Figure 10. Relative viscosity change in n-butane by Silanol at T=25oC and average shear rate of 1750-7100 s-1. Δ 2 wt% Silanol; ○ 1 wt% Silanol.....	25

Figure 11. Relative viscosity (viscosity of pentane solution/viscosity of pentane) associated with high molecular weight polymers at 25C, 1 atm, 100-375 s-1. □ PIB 10,000,000; ◇ PIB 4,200,000; + PIB 500,000..... 28

Figure 12. Relative viscosity (viscosity of hexane solution/viscosity of hexane) associated with high molecular weight polymers at 25C, 1 atm, 100-375 s-1. □ PIB 10,000,000; ◇ PIB 4,200,000; + PIB 500,000..... 28

Figure 13. Relative viscosity (viscosity of alkane solution/viscosity of alkane) associated with DRA at 25C, 1 atm, 375 s-1. ◇ pentane; □ hexane; ○ heptane; Δ octane; x decane; + dodecane. 31

Figure 14. Viscosity change in ethane at 25oC and average shear rate of 1500-7100 s-1 (Logarithmic Y axis). + DRA at 0.5 wt%; x DRA at 0.25 wt%; □ DRA at 0.2 wt%; ◇ DRA at 0.1 wt%; ○ DRA 0.04 wt%; Δ DRA 0.01 wt%. 34

Figure 15. Viscosity change in ethane at 40oC and average shear rate of 1500-7100 s-1 (Logarithmic Y axis). + DRA at 0.5 wt%; x DRA at 0.25 wt%; □ DRA at 0.2 wt%; ◇ DRA at 0.1 wt%; ○ DRA 0.04 wt%; Δ DRA 0.01 wt%. 34

Figure 16. Viscosity change in ethane at 60oC and average shear rate of 800-7100 s-1 (Logarithmic Y axis). + DRA at 0.5 wt%; x DRA at 0.25 wt%; □ DRA at 0.2 wt%; ◇ DRA at 0.1 wt%; ○ DRA 0.04 wt%; Δ DRA 0.01 wt%. 35

Figure 17. Viscosity change in propane at 25oC and average shear rate of 1000-7100 s-1 (Logarithmic Y axis). + DRA at 0.5 wt%; x DRA at 0.25 wt%; □ DRA at 0.2 wt%; ◇ DRA at 0.1 wt%; ○ DRA 0.04 wt%; Δ DRA 0.01 wt%. 35

Figure 18. Viscosity change in propane at 40oC and average shear rate of 1200-7100 s-1 (Logarithmic Y axis). + DRA at 0.5 wt%; x DRA at 0.25 wt%; □ DRA at 0.2 wt%; ◇ DRA at 0.1 wt%; ○ DRA 0.04 wt%; Δ DRA 0.01 wt%. 36

Figure 19. Viscosity change in propane at 60oC and average shear rate of 800-7100 s-1 (Logarithmic Y axis). + DRA at 0.5 wt%; x DRA at 0.25 wt%; □ DRA at 0.2 wt%; ◇ DRA at 0.1 wt%; ○ DRA 0.04 wt%; Δ DRA 0.01 wt%. 36

Figure 20. Viscosity change in butane by DRA at 25oC and average shear rate of 400-7100 s-1 (Logarithmic Y axis). + DRA at 0.5 wt%; x DRA at 0.25 wt%; □ DRA at 0.2 wt%; ◇ DRA at 0.1 wt%; ○ DRA 0.04 wt%; Δ DRA 0.01 wt%. 37

Figure 21. Viscosity change in butane by DRA at 40oC and average shear rate of 400-7100 s-1 (Logarithmic Y axis). + DRA at 0.5 wt%; x DRA at 0.25 wt%; □ DRA at 0.2 wt%; ◇ DRA at 0.1 wt%; ○ DRA 0.04 wt%; Δ DRA 0.01 wt%.	37
Figure 22. Viscosity change in butane by DRA at 60oC and average shear rate of 400-7100 s-1 (Logarithmic Y axis). + DRA at 0.5 wt%; x DRA at 0.25 wt%; □ DRA at 0.2 wt%; ◇ DRA at 0.1 wt%; ○ DRA 0.04 wt%; Δ DRA 0.01 wt%.	38
Figure 23. Association in trialkyl tin fluoride.....	39
Figure 24. Structure of triphenyltin fluoride and tributyltin fluoride	41
Figure 25. Dimethyldiphenyltin, purchased from Alfa Aesar	41
Figure 26. Dimethylphenyltin iodide, produced by iodination of Dimethyldiphenyltin	42
Figure 27. Dimethylphenyltin fluoride, produced by halogen exchange of Dimethylphenyltin iodide with potassium fluoride.....	42
Figure 28. Relative viscosity (viscosity of pentane solution/viscosity of pentane) x tributyltin fluoride ; □ dimethylphenyltin fluoride at 23oC.....	43
Figure 29. Relative viscosity (viscosity of hexane solution/viscosity of pentane) x tributyltin fluoride ; □ dimethylphenyltin fluoride at 23oC.....	44
Figure 30. Viscosity change in ethane by TBTF at 25oC and average shear rate of 100-7100 s-1 (Logarithmic Y-axis). x TBTF at 1 wt%; Δ TBTF at 0.75 wt%; □ TBTF 0.5 wt%; ○ TBTF 0.2 wt%.	46
Figure 31. Viscosity change in ethane by TBTF at 40oC and average shear rate of 100-7100 s-1 (Logarithmic Y-axis). x TBTF at 1 wt%; Δ TBTF at 0.75 wt%; □ TBTF 0.5 wt%; ○ TBTF 0.2 wt%.	46
Figure 32. Viscosity change in ethane by TBTF at 60oC and average shear rate of 350-7100 s-1 (Logarithmic Y-axis). x TBTF at 1 wt%; Δ TBTF at 0.75 wt%; □ TBTF 0.5 wt%; ○ TBTF 0.2 wt%.	47

Figure 33. Viscosity change in ethane by TBTF at 80oC and average shear rate of 1500-7100 s-1 (Logarithmic Y-axis). x TBTF at 1 wt%; Δ TBTF at 0.75 wt%; □ TBTF 0.5 wt%; ○ TBTF 0.2 wt%.	47
Figure 34. Viscosity change in ethane by TBTF at 100oC and average shear rate of 3500-7100 s-1 (Logarithmic Y-axis). x TBTF at 1 wt%; Δ TBTF at 0.75 wt%; □ TBTF 0.5 wt%; ○ TBTF 0.2 wt%.	48
Figure 35. Viscosity change in propane by TBTF at 25oC and average shear rate of 70-710 s-1 (Logarithmic Y-axis). x TBTF at 1 wt%; □ TBTF 0.5 wt%.....	48
Figure 36. Viscosity change in propane by TBTF at 40oC and average shear rate of 70-710 s-1 (Logarithmic Y-axis). x TBTF at 1 wt%; □ TBTF 0.5 wt%.....	49
Figure 37. Viscosity change in propane by TBTF at 60oC and average shear rate of 100-1000 s-1 (Logarithmic Y-axis). x TBTF at 1 wt%; □ TBTF 0.5 wt%.....	49
Figure 38. Viscosity change in n-butane by TBTF at 25oC and average shear rate of 70-710 s-1 (Logarithmic Y-axis). x TBTF at 1 wt%; □ TBTF 0.5 wt%.....	50
Figure 39. Viscosity change in n-butane by TBTF at 40oC and average shear rate of 70-710 s-1 (Logarithmic Y-axis). x TBTF at 1 wt%; □ TBTF 0.5 wt%.....	50
Figure 40. Viscosity change in n-butane by TBTF at 60oC and average shear rate of 100-1000 s-1 (Logarithmic Y-axis). x TBTF at 1 wt%; □ TBTF 0.5 wt%.....	51
Figure 41. Possible association of HAD2EH molecules (Pilpel, 1963)	52
Figure 42. Viscosity change in pentane	55
Figure 43. Viscosity change in hexane	55
Figure 44. Viscosity change in propane by HADEH at 40oC and average shear rate of 350-2500 s-1 (Logarithmic Y-axis). x HAD2EH at 1 wt%; □ HADEH 0.5 wt%.	57
Figure 45. Viscosity change in propane by HADEH at 60oC and average shear rate of 450-2500 s-1 (Logarithmic Y-axis). x HADEH at 1 wt%; □ HADEH 0.5 wt%.	57

Figure 46. Viscosity change in propane by HADEH at 80oC and average shear rate of 450-2800 s-1 (Logarithmic Y-axis). x HADEH at 1 wt%; □ HADEH 0.5 wt%.	58
Figure 47. Viscosity change in propane by HADEH at 100oC and average shear rate of 500-2800 s-1 (Logarithmic Y-axis). x HADEH at 1 wt%; □ HADEH 0.5 wt%.	58
Figure 48. Viscosity change in n-butane by HADEH at 40oC and average shear rate of 250-400 s-1 (Logarithmic Y-axis). □ HADEH 0.5 wt%.....	59
Figure 49. Viscosity change in n-butane by HADEH at 60oC and average shear rate of 280-450 s-1 (Logarithmic Y-axis). □ HADEH 0.5 wt%.....	59
Figure 50. Viscosity change in n-butane by HAD2EH at 80oC and average shear rate of 300-450 s-1 (Logarithmic Y-axis). □ HADEH 0.5 wt%.....	60
Figure 51. Viscosity change in n-butane by HAD2EH at 100oC and average shear rate of 350-550 s-1 (Logarithmic Y-axis). □ HADEH 0.5 wt%.....	60
Figure 52. Phosphate di-ester, Phosphate mono-ester, Phosphonic acid ester and dialkyl phosphinic acid.....	61
Figure 53. Mechanism of chelating complex (phosphate ester with metal ion cross linker) (Funkhouser et al., 2009; George et al., 2006, 2008; Page and Warr, 2009).....	62
Figure 54. Relative viscosity (viscosity of pentane solution/viscosity of pentane) x HGA70C6 + HGA65 at 23oC; Δ DRA at 23oC; □ HAD2EH at 30oC; ○ TBTF at 23oC.....	64
Figure 55. Relative viscosity (viscosity of hexane solution/viscosity of hexane) x HGA70C6 + HGA65 at 23oC; Δ DRA at 23oC; □ HADEH at 30oC; ○ TBTF at 23oC.....	64
Figure 56. Viscosity change in ethane by HGA70 C6+ HGA 65 at 25oC and average shear rate of 3500-7100 s-1 (Logarithmic Y-axis). x 1 wt% ; □ 0.5 wt%; ○ 0.25 wt%.	66
Figure 57. Viscosity change in ethane by HGA70 C6+ HGA 65 at 40oC and average shear rate of 3500-7100 s-1 (Logarithmic Y-axis). x 1 wt% ; □ 0.5 wt%; ○ 0.25 wt%.	67
Figure 58. Viscosity change in ethane by HGA70 C6+ HGA 65 at 60oC and average shear rate of 3500-7100 s-1 (Logarithmic Y-axis). x 1 wt% ; □ 0.5 wt%; ○ 0.25 wt%.	67

- Figure 59. Viscosity change in propane by HGA70 C6+ HGA 65 at 25oC and average shear rate of 2000-7100 s-1 (Logarithmic Y-axis). x 1 wt% ; □ 0.5 wt% ; ○ 0.25 wt%..... 68
- Figure 60. Viscosity change in propane by HGA70 C6+ HGA 65 at 40oC and average shear rate of 2200-7100 s-1 (Logarithmic Y-axis). x 1 wt% ; □ 0.5 wt% ; ○ 0.25 wt%..... 68
- Figure 61. Viscosity change in propane by HGA70 C6+ HGA 65 at 60oC and average shear rate of 2500-7100 s-1 (Logarithmic Y-axis). x 1 wt% ; □ 0.5 wt% ; ○ 0.25 wt%..... 69
- Figure 62. Viscosity change in butane by HGA70 C6+ HGA 65 at 25oC and average shear rate of 1500-3500 s-1 (Logarithmic Y-axis). □ 1.0 wt% ; ○ 0.5 wt%..... 69
- Figure 63. Viscosity change in butane by HGA70 C6+ HGA 65 at 40oC and average shear rate of 1500-3500 s-1 (Logarithmic Y-axis). □ 1.0 wt% ; ○ 0.5 wt%..... 70
- Figure 64. Viscosity change in butane by HGA70 C6+ HGA 65 at 60oC and average shear rate of 1500-3500 s-1 (Logarithmic Y-axis). □ 1.0 wt% ; ○ 0.5 wt%..... 70

ACKNOWLEDGEMENTS

First and foremost, I would like to express my sincere thanks to my adviser Dr. Robert Enick, who has guided me throughout the preparation of this thesis. Without his timely advice and kind guidance, this report would not have materialized. Honestly, it was a wonderful learning experience for me both in professional as well as social aspects. I am delighted to have such a great adviser. I would also take this opportunity to express my sincere thanks to Dr. Giannis Mpourmpakis and Dr. Eric Beckman. It was indeed a pleasure listening Dr. Beckman suggestions in group meetings. I thank my lab mates Stephen Cummings and Jason Lee for their great help during my initial phase of lab-work.

I owe a special mention to some really good friends I have made over the past few years, and with whom I shared some of the most unforgettable memories of my life. Without Sarwesh Parbat, Hussein Baled, Swapnil Nerkar, Shardul Wadekar, Brandon Grainger, Prasad Patel, Bharat Gattu, Rakesh Reddy, Saurabh Bhavsar, Amey More, Sameer Damle and Shrinath Ghadge this journey would not have been as much fun and Pittsburgh as exciting. I also want to express my appreciation to the Chemical Engineering department staff comprising of Bob Maniet, Adrian Starke, Rita Leccia and the most beloved person, Patricia Park for their assistance and cooperation. In fact, I would like to thank the entire Pitt family for the great memories that I will be taking with me.

Last but not the least, I owe a lot of gratitude to my family members whose perpetual support and encouragement to do the best and overall to be a good human being. I am blessed and humbled by the unconditional love, warmth and affection shown by my parents and brother, Chetan, throughout my life.

1.0 INTRODUCTION

This section addresses two vital areas in the oil and gas industry where dense NGLs has significant demand i.e. enhanced oil recovery and NGL fracking.

1.1 DENSE NGL FOR ENHANCED OIL RECOVERY

Domestic oil production occurs in three phases; primary recovery, secondary recovery, and tertiary recovery (enhanced oil recovery). In many domestic formations that retain light oils, 6-15% of OOIP is recovered by primary recovery method which is limited to hydrocarbons naturally rising up to the surface. Additional 6-30% of the Original Oil in Place (OOIP) is recovered by secondary recovery treatments which essentially an injection of water or a pressurizing gas with no solvent strength (N₂) deep into the reservoir and displacing the oil and directing it to the production well, known as water/gas flooding. Primary and secondary processes leave behind almost 65-88% of the OOIP. The recovery of the remaining oil requires a good crude oil solvent such as high pressure CO₂, natural gas liquids (NGL's) and good volumetric sweep of the formation. In tertiary production, injectants such as CO₂ and NGL's get used which mix with oil to alter its properties and allow it to flow more freely in the reservoir. These injectants have the ability to mix with oil to swell it, make it less viscous, detach it from the rock surface, lower or eliminate interfacial tension between the injectants and the oil, and cause the oil to flow more free within the reservoir

towards production well. (Advanced Resources International (ARI), 2010; The National Enhanced Oil Recovery Initiative (NEORI), 2012)

According to the report published by Oil & Gas Journal in 2014 (Kootungal, 2014), hydrocarbon miscible enhanced oil recovery (EOR) has contributed 1.5-2.0% of overall oil production in US over the past several decades. Hydrocarbon miscible flooding typically involves the injection of natural gas liquids (NGL) (Taber, 1983), which is primarily a mixture of ethane, propane, butane and a small amount of pentanes and higher alkanes. This mixture is an excellent solvent for the displacement of oil because it often exhibits complete miscibility with crude oil in all proportions at reservoir conditions (i.e. first contact miscibility).

Table 1. Data on US - hydrocarbon flooding (Kootungal, 2014)

Year	Miscible hydrocarbon flooding		
	Production (bbl/day)	% Contribution	No. of treatments
1992	113,072	1.49%	25
1994	99,693	1.41%	15
1996	96,263	1.33%	14
1998	102,053	1.34%	11
2000	124,500	1.66%	6
2002	95,300	1.43%	7
2004	97,300	1.47%	8
2006	95,800	1.47%	13
2008	81,000	1.26%	13
2010	81,100	1.22%	12
2012	81,100	1.06%	13
2014	127,500	1.64%	14

Hydrocarbon miscible EOR is not as pervasive in the United States as CO₂ EOR because most of the CO₂ is obtained from massive natural deposits and is transported through an extensive CO₂ distribution pipelines, whereas the NGLs used for EOR originate in gas processing plants associated with oil recovery projects (including CO₂ EOR). Therefore the hydrocarbon miscible EOR activity is typically done in remote fields that have access to stranded NGL supplies. However NGL flooding is more efficient than CO₂ flooding because the amount of oil recovered per amount of solvent injected is more. NGLs are more expensive than CO₂, however, because ethane can be sold as a chemical building block to make ethylene, while propane and butane can be sold as LPG for fuel. In some large formations where there are no nearby markets for NGLs, however, it makes more economic sense to separate the NGLs from produced petroleum and re-inject them into the formation for oil recovery.(Frazier and Todd, 1984; Holm, 1976)

Although the solvent strength of a NGL mixture is exemplary, this fluid has the same two fundamental disadvantages as CO₂; low density and viscosity relative to crude oil. The density of high pressure NGL at typical hydrocarbon miscible conditions is roughly 0.5 gm/cm³. At EOR conditions i.e. T = 20-80°C, P = 300-2500 psi ethane, propane and butane has density of roughly 0.4 g/cm³, 0.5 g/cm³ and 0.6 g/cm³ respectively. (Friend et al., 1991; Miyamoto and Watanabe, 2000, 2001). Because the NGL density value is less than that of crude oil, NGLs tend to exhibit gravity override as they flow through the formation, reducing oil recovery in the lower portions of reservoir. It is not possible to substantially increase the density of NGL with a dilute concentration of an additive at a specified temperatures and pressures, however.

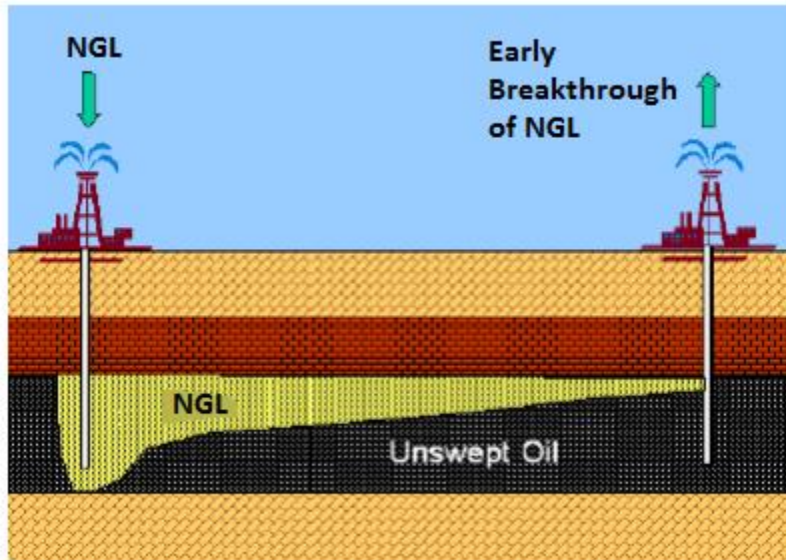


Figure 1. Early breakthrough of NGL resulting in low areal and vertical sweep efficiencies

The viscosity of NGL at reservoir conditions is roughly 0.1 mPa-s (centipoise, cP), a value that can be significantly lower than brine and oil viscosity. For example, the range of crude oil viscosity values associated with most hydrocarbon miscible projects in the US is 1-2 mPa-s (cP) with several other projects having crude oil with a viscosity of 7-140 mPa-s (cP). In Canada crude oil viscosity values in hydrocarbon miscible projects range between 0.1 – 0.8 m Pa-s (cP). The low viscosity of NGL relative to the crude oil being displaced leads to unfavorable mobility ratio which, in turn, results in viscous fingering, early NGL breakthrough, high NGL utilization ratios, high gas-to-oil ratios, poor sweep efficiency, depressed oil production and a disappointingly low percent of OOIP recovery (Habermann, 1960). Further, in stratified formations, the viscosity contrast enhances the flow of NGLs into thief zones.

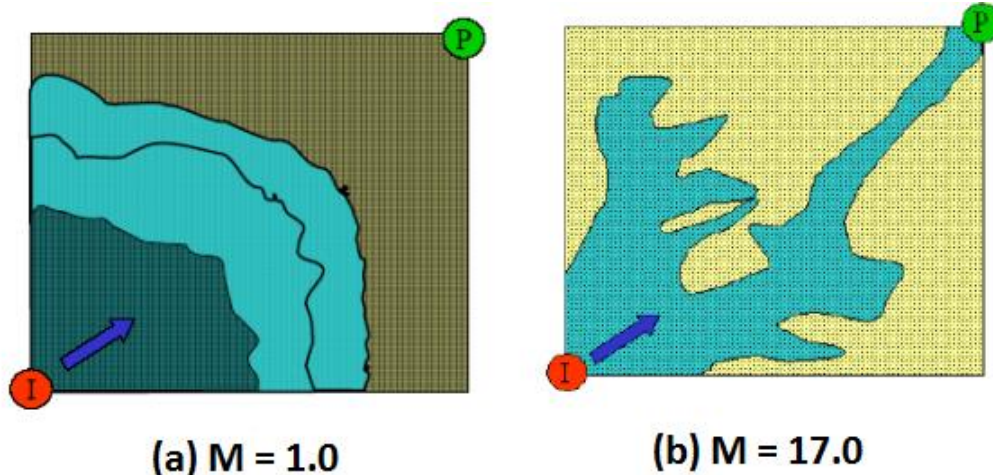


Figure 2. Model showing sweeping efficiency as a function of mobility ration (M)

(a) Ideal flow of NGL solvent from injection well (I) to production well (P) for maximum oil recovery

(b) Viscous fingering leaving behind large volume

It is possible to diminish the mobility of dense NGL by reducing its permeability via water-alternating gas (WAG) injection process. It is easy to thicken conventional oils and hydrocarbons that are liquids at ambient conditions, such as octane, hexane and pentane. However, challenges arise as one considers polymers thickeners for butane, propane and ethane because high pressure equipment is required for testing. Further, the alkanes become increasing poor solvents for polymers as once progresses to from pentane to ethane.

The idea of thickening NGLs for making NGL flooding more efficient is not completely new and substantial amount of work is reported in literature on thickening propane and butane since 1960s. However, to the best of our knowledge, not a single report is yet published about thickening of liquid or supercritical ethane.

1.2 NGL GEL FOR DRY FRACKING

In addition to its use as an EOR solvent, NGL or LPG serve as a dry hydraulic fracturing fluid in water-sensitive formations. In the process, LPG fluid is injected into the formation at extremely high pressure (e.g. 10,000 psi) until the formation fractures as indicated by a sudden and dramatic decrease in pressure (e.g. 5000 psi). At this point, a slurry and sand is injected into the well in order to prop the 1/8” – 1/4” wide fracture open before it collapses upon itself, which typically takes about one minute. This creates a narrow, high permeability, sand-packed channel for the gas to flow from the formation to the well. This process is efficient when the fracture is deep, wide and propped open with large sand particles.

Petroleum fluids have been used for fracturing purpose since 1950, sometimes in combination with dissolved CO₂ (Hurst, 1972; Smith, 1973). More recently (Taylor et al., 2006; Tudor et al., 2009) described the properties of gelled liquefied petroleum gas (LPG), primarily a mixture of propane and butane, for fracturing applications. Because of its volatility, LPG leaves no residue behind. Intensified concerns by the public regarding water pollution (requires ~3-6 million gallons of water per well) for hydrofracturing have prompted many companies to search for alternatives to hydrofracturing, especially in water-sensitive formations. The benefits of using high pressure volatile light alkanes for fracturing include the elimination of the formation damage associated with conventional aqueous fluids, and the ease of removal of the hydrocarbons via depressurization, the absence of waste water, and the ability to recapture the alkanes at the wellhead after the proppant is placed. The “gelation” or “thickening” of the light liquid alkanes enables them to generate larger fractures and to carry higher concentrations of larger sand proppant particles.

Despite the numerous reports of “gelled” LPG found in many references (Hurst, 1972; Lestz et al., 2007; Smith, 1973; Taylor et al., 2006; Tudor et al., 2009), to the best of our knowledge a detailed analysis of the phase behavior of gellant additive in ethane, propane, butane, NGL or LPG has not been published, nor has a detailed description of the viscosity of such mixtures in a viscometer or rheometer been presented. Rheological data for gelled LPG is very scarce in the literature (Taylor et al., 2005a). Moreover, rheology and protocols for gelling and mixing remain confidential.

2.0 OBJECTIVE

The objective of this work is to increase the viscosity of NGL at laminar flow condition for EOR application and/or to make an NGL gel for fracking application with the very low concentration (~ 0.1 – 2.0 wt%) of thickener additive. Alkanes become increasingly poor solvents as one progresses from hexane to ethane, as reflected by the decreasing solubility parameter values of the alkanes with decreasing carbon number. Therefore candidate thickeners are first screened with liquid hexane and pentane at ambient pressure. If the candidate is not effective in these east-to-perform higher alkanes, further high pressure testing in the lower alkanes is not carried out. The concentration range needed to increase the viscosity of NGL constituents (ethane, propane and butane) is first determined by thickening normal liquids alkanes such as pentane and hexane at ambient pressure, followed by conducting experiments at high pressures in butane, propane and ethane. In high pressure tests, the candidate which is not soluble at extreme conditions of 10,000 psi and 100°C is considered to be insoluble.

The solubility tests are carried out in high pressure (rated to 10,000 psi and 180°C), windowed, agitated, invertible, variable-volume cell in a controlled air bath. The cloud point, the pressure at which a transparent solution becomes a two-phase dispersion, is determined visually during the slow expansion of the cell and its contents. Typically this cloud point should be less than the minimum miscibility pressure (MMP) of EOR, or the fracturing pressure in order to get proper one phase solution with complete miscibility and the desired viscosity.

Any candidates that are soluble in an NGL component are later assessed for viscosity measurement. Falling ball viscometry is employed via measuring the terminal velocity of a close-clearance glass that falls through the solution after the cell is rapidly inverted. Relative viscosity (solution viscosity/viscosity of the pure alkane) is obtained as a function of concentration, pressure and temperature.

In order to increase the viscosity of NGL constituents at very dilute concentration of thickener additive two types of thickeners are employed: high molecular weight polymers and small associating molecules. In either cases the resultant thickened NGL solution should be a thermodynamically stable, transparent fluid capable of flowing through the pore throats (~1 micron) of sandstone and carbonate rocks.

3.0 METHODOLOGY

In this section, the experimental apparatus and methodologies used for phase behavior and viscosity studies are introduced.

3.1 LOW PRESSURE VISCOMETRY

A commercially available rotating dish and cup type viscometer (Brookfield DV-II+ Programmable Viscometer, M/97-164-D1000) instrument was used for measuring the viscosity of liquid solutions at atmospheric pressure. Using a pipette, 0.5 μL of sample was placed in the temperature-controlled sample chamber. After assembly, the dish spindle was lowered to contact the surface of the sample, on which it could be controlled to rotate at various shear rates. The dish spindle is calibrated to provide an accurate digital output of viscosity value onto a display screen. Measurements were repeated multiple times (4-5 times) and the mean average of the values is reported. The size of the data markers reflects the range of viscosity values obtained at each condition.

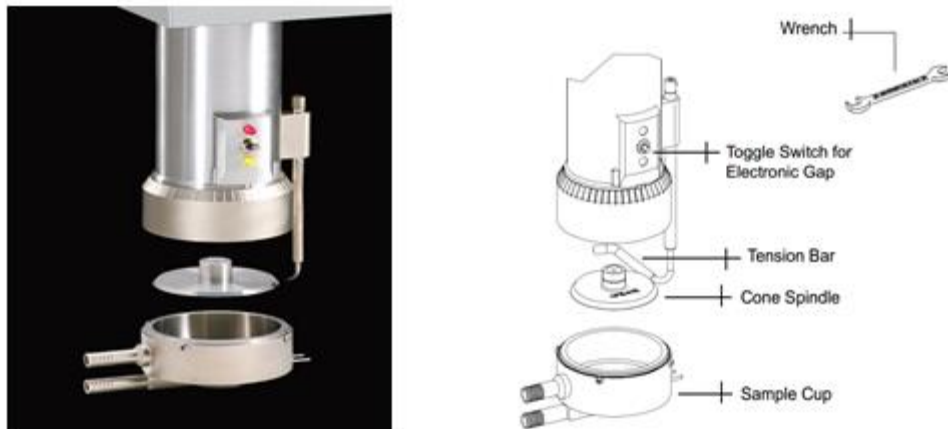


Figure 3. Low pressure viscometry apparatus (Brookfield Viscometer)

3.2 PHASE BEHAVIOR APPARATUS

Phase behavior studies were conducted in high-pressure, variable-volume, agitated and windowed cell. The schematic of this high pressure SS cell (formerly D. B. Robinson and Associates and now DBR-Schlumberger) is shown in Figure 4. A standard non-sampling techniques for determining the cloud point of mixture with known overall composition is employed. During the course of heating or cooling, a typical isobaric condition is employed. Details of the phase behavior measurement are provided elsewhere (Hong et al., 2008; Kilic et al., 2003; Miller et al., 2009). Basically, specified amounts of a thickener and high pressure fluid are combined in a variable-volume view cell and mixed at high pressure until a single- phase is attained in the cylindrical sample volume of a thick-walled Pyrex tube. This phase of known composition is then very slowly expanded (~100 cc/hr) at constant temperature until the first appearance of a second phase, typically a cloud point, is observed. Cloud points can be determined at several compositions. The

error associated with the measurement of cloud point data for polydisperse polymers in a high pressure solvent is ± 0.7 MPa.

Typically heating and cooling operations are performed isobarically. In the case of the two-component (phosphate ester + crosslinker) thickener, the phosphate ester was placed in a small open glass dish on top of the sliding piston at the bottom of the sample volume, while the crosslinker solution was placed on the sliding piston itself. This prevented the phosphate ester and the crosslinker from reacting prior to being dissolved in the high pressure alkane.

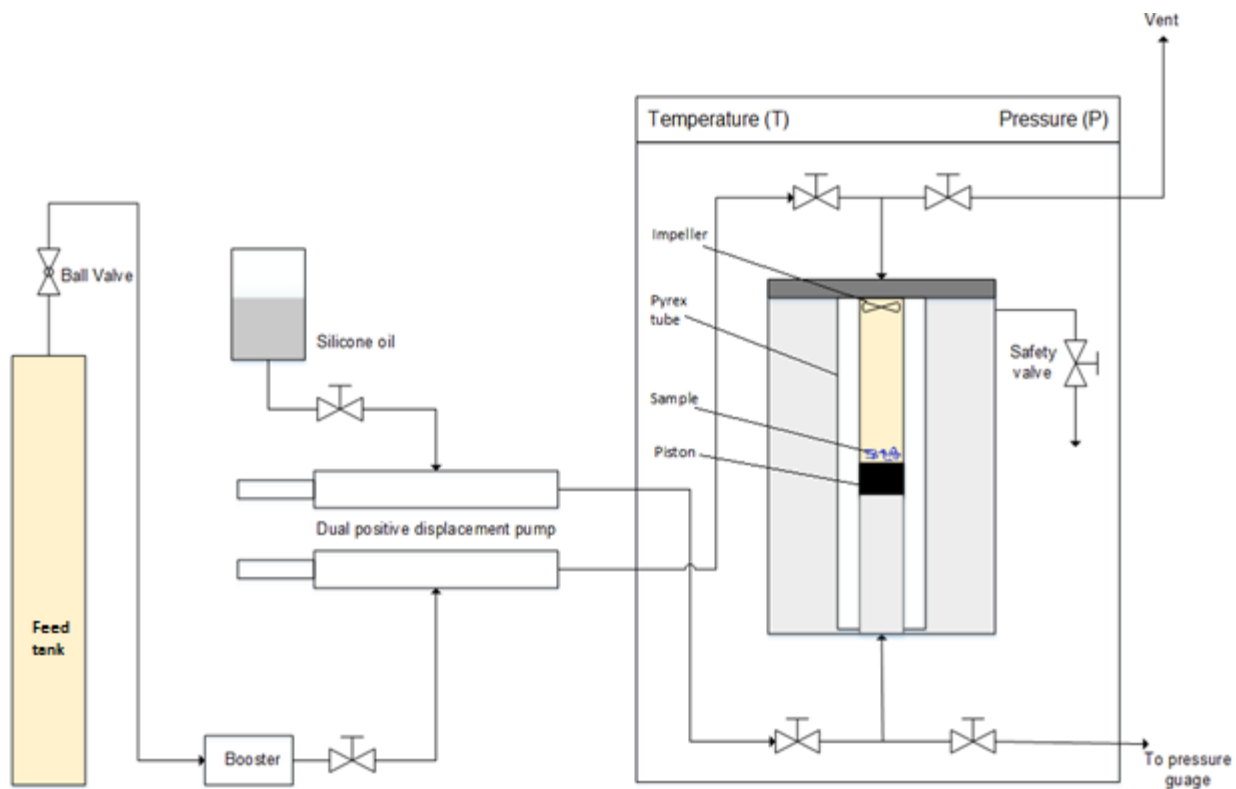


Figure 4. Schematic of phase behavior apparatus (Robinson Cell)

3.3 HIGH PRESSURE FALLING BALL VISCOMETRY

High pressure, close clearance falling ball viscometry in the high pressure windowed cell phase behavior cell is employed to measure the viscosity of single-phase mixtures of thickener compound and NGL constituents such as ethane, propane and butane. Just as in the case of a solubility test, a transparent single phase solution at a pressure above the cloud point pressure of the mixture composition is established in the sample volume of a Pyrex tube (3.175 cm inside diameter). A Pyrex ball (2.23 gr/cm³, 3.1587 cm diameter) is also present at the bottom of the sample volume. The entire cell is then rapidly inverted, and the ball is permitted to fall through the entire 14cm column of the high pressure sample. The terminal velocity of the falling ball is measured as the time required for the ball to fall 2 cm at a position at the midpoint of the sample volume. Measurements are repeated 10 times and the average terminal velocity is recorded. The terminal velocity of the same fluid with no polymer present was also recorded at the same temperature and pressure. The governing equation for a falling ball viscometer can be used to estimate the degree of viscosity enhancement associated with a thickener. For a falling ball viscometer,

$$\mu = K \frac{(\rho_{ball} - \rho_{fluid})}{V_t} \quad (1)$$

K is the viscometer constant that is dependent upon the ball and tube diameter and is typically determined via calibration with a fluid of known density and viscosity. ρ_{ball} and ρ_{fluid} are densities of ball and fluid, respectively. V_t is terminal velocity of the falling ball.

Relative viscosity is the ratio of the viscosity of the fluid with a dissolved thickener to the viscosity of the pure fluid, $\frac{\mu_{sol}}{\mu_o}$. If one assumes that the dilute concentration of polymer does not significantly affect fluid density, then the relative viscosity can be expressed as follows

$$\text{Relative Viscosity} = \frac{\mu_{\text{sol}}}{\mu_0} = \frac{V_{\text{to}}}{V_{\text{tsol}}} \quad (2)$$

where, μ_{sol} is viscosity of solution containing a specified amount of thickener, μ_0 is viscosity of the pure fluid, V_t is terminal velocity of ball in the pure fluid and V_{tsol} is terminal velocity of ball in solution with polymer. Our group used this procedure previously for falling cylinder viscometry (Enick, 1991a; Xu et al., 2003). The schematic of the falling ball viscometer and its operation are shown below.

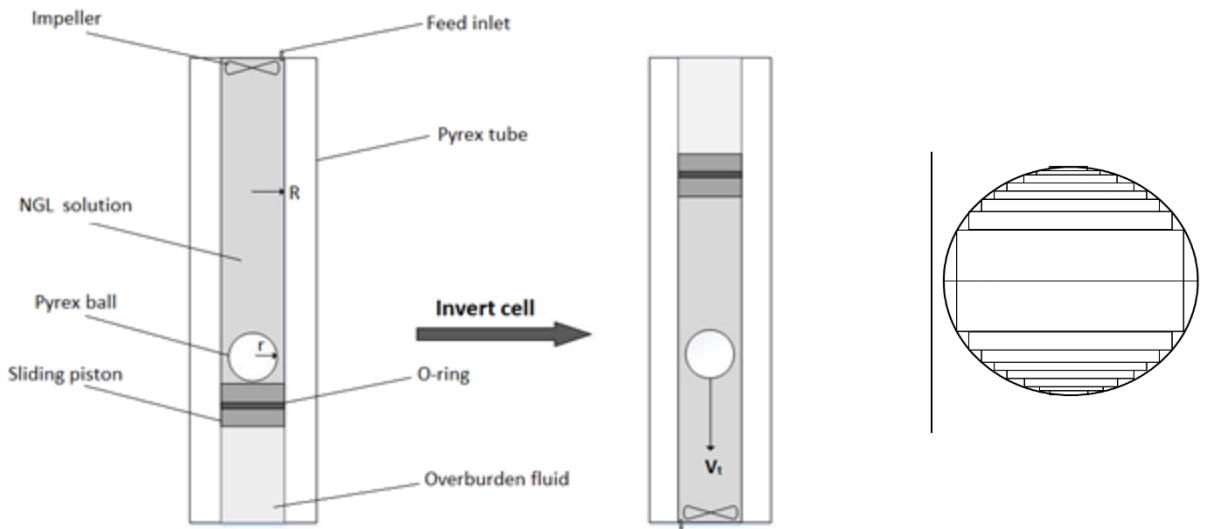


Figure 5. (left and center) Close-clearance falling ball viscometer operation; (right) multiple cylinder approximation of sphere used to derive average shear rate expression based on cylindrical coordinates

The only literature that presents an expression for the average shear rate on the surface of a ball falling at its terminal velocity in a column of a Newtonian fluid retained in a tube with a slightly larger diameter than the ball (i.e. a close clearance falling ball viscometer) was presented by Doffin et al., 1984. These researchers stated that the maximum shear rate on the surface of the

sphere occurs at the position along the equatorial plane where the gap between the ball and sphere is smallest. They expressed this maximum shear rate γ as

$$\gamma_{max} = \left\{ \frac{V_t (3R^2 + r^2 + 2Rr)}{(R + r)e^2} \right\} \quad (3)$$

where V_t is terminal settling velocity of ball, R is the inside radius of the tube, r is the radius of the ball, and e is the smallest gap between the ball and the tube ($R-r$). The authors then stated that the average shear rate on the falling ball, γ_{avg} , was equal to one half of the maximum value

$$\gamma_{avg} = 0.5 \left\{ \frac{V_t (3R^2 + r^2 + 2Rr)}{(R + r)e^2} \right\} \quad (4)$$

These expressions have been used by others to estimate the average shear rate on the falling ball, although Fons and co-workers mistakenly set the parameter e equal to the difference in diameters rather than radii. (Fons et al., 1993)

In this work we equate the maximum shear rate at the position of the smallest gap to the analytic solution for the shear rate at the wall of a falling cylinder (with the same radius as the ball) that falls at the same velocity as the ball (Barrage, 1987; Heller and Taber, 1982; Huang et al., 2000).

$$\gamma_{max} = V_t \left(\frac{-2r - (R^2 - r^2) \frac{1}{r \ln\left(\frac{r}{R}\right)}}{\ln\left(\frac{r}{R}\right) (r^2 + R^2) + (R^2 - r^2)} + \frac{1}{r \ln\left(\frac{r}{R}\right)} \right) \quad (5)$$

Equations 3 and 5 yield virtually identical results for the maximum shear rate. Rather than arbitrarily setting the average shear rate equal to one-half of the maximum value, we determine a surface-area averaged value. This is accomplished by modeling the ball as a stack of thin horizontal

cylinders of incrementally different diameter that, as an aggregate, closely simulates the shape of the sphere. For our geometry, the results are insensitive to the number of cylinders if at least 2000 cylinders are used, therefore 4000 cylinders were used in the calculations below.

It is assumed that the volumetric flow rate of the fluid displaced by the falling ball, Q , remains invariant for each of the annular spaces associated with the 4000 cylinders.

$$Q = \pi r^2 V_t \quad (6)$$

The shear rate along the wall of each cylinder can therefore be determined using equation 5, with r corresponding to the radius of the thin cylinder (r_c) and with V_t set equal to the velocity of the cylinder required to attain the volumetric flow rate in the annular gap, V_{tc} .

$$V_{tc} = Q/\pi r_c^2 \quad (7)$$

To obtain a surface area-average shear rate, the products of the shear rate and the surface area of the short vertical wall of each for each cylinder are summed. This summation is then divided by the total area of the vertical walls of the cylinders. These calculations were repeated for numerous examples with ratios of $0.95 < r/R < 0.9999$, and in each case the surface area-averaged shear rate was compared to the maximum shear rate. The results are expressed in the following equation;

$$\begin{aligned} \frac{\gamma_{avg}}{\gamma_{max}} = & -4.354 \times 10^8 \left(\frac{r}{R}\right)^6 + 2.540 \times 10^9 \left(\frac{r}{R}\right)^5 - 6.175 \times 10^9 \left(\frac{r}{R}\right)^4 + 8.005 \\ & \times 10^9 \left(\frac{r}{R}\right)^3 \\ & -5.837 \times 10^9 \left(\frac{r}{R}\right)^2 + 2.270 \times 10^9 \left(\frac{r}{R}\right) - 3.678 \times 10^8 \end{aligned} \quad (8)$$

This result is dominated by the portion of the sphere surface near the gap, where the shear rates are the highest and the surface areas of the thin cylinders are the greatest.

A very similar result for the ratio of the average shear rate to the maximum shear rate is obtained for the surface area average shear rate of a close clearance falling ball viscometer if the terminal velocity of each thin falling cylinder is maintained at a single value; the terminal velocity of the ball.

$$\begin{aligned} \frac{\gamma_{avg}}{\gamma_{max}} = & -4.372 \times 10^8 \left(\frac{r}{R}\right)^6 + 2.551 \times 10^9 \left(\frac{r}{R}\right)^5 - 6.200 \times 10^9 \left(\frac{r}{R}\right)^4 + 8.038 \\ & \times 10^9 \left(\frac{r}{R}\right)^3 \\ & -5.861 \times 10^9 \left(\frac{r}{R}\right)^2 + 2.279 \times 10^9 \left(\frac{r}{R}\right) - 3.693 \times 10^8 \end{aligned} \quad (9)$$

Note that both the maximum shear rate and average shear rate are dependent variables in a falling object viscometer; their values are proportional to the terminal velocity of the falling ball.

Values for the ball and tube diameter and related parameters are provided below.

D	inside diameter of Pyrex tube	=	3.175×10^{-2}	m
d	diameter of Pyrex Ball	=	3.1587×10^{-2}	m
e	R - r minimum gap size	=	8.15×10^{-5}	m
R	D/2 Pyrex tube inner radius	=	1.5875×10^{-2}	m
r	d/2 Pyrex ball radius	=	1.57935×10^{-2}	m
R/r	dimensionless ratio of ball/tube radii	=	0.99487	
$\gamma_{avg}/\gamma_{max}$	eq. 8	=	0.09934	
$\gamma_{avg}/\gamma_{max}$	eq. 9	=	0.09828	

The maximum shear rate at the ball surface occurs in the smallest gap position between the ball and tube, and both equation 3 and 5 give a maximum shear rate of

$$\gamma_{max}(s^{-1}) = 71700 V_t \left(\frac{cm}{s} \right) \quad (10)$$

Therefore, based on equation 4 (Doffin et al., 1984) the average shear rate is

$$\gamma_{avg}(s^{-1}) = 0.5 (71700) V_t \left(\frac{cm}{s} \right) = 35850 V_t \left(\frac{cm}{s} \right) \quad (11)$$

While based on equations 5 and 8 from this work, the surface area-average shear rate (based on the assumption that the volumetric flow rate in the horizontal annuli between the falling ball and tube remains constant for each of the 4000 cylinders) is

$$\gamma_{avg}(s^{-1}) = 0.09934 (71700) V_t \left(\frac{cm}{s} \right) = 7120 V_t \left(\frac{cm}{s} \right) \quad (12)$$

Similarly, based on equations 5 and 9 from this work, the surface area-average shear rate (based on the assumption that the terminal velocity of each of the 4000 cylinders is the same as the terminal velocity of the sphere) is

$$\gamma_{avg}(s^{-1}) = 0.09828 (71700) V_t \left(\frac{cm}{s} \right) = 7050 V_t \left(\frac{cm}{s} \right) \quad (13)$$

These expressions are intended to provide estimates of the approximate average shear rate experienced on the surface of a ball falling through a closed tube with a slightly larger diameter that is filled with a Newtonian fluid. Although the pure alkanes used in this study are Newtonian, the dilute polymer solutions prepared in this study are likely to be non-Newtonian shear thinning solutions. Therefore equations 3-12 should be viewed as a means of estimating the order-of-magnitude of the shear rate associated with the falling ball viscometer for these solutions rather than a precise determination of the exact average shear rate.

4.0 POLYMERIC THICKENER

This section covers the various polymeric thickeners considered for NGL constituents. Mainly an eco-friendly and less-expensive polymers are investigated and these polymers can broadly be classified as silicone polymers and hydrocarbon polymers.

4.1 SILICONE POLYMERS

The remarkable solubility of polydimethylsiloxane (PDMS) in non-polar CO₂ and non-polarity of ethane, propane and butane solvents, made us pursue silicone based polymers. Literature also suggested the used of silicone based polymers as a drag reducing agent in transportation of various hydrocarbon liquids. So we decided to perform viscosity studies in NGL constituents.

Materials: A trimethyl silyl-terminated polydimethylsiloxane (PDMS) silicone polymer of viscosity 20000000 cSt (Mw 417300) was obtained from Gelest, and a silanol-terminated PDMS (Silanol SE 30) (Mw 972540) was obtained from Momentive. Both samples were used as received. The Momentive Silanol product is, to the best of our knowledge, the highest molecular weight commercially available polydimethyl siloxane polymer. These polymer are designated to be PDMS-1 and Silanol respectively. Various other forms of silicone polymers such as PDMS-2, Silanol-1, Silanol-2 and Silanol-3 were obtained from GE Global Research and used as received. The weight-average molecular weight (Mw) and Number-average molecular weight (Mn) values

for all these silicone polymers were measured by Gel Permeation Chromatography (GPC) technique at GE Global Research, Niskayuna.

Table 2. High molecular weight silicone polymers

Name	Structure	Molecular weight (obtained by GPC)
PDMS-1	$\text{H}_3\text{C}-\underset{\text{CH}_3}{\overset{\text{CH}_3}{\text{Si}}}-\text{O}-\left[\underset{\text{CH}_3}{\overset{\text{CH}_3}{\text{Si}}}-\text{O}\right]_n-\underset{\text{CH}_3}{\overset{\text{CH}_3}{\text{Si}}}-\text{CH}_3$	Mw-417,300 g/mol, Mn- 198,660 g/mol
PDMS-2	$\text{CH}_2=\underset{\text{CH}_3}{\overset{\text{CH}_3}{\text{Si}}}-\text{O}-\left[\underset{\text{CH}_3}{\overset{\text{CH}_3}{\text{Si}}}-\text{O}\right]_m-\left[\underset{\text{CH}_3}{\overset{\text{CH}_3}{\text{Si}}}-\text{O}\right]_n-\text{Si}(\text{CH}_3)_2-\text{CH}=\text{CH}_2$	Mw-749,000 g/mol, Mn- 431,000 g/mol
Silanol	$\text{HO}-\underset{\text{CH}_3}{\overset{\text{CH}_3}{\text{Si}}}-\text{O}-\left[\underset{\text{CH}_3}{\overset{\text{CH}_3}{\text{Si}}}-\text{O}\right]_n-\underset{\text{CH}_3}{\overset{\text{CH}_3}{\text{Si}}}-\text{OH}$	Mw-972,540 g/mol, Mn-454,000 g/mol
Silanol-1	$\text{HO}-\underset{\text{CH}_3}{\overset{\text{CH}_3}{\text{Si}}}-\text{O}-\left[\underset{\text{CH}_3}{\overset{\text{CH}_3}{\text{Si}}}-\text{O}\right]_n-\underset{\text{CH}_3}{\overset{\text{CH}_3}{\text{Si}}}-\text{OH}$	Mw-934,680 g/mol, Mn- 379,830 g/mol
Silanol-2	$\text{HO}-\underset{\text{CH}_3}{\overset{\text{CH}_3}{\text{Si}}}-\text{O}-\left[\underset{\text{CH}_3}{\overset{\text{CH}_3}{\text{Si}}}-\text{O}\right]_m-\left[\underset{\text{Ph}}{\overset{\text{Ph}}{\text{Si}}}-\text{O}\right]_n-\underset{\text{CH}_3}{\overset{\text{CH}_3}{\text{Si}}}-\text{OH}$	Mw-712,000 g/mol, Mn- 351,000 g/mol
Silanol-3	$\text{HO}-\underset{\text{CH}_3}{\overset{\text{CH}_3}{\text{Si}}}-\text{O}-\left[\underset{\text{CH}_3}{\overset{\text{CH}_3}{\text{Si}}}-\text{O}\right]_m-\left[\underset{\text{Ph}}{\overset{\text{Ph}}{\text{Si}}}-\text{O}\right]_n-\underset{\text{CH}_3}{\overset{\text{CH}_3}{\text{Si}}}-\text{OH}$	Mw-639,000 g/mol, Mn- 298,000 g/mol

4.1.1 Ambient pressure testing

All these high molecular weight silicone polymers exhibited the very high solubility in pentane and hexane. Polymers dissolved very easily and required just a rigorous shaking of vials for few minutes. The degree of thickening increased with concentration for all the polymers. Silanol was

the most effective thickener among all silicone polymers, inducing 4-folds increase in viscosity at a concentration of 1 wt%. Silanol also was the highest molecular weight silicone polymer.

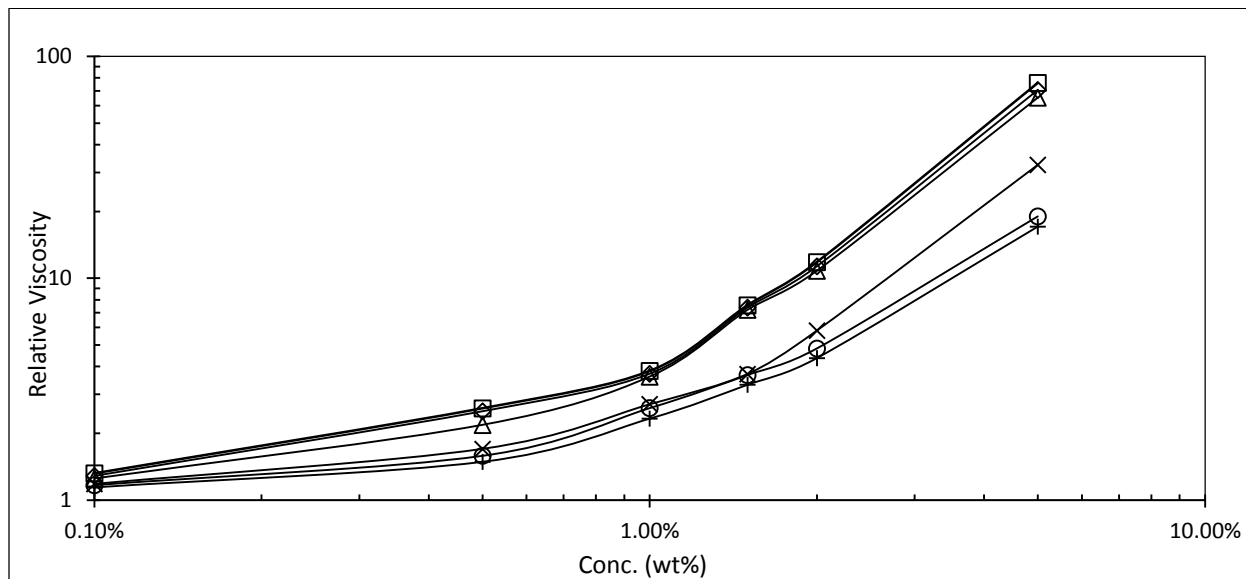


Figure 6. Relative viscosity (viscosity of pentane solution/viscosity of pentane) associated with silicone polymers at 25°C, 1 atm, 100-375 s⁻¹. □ Silanol; ◇ Silanol-1; △ PDMS-2; × PDMS-1; ○ Silanol-2; + Silanol-3.

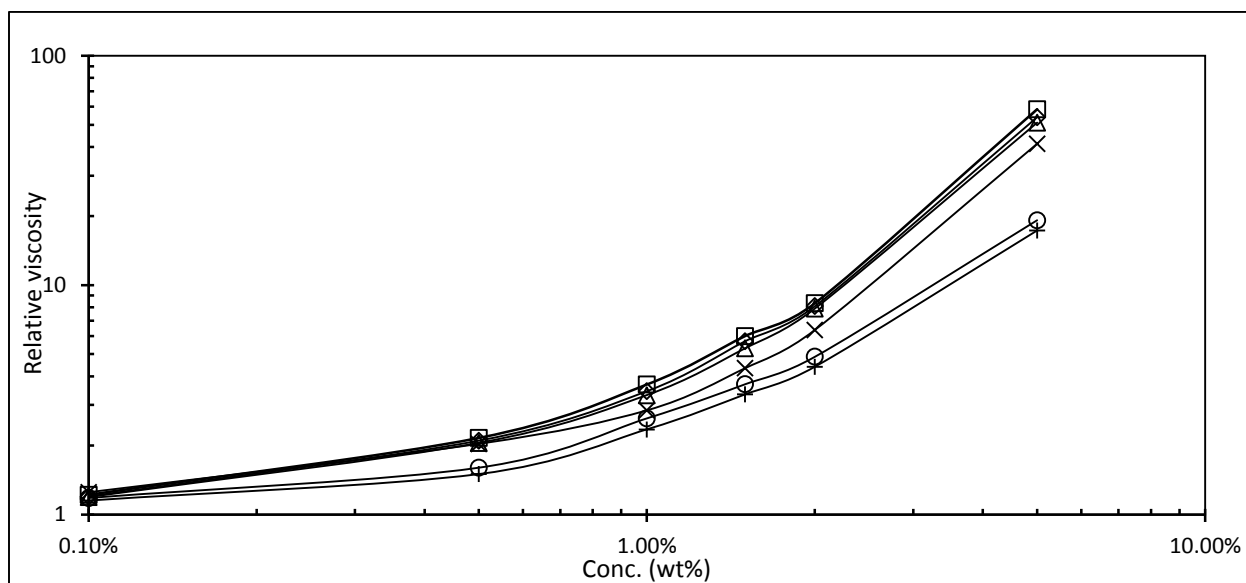


Figure 7. Relative viscosity (viscosity of hexane solution/viscosity of hexane) associated with silicone polymers at 25°C, 1 atm, 100-375 s⁻¹. □ Silanol; ◇ Silanol-1; △ PDMS-2; × PDMS-1; ○ Silanol-2; + Silanol-3.

4.1.2 High pressure testing

Silanol dissolves readily at concentrations up to 2wt% (higher concentrations were not assessed) in ethane, propane and butane at pressures above the cloud point pressure values listed in Table 3. Silanol was soluble at pressures slightly above the vapor pressure of propane and butane. In ethane, however, pressures much greater than the vapor pressure are required for dissolution. The vapor pressures of these light alkanes are provided in Table 4. The high solubility of polydimethylsiloxane (PDMS) in NGL constituents has been previously attributed to the high thermal expansion coefficient for PDMS (Zeman et al., 1972), which exhibits LCST behavior in various fluids. LCST behavior refers to the fact that as the temperature increases one needs higher pressures to put the polymer into solution; most polymers exhibit this behavior in highly compressible fluids. This behavior is generally thought to be entropically driven because as the free volume of the solvent and polymer become significantly different, the system phase splits so that the solvent can maximize its entropy. As such, the key variable is the coefficient of thermal expansion of each of the components; PDMS has a very high expansion coefficient and hence it will maintain a single phase with very compressible fluids long after others have phase split. Further, the miscibility of PDMS with the light alkanes is consistent with their respective solubility parameter values. PDMS has a solubility parameter in the $7.3\text{-}7.6 \text{ (cal/cm}^3\text{)}^{0.5}$ range. The solubility parameter values for n-hexane, n-pentane, and n-butane, which are excellent solvents for PDMS, are 7.24, 7.0 and 6.89 $\text{(cal/cm}^3\text{)}^{0.5}$, respectively. The solubility parameter for liquid propane and liquid ethane are 6.4 and 5.8 $\text{(cal/cm}^3\text{)}^{0.5}$ respectively, as estimated using a group contribution method (Hansen, 2007). The difference between the solubility parameter values of PDMS and the hexane-propane alkanes differ by less than 1 $\text{(cal/cm}^3\text{)}^{0.5}$, which is consistent with the high degree of solubility in these alkanes. The difference between the solubility parameter

values of PDMS and ethane is greater than 1 (cal/cm^3)^{0.5}, however. Therefore it is not surprising that extremely high pressures were required for the PDMS to dissolve in ethane.

Table 3. Cloud point pressures of Silanol 980,000 in NGL

Solvent	Concentration (wt%)	Cloud point (psi)		
		25°C	40°C	60°C
Ethane	1	1720	1960	2570
	2	1740	2030	2610
Propane	1	145	225	355
	2	155	237	371
n-butane	1	40	60	110
	2	45	68	134

Table 4. Vapor pressure of light alkanes

Solvent	Vapor Pressure in psi		
	25°C	40°C	60°C
Ethane	607.7	Supercritical	Supercritical
Propane	138.1	198.6	307.1
n-butane	35.3	54.9	92.6

The relative viscosity (viscosity of the solution/viscosity of the pure alkane at the same temperature and pressure) of high pressure ethane, propane and butane-rich solutions containing 1wt% or 2wt% Silanol is illustrated in Figures 8, 9 and 10, respectively. Despite its high molecular weight and ability to dissolve in ethane, Silanol is ineffective at thickening ethane; hardly any increase is observed at 1wt% and only a 20% increase is observed at 2wt% Silanol and 9000 psi at 25°C. Silanol was more effective in thickening propane. For example, at a concentration of 2wt% Silanol the propane-rich solution was twice as viscous as pure propane at 9000 psi. The greatest thickening effect at a specified mass concentration is achieved in butane, where a 4-fold

increase in butane viscosity is realized at 2wt% Silanol and 9000 psi. In all cases, the Silanol polymer is a better thickener at higher pressures. All of these effects are consistent with alkane solvent strength increasing with pressure and with an increasing carbon chain length. The stronger solvent, such as high pressure butane, not only dissolves the polymer but also cause the polymer molecules to swell and uncoil, leading to the greater viscosity increases of the solution. In poorer solvents, such as low pressure ethane, the dissolved polymer may remain more tightly coiled and is thereby less effective at increasing solution viscosity.

The relative viscosity increases associated with dilute amounts of Silanol in pentane and hexane, Figures 6 and 7 respectively, are similar to those observed for butane, although they were determined with a different type of viscometer at a different shear rate. Therefore it appears that a dramatic decrease in the ability of a linear alkane to both dissolve and swell Silanol 980000 such that it thickens the solution occurs for propane and especially for ethane.

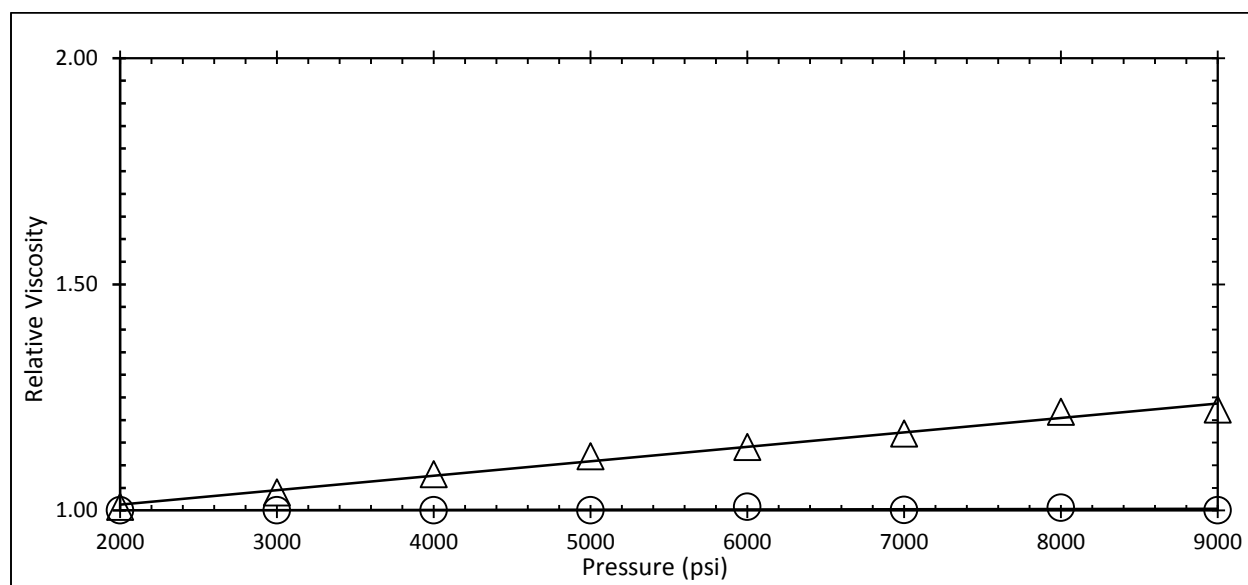


Figure 8. Relative viscosity change in ethane by Silanol at $T=25^{\circ}\text{C}$ and average shear rate of 6000-7100 s^{-1} . Δ 2 wt% Silanol; \circ 1 wt% Silanol.

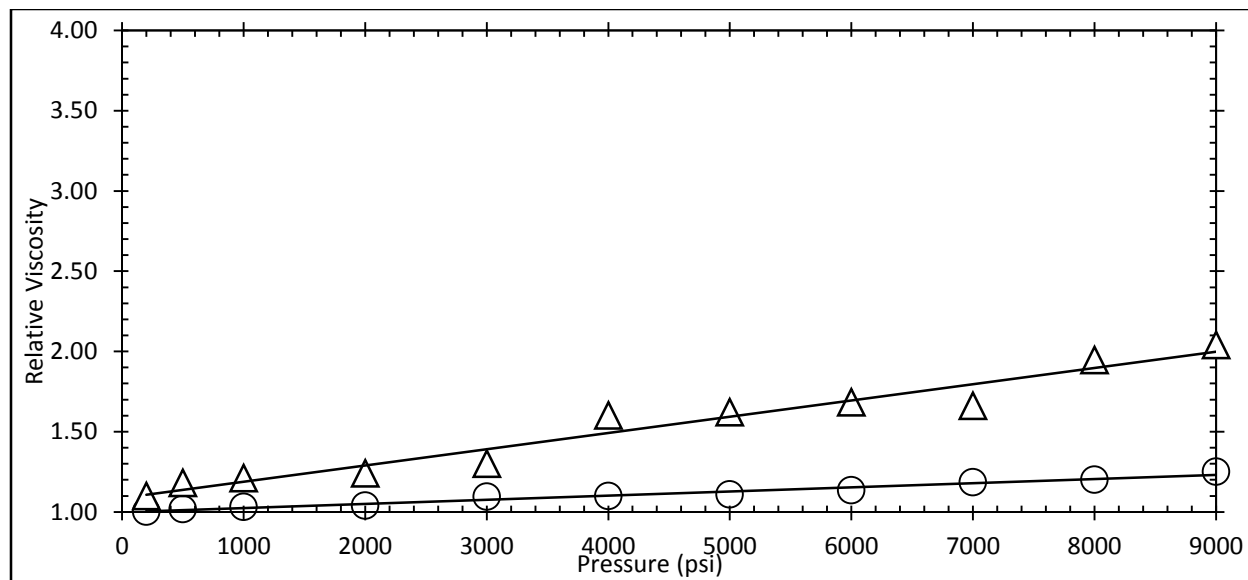


Figure 9. Relative viscosity change in propane by Silanol at $T=25^{\circ}\text{C}$ and average shear rate of $3500\text{-}7100\text{ s}^{-1}$. Δ 2 wt% Silanol; \circ 1 wt% Silanol.

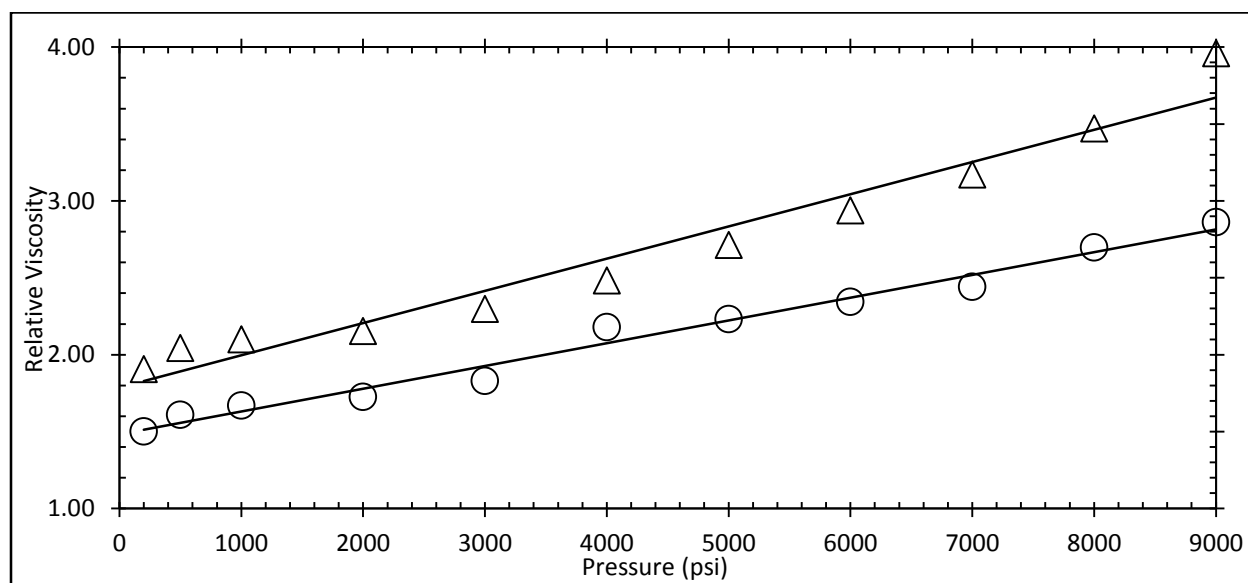


Figure 10. Relative viscosity change in n-butane by Silanol at $T=25^{\circ}\text{C}$ and average shear rate of $1750\text{-}7100\text{ s}^{-1}$. Δ 2 wt% Silanol; \circ 1 wt% Silanol.

4.2 HYDROCARBON POLYMER

There have been reports of dissolution of high molecular weight hydrocarbon polymers and oxygenated hydrocarbon polymers in NGLs, such as polyethylene Mw 108246 in ethane, polyethylene Mw 340000 in propane, polyethylene Mw 420000 in butane; poly(ethylene-co-methyl acrylate) Mw 100000 in ethane, poly(ethylene-co-methyl acrylate) Mw 140000 in propane and butane; poly(ethylene-co-octene) Mw 200000 in propane; polypropylene Mw 210000 in propane; and poly(ethylene-co-acrylic acid) Mw 100000 in propane and butane (Kirby and McHugh, 1999). With regard to the highest molecular weight polymers, polyisobutylene (PIB) Mw 1660000 is slightly soluble in compressed liquid butane, but is insoluble in propane and ethane.

4.2.1 PIB polymer

In the late 1960's, several patents were published citing the advantages of thickening liquid propane with dissolved polymers (Henderson et al., 1967; Roberts et al., 1969). For example, Dauben and co-workers studied poly-isobutylene polymer (PIB, Mw ~130,000) in a solution of propane (75 vol%) and a C7-rich condensate (25 vol%). This patent claimed to achieve a 2-3 fold viscosity enhancement at 0.25wt% polymer (Dauben et al., 1971). However, the method used for measuring the viscosity was not reported. While studying various polymers for CO₂ and NGL thickening, Heller and co-workers found poly α -olefins based on n-decene, n-pentene, n-hexene to be only sparingly CO₂-soluble, but quite soluble in liquid n-butane. A 5-fold viscosity enhancement for liquid butane was measured with a falling cylinder viscometer with these polymers at concentrations of 2.2 wt% (Dandge and Heller, 1987). They did not report testing of these polymers in liquid propane or in ethane.

Materials: A series of high molecular weight polyisobutylene (PIB) polymer of weight-average molecular weights Mw 500000, Mw 1000000 and Mw 4200000 were obtained from Sigma Aldrich and used as received. An ultrahigh molecular weight PIB, Mw 10000000 (Oppanol B250), was obtained from BASF and used as received.

Table 5. High molecular weight polyisobutylene (PIBs)

Structure	Molecular weight (obtained by GPC)
$\text{H}_3\text{C}-\left[\begin{array}{c} \text{CH}_3 \\ \\ \text{C}-\text{CH}_2 \\ \\ \text{CH}_3 \end{array} \right]_n-\text{CH}_3$	Mw-500,000 g/mol
$\text{H}_3\text{C}-\left[\begin{array}{c} \text{CH}_3 \\ \\ \text{C}-\text{CH}_2 \\ \\ \text{CH}_3 \end{array} \right]_n-\text{CH}_3$	Mw-4,200,000 g/mol
$\text{H}_3\text{C}-\left[\begin{array}{c} \text{CH}_3 \\ \\ \text{C}-\text{CH}_2 \\ \\ \text{CH}_3 \end{array} \right]_n-\text{CH}_3$	Mw-10,00,000 g/mol

4.2.1.1 Ambient pressure testing

The polyisobutylene (PIBs) were soluble in pentane and hexane. However the dissolution of polymer was bit tough, required 1-2 days of mixing to attain complete homogeneity in the solution. The viscosity enhancement is illustrated in the Figure 11-12. The highest molecular weight PIB, Mw 10000000 was clearly the most effective thickener.

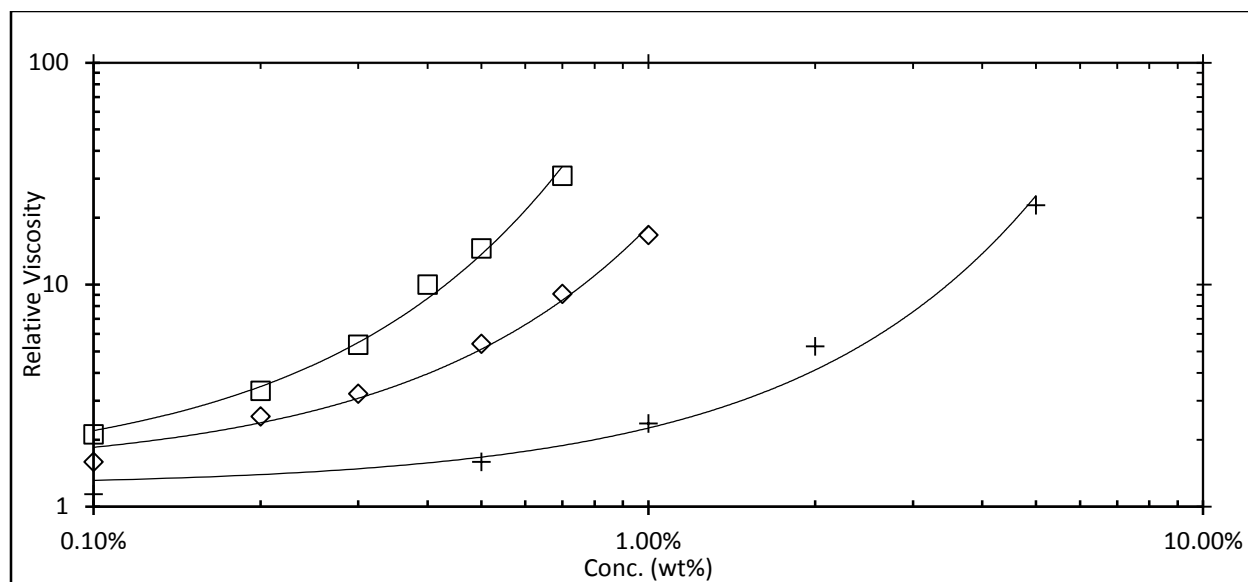


Figure 11. Relative viscosity (viscosity of pentane solution/viscosity of pentane) associated with high molecular weight polymers at 25C, 1 atm, 100-375 s⁻¹. □ PIB 10,000,000; ◇ PIB 4,200,000; + PIB 500,000.

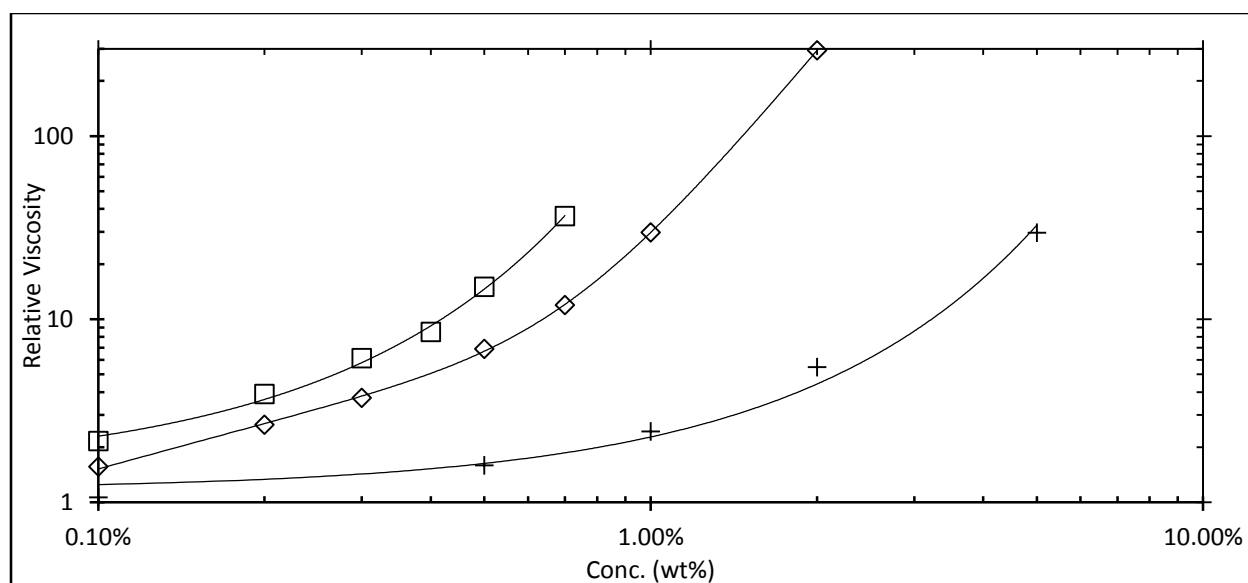


Figure 12. Relative viscosity (viscosity of hexane solution/viscosity of hexane) associated with high molecular weight polymers at 25C, 1 atm, 100-375 s⁻¹. □ PIB 10,000,000; ◇ PIB 4,200,000; + PIB 500,000.

4.2.1.2 High pressure testing

PIB 10000000 is insoluble in high pressure ethane, propane and butane; there were no signs of polymer swelling or dissolution after 6 hours of mixing at 25-80°C. Even when a transparent solution of 1wt% PIB 10000000 in hexane is first prepared, the PIB immediately precipitates when the high pressure ethane, propane and butane is added as the mixture is agitated.

4.2.2 DRA polymer

The main intention of trying high and ultrahigh molecular weight drag reducing agent (DRA) polymers used in oil pipelines as NGL thickeners. DRA polymers typically have molecular weights greater than 5000000 and are used in concentrations of only 10-20 ppm to attain substantial increases in throughput at a specified pressure drop or significant power reduction for a specified volumetric flow rate. At these dilute concentrations, the polymers do not significantly change the fluid properties; therefore the viscosity of the solution of oil and dissolved DRA at 10-20 ppm as measured in a laminar flow viscometer will be essentially the same as the oil. In general, the higher the molecular weight of the polymer, the smaller the concentration required to achieve a targeted level of drag reduction. Therefore DRA polymers with molecular weights in excess of 5000000 g/mol are particularly well suited for drag reduction (Milligan et al., 2009). Polymers that have been studied as DRAs for organic liquids include polydimethyl siloxane (PDMS), poly- α -olefins (of hexene, octene, decene, dodecene), polyethylene, polyethylene terephthalate, polyethylene oxide, polyisopropene, polyisobutylene, polybutadiene, ethyl cellulose, ethylene and vinyl alcohol copolymer, and epichlorohydrin and ethylene oxide copolymers. (Burger et al., 1980; Canevari and Peruyero, 1970; Evans, 1974; Liaw, 1968; Ma et al., 2003). Typically the DRA,

which is a powder or extraordinarily viscous liquid in pure form for most polymers, is pumped into the oil pipeline as either a extremely viscous concentrated solution of several wt% DRA in an organic solvent, or as a dispersion of fine DRA polymer particles carried in an oil-soluble organic solvent that is a poor polymer solvent.

To increase viscosity at laminar flow conditions with low concentrations of an ultra-high molecular weight DRA, polymer concentrations greater than 100 ppm are likely required.

Materials: Attempts to rapidly dissolve polymeric DRAs in hydrocarbons with intense mixing results in shear degradation of the polymer and a loss in its drag reducing or thickening capability. However, prolonged mixing at low rpm in the high pressure phase behavior cell and viscometer would not be practical. Therefore pre-made concentrated 1 wt% DRA and 2wt% solutions of a proprietary ultra-high molecular weight DRA in hexane were obtained from a vendor and used as received. Each solution prepared in this study using DRA-1% or DRA-2% therefore contains 99 or 49 times, respectively, as much hexane as DRA on a weight basis.

4.2.2.1 Ambient pressure testing

DRA is an excellent thickener for liquid alkanes such as pentane, hexane, octane, decane and dodecane as shown in the Figure 13. At a very dilute concentration of 0.2 wt%, it induces viscosity increase by 7-16 folds in liquid alkanes.

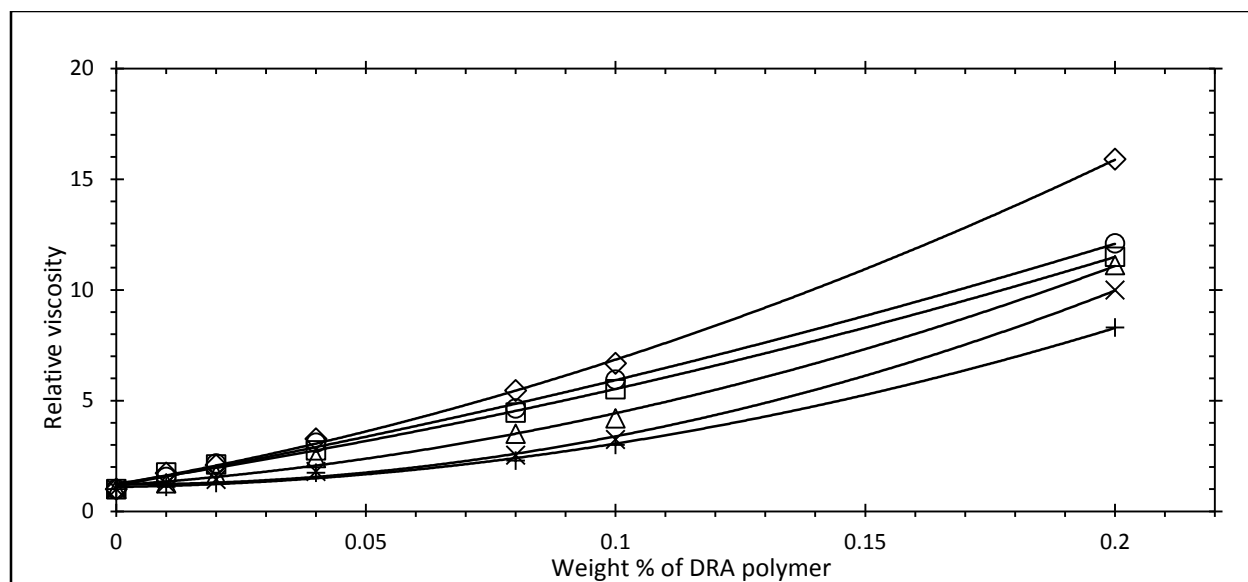


Figure 13. Relative viscosity (viscosity of alkane solution/viscosity of alkane) associated with DRA at 25°C, 1 atm, 375 s^{-1} . ◇ pentane; □ hexane; ○ heptane; △ octane; x decane; + dodecane.

4.2.2.2 High pressure testing

The solubility of the DRA in ethane, propane and butane at 25°C, 40°C and 60°C is represented by the cloud point data found in Table 6 for solutions containing up to 0.5 wt% DRA. For concentrations up to and including 0.2 wt% DRA in NGL component, the DRA 1% solution was used to prepare the mixture. Therefore every high pressure solution contained 99 times as much hexane as the DRA. For example, the 0.04% DRA solution in butane actually was composed of 0.04% DRA, 3.96% hexane, and 96% butane. For concentrations of 0.25wt% and higher DRA in NGL component, the DRA 2% solution was used to prepare the mixture. These high pressure solutions contained 49 times as much hexane as the DRA. For example, the 0.50% DRA solution in butane actually was composed of 0.50% DRA, 24.50% hexane, and 75% butane. The hexane can be considered as a co-solvent for the DRA polymer.

Solubility results are presented in Table 6. At dilute DRA concentrations, this polymer is soluble in butane and propane at pressures close to the vapor pressure of butane and propane. In ethane, however, much higher pressures are required to attain solubility. As in the case of Silanol, this reflects that ethane is a substantially weaker solvent for a high molecular weight polymer than propane or butane.

Because the DRA is not available in its neat form, the solubility of the DRA in the NGL constituents absent the presence of hexane could not be determined. Further, dissolution of the neat polymer in these light alkanes would have likely required impractically long, gentle mixing to avoid shear degradation.

Table 6. Cloud point pressure of DRA in light alkanes. DRA is part of a 1wt% DRA in 99% hexane solution except for mixtures designated as *, in which case a 2wt% DRA in hexane solution was used to prepare mixtures with NGLs.

Solvent	DRA concentrations (wt%)	Hexane concentration (wt%)	Cloud point (psi)		
			25C	40C	60C
Ethane	0.01	0.99	5140	5770	5936
	0.04	3.96	4940	5425	5855
	0.10	9.90	4312	4810	5420
	0.20	19.80	3140	3660	4120
	0.25*	12.25	6430	6710	6884
	0.50*	24.50	6135	6520	6810
Propane	0.01	0.99	145	225	355
	0.04	3.96	143	224	348
	0.10	9.90	142	223	345
	0.20	19.80	141	221	340
	0.25*	12.25	208	335	434
	0.50*	24.50	210	315	445
Butane	0.01	0.99	38	59	96
	0.04	3.96	38	59	96
	0.10	9.90	38	59	93
	0.20	19.80	38	59	92
	0.25*	12.25	42	62	103
	0.50*	24.50	42	64	112

The increases in viscosity attained with dilute concentrations of DRA (along with hexane as a co-solvent) are presented in Figures 14-22. In all cases the relative viscosity of the solution increases slightly with increasing pressure, reflecting the increasing solvent strength of the alkane to uncoil the polymer in solution. Further, the viscosity increases attained in ethane and propane are comparable and significantly less than those realized in butane. For example, a 0.25wt% DRA concentration is required to roughly double the viscosity of ethane and propane, Figures 14-22, while only 0.10wt% DRA is required to double the butane viscosity, Figures 20-22. At 0.5wt% DRA, 3-9-fold increases in ethane and propane viscosity occur, while 23-30 fold increases occur in butane at a 0.5wt% DRA concentration. These results indicate that butane is a significantly stronger solvent for the dissolution and swelling of ultrahigh molecular weight polymers than ethane or propane.

In general, these results indicate that an attempt to increase the viscosity (as measured in a falling ball viscometer) of NGLs by roughly an order-of-magnitude with ultrahigh molecular weight polymers such as the DRA will probably require the dissolution of many thousands of ppm (tenths of a wt%), as opposed to hundreds of ppm or tens of thousands of ppm.

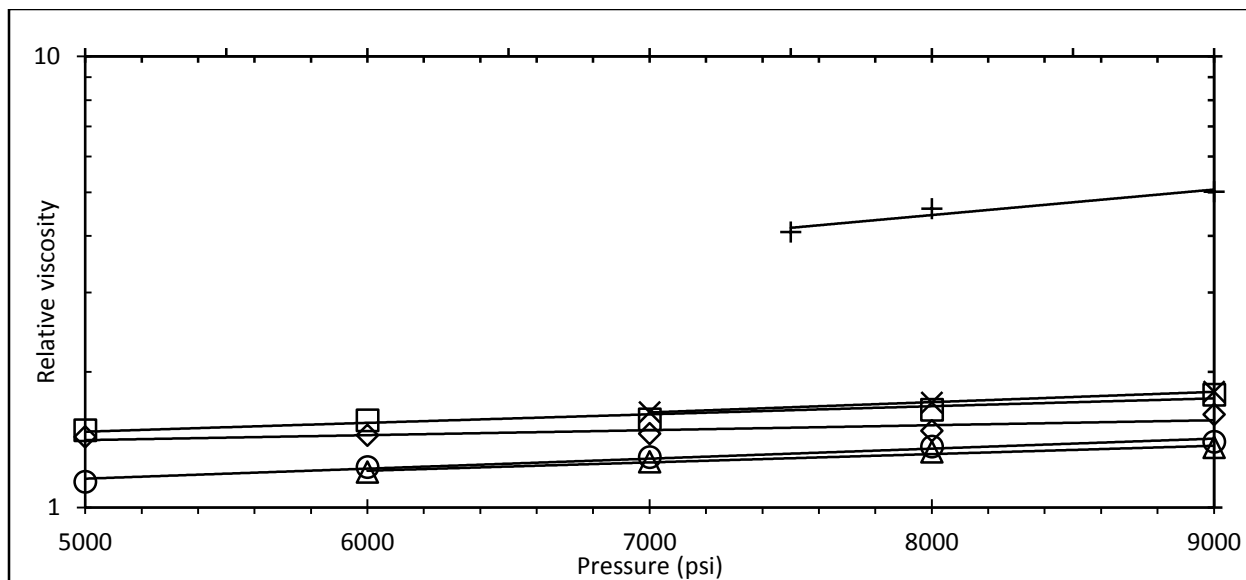


Figure 14. Viscosity change in ethane at 25°C and average shear rate of 1500-7100 s⁻¹ (Logarithmic Y axis). + DRA at 0.5 wt%; x DRA at 0.25 wt%; □ DRA at 0.2 wt%; ◇ DRA at 0.1 wt%; ○ DRA 0.04 wt%; △ DRA 0.01 wt%.

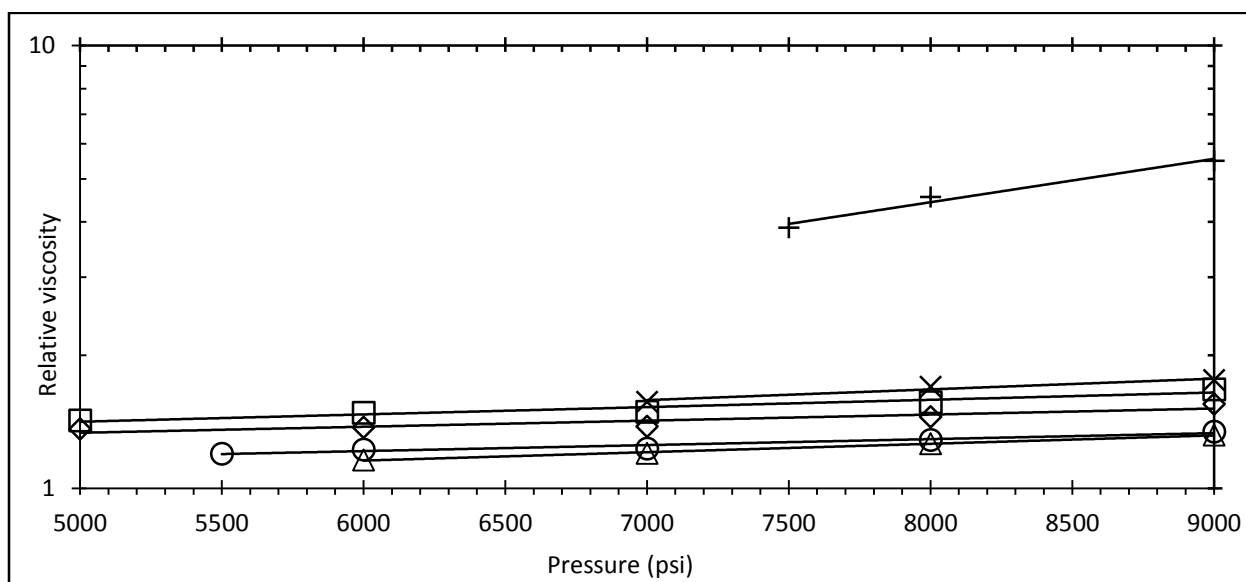


Figure 15. Viscosity change in ethane at 40°C and average shear rate of 1500-7100 s⁻¹ (Logarithmic Y axis). + DRA at 0.5 wt%; x DRA at 0.25 wt%; □ DRA at 0.2 wt%; ◇ DRA at 0.1 wt%; ○ DRA 0.04 wt%; △ DRA 0.01 wt%.

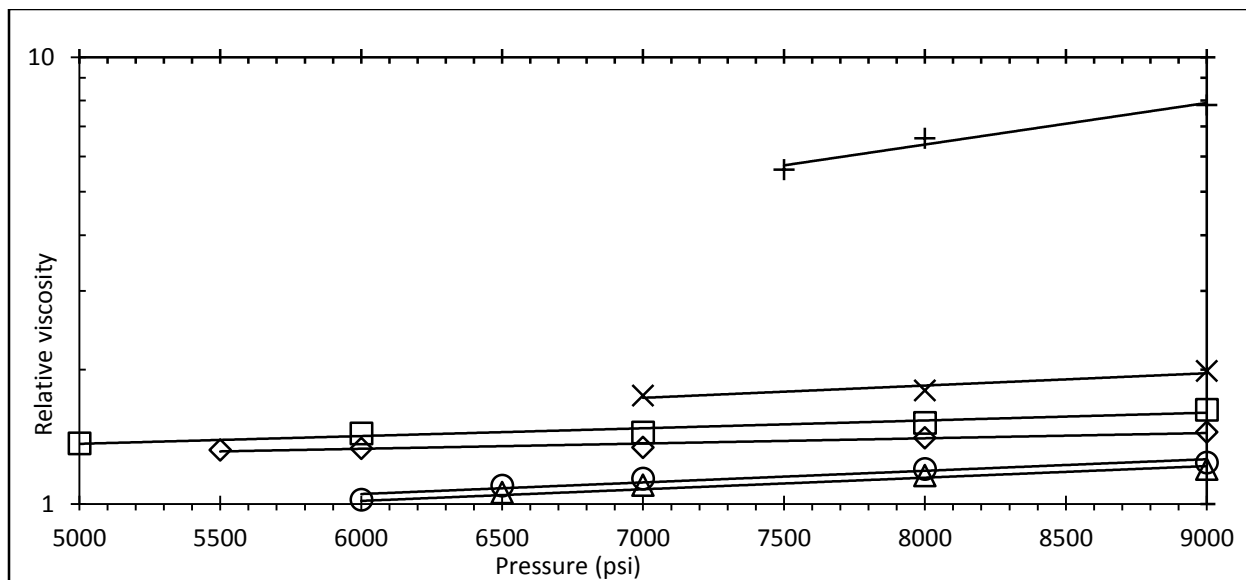


Figure 16. Viscosity change in ethane at 60°C and average shear rate of 800-7100 s^{-1} (Logarithmic Y axis). + DRA at 0.5 wt%; x DRA at 0.25 wt%; □ DRA at 0.2 wt%; ◇ DRA at 0.1 wt%; ○ DRA 0.04 wt%; Δ DRA 0.01 wt%.

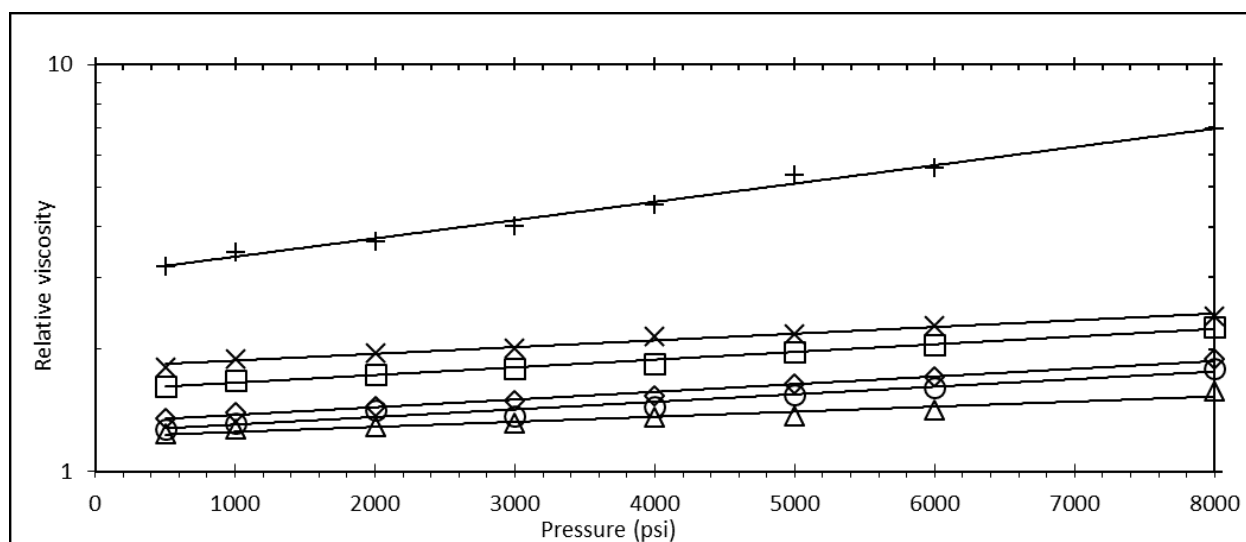


Figure 17. Viscosity change in propane at 25°C and average shear rate of 1000-7100 s^{-1} (Logarithmic Y axis). + DRA at 0.5 wt%; x DRA at 0.25 wt%; □ DRA at 0.2 wt%; ◇ DRA at 0.1 wt%; ○ DRA 0.04 wt%; Δ DRA 0.01 wt%.

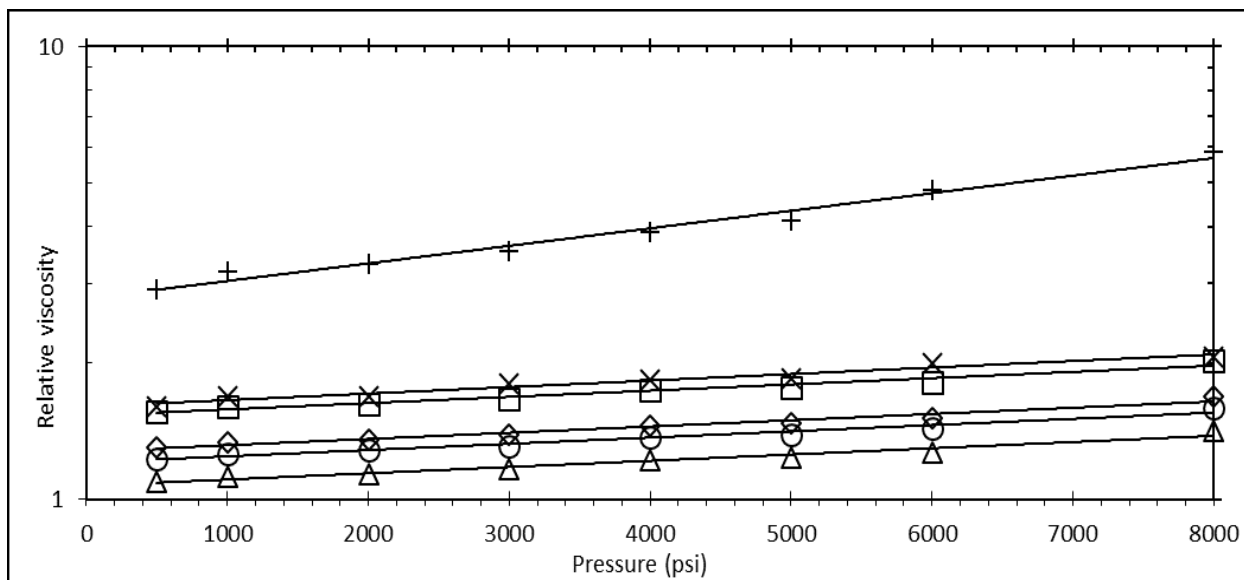


Figure 18. Viscosity change in propane at 40°C and average shear rate of 1200-7100 s⁻¹ (Logarithmic Y axis). + DRA at 0.5 wt%; x DRA at 0.25 wt%; □ DRA at 0.2 wt%; ◇ DRA at 0.1 wt%; ○ DRA 0.04 wt%; △ DRA 0.01 wt%.

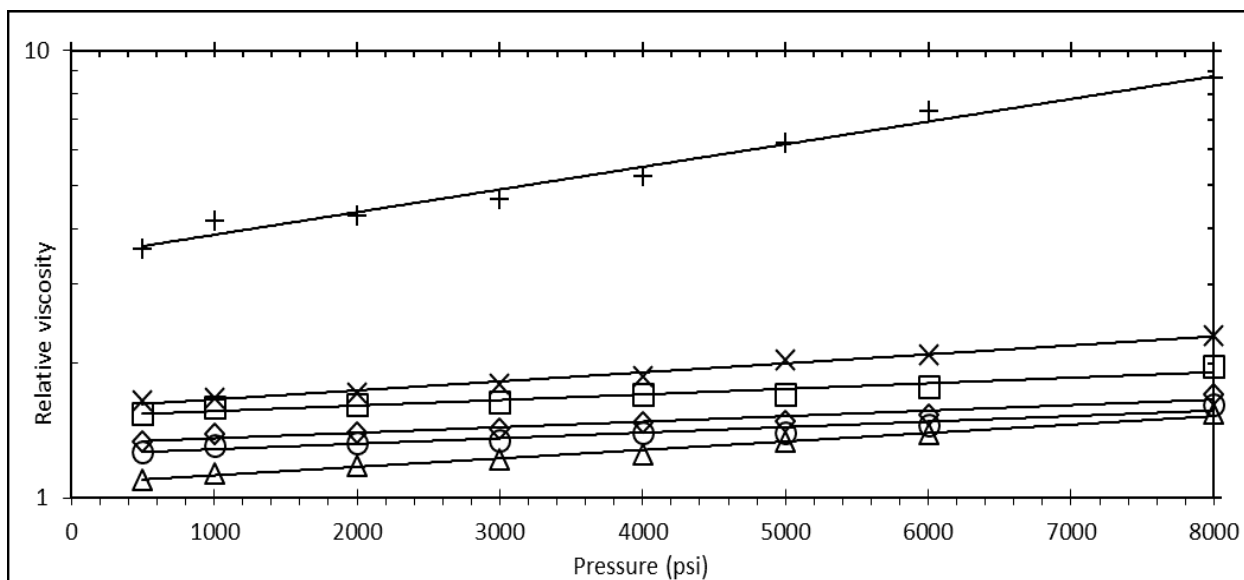


Figure 19. Viscosity change in propane at 60°C and average shear rate of 800-7100 s⁻¹ (Logarithmic Y axis). + DRA at 0.5 wt%; x DRA at 0.25 wt%; □ DRA at 0.2 wt%; ◇ DRA at 0.1 wt%; ○ DRA 0.04 wt%; △ DRA 0.01 wt%.

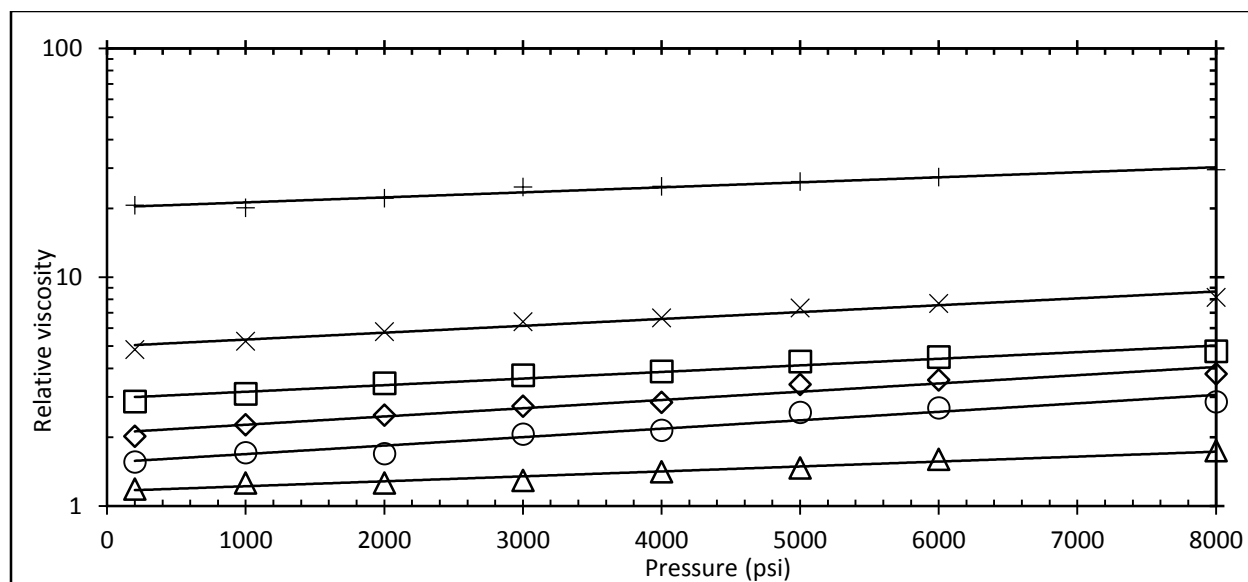


Figure 20. Viscosity change in butane by DRA at 25°C and average shear rate of 400-7100 s⁻¹ (Logarithmic Y axis). + DRA at 0.5 wt%; x DRA at 0.25 wt%; □ DRA at 0.2 wt%; ◇ DRA at 0.1 wt%; ○ DRA 0.04 wt%; Δ DRA 0.01 wt%.

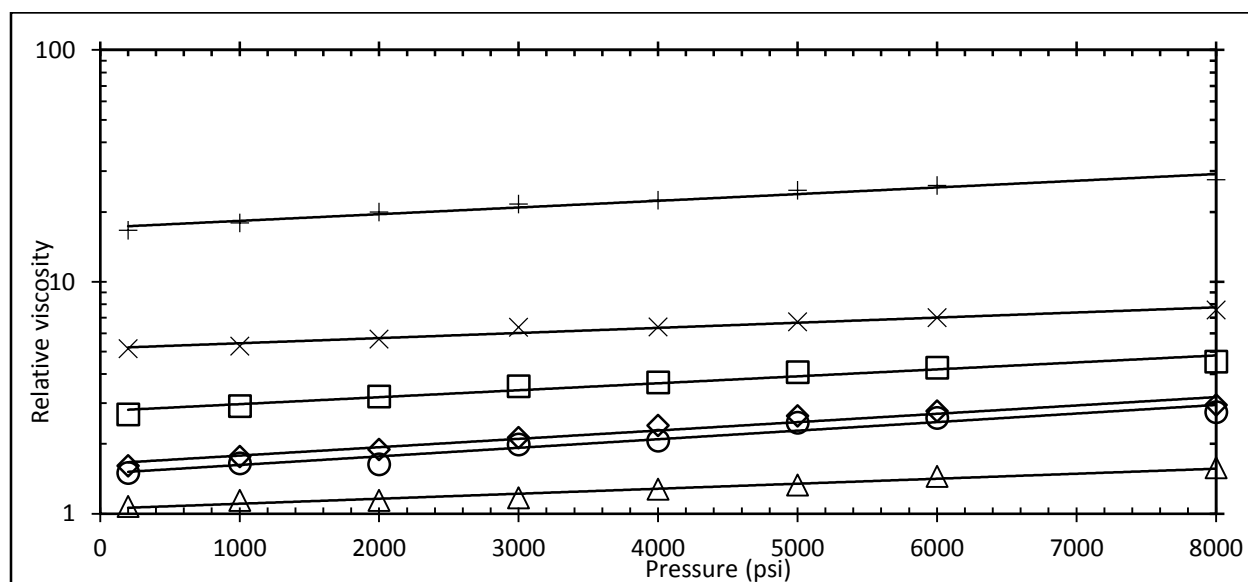


Figure 21. Viscosity change in butane by DRA at 40°C and average shear rate of 400-7100 s⁻¹ (Logarithmic Y axis). + DRA at 0.5 wt%; x DRA at 0.25 wt%; □ DRA at 0.2 wt%; ◇ DRA at 0.1 wt%; ○ DRA 0.04 wt%; Δ DRA 0.01 wt%.

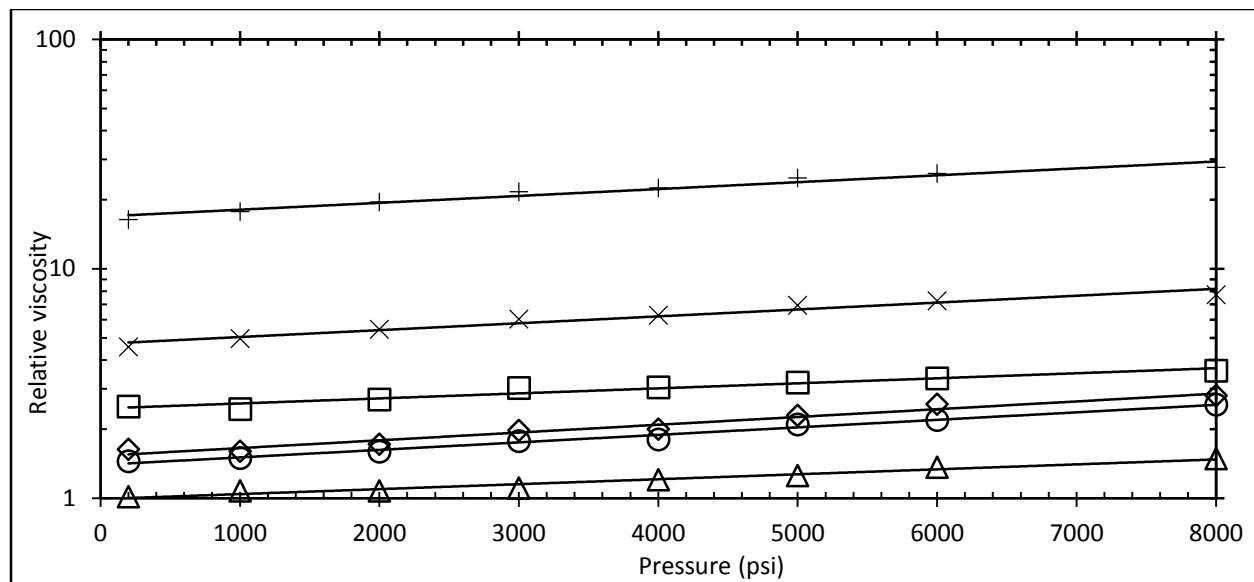


Figure 22. Viscosity change in butane by DRA at 60°C and average shear rate of 400-7100 s⁻¹ (Logarithmic Y axis).
 + DRA at 0.5 wt%; x DRA at 0.25 wt%; □ DRA at 0.2 wt%; ◇ DRA at 0.1 wt%; ○ DRA 0.04 wt%; Δ DRA 0.01 wt%.

5.0 SMALL ASSOCIATING MOLECULE THICKENER

This section covers small associating molecules which self-assemble among themselves and result in increase in viscosity of solution.

5.1 TRIALKYLTIN FLUORIDES

It has been reported that organotin fluorides having structure R_3SnF , where R being independently an alkyl, alkyl-aryl or aryl group form linear high molecular weight polymer chains by transient association in non-polar hydrocarbon solvents. (Clark et al., 1964; Dunn and Oldfield, 1970) These trialkyl tin fluorides form long linear transient polymeric chains via intermolecular associations between the electropositive tin atom and the electronegative fluorine atom of the neighboring molecule, with the three alkyl chains enhancing solubility in the hydrocarbon solvent and a low enough level of steric hindrance so as to not disrupt the tin-fluorine associations (Dunn and Oldfield, 1970)

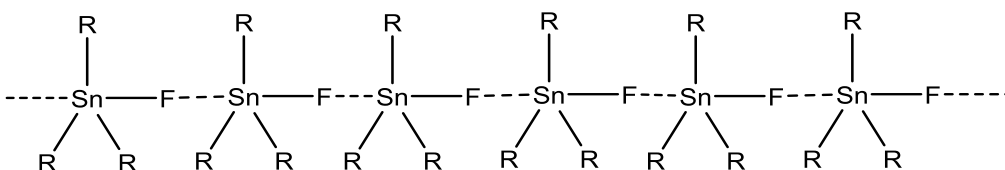


Figure 23. Association in trialkyl tin fluoride

Tributyltin fluoride: One of the most effective light hydrocarbon thickeners that has even been reported is tributyltin fluoride (TBTF), a white powder with a melting point of 271°C. This Tributyltin fluorides typically dissolve in organic liquids after a relatively short period of agitation or stirring (~minutes); although heating hastens the dissolution a heating/cooling cycle is not required to thicken the organic liquid. Dunn and co-workers first reported that TBTF increases the viscosity of non-polar liquid solvents such as n-hexane and carbon tetrachloride. Heller and co-workers found that TBTF increases the viscosity of high pressure Liquefied Petroleum Gas (LPG), which is composed primarily of propane and butane. For example, 2-10 fold increases in the viscosity of liquid propane and butane are induced at TBTF concentrations of 0.15 - 0.30 wt% at 25°C and 8.3 MPa (~1200 psi), as determined with a high pressure, falling cylinder, close-clearance viscometer. Enick and co-worker later confirmed that liquid propane and butane could be thickened with TBTF (Iezzi et al., 1989). Although Heller claimed that TBTF could also thicken ethane, Heller's group reported that TBTF was only sparingly soluble in ethane and induced no viscosity change in their sapphire crystal viscometer that was rated to 3000 psi.

Because tripropyltin fluoride is insoluble in hydrocarbon solvents (the C3 arms are too short to promote dissolution in the solvent) (Van Den Berghe and Van Der Kelen, 1971), trialkyl tin fluorides with longer n-alkyl arms have been studied. Dandge and co-workers found that triamyl, trihexyl, trioctyl and tridecyl armed tin fluorides were soluble (> 0.4 wt%) in normal alkanes higher than propane as well as in many more solvents such as cyclopentane and cyclohexane in which tributyltin fluoride was insoluble. However, in comparison of viscosity change induced in solvents like n-hexane (at 0.1 MPa and 25°C) and n-butane (at 8.3 MPa and 25°C), tributyltin fluoride clearly outperformed the others at equivalent mass concentrations in the alkane. (Dandge et al., 1989)

Material: A white colored powder of tributyltin fluoride and triphenyltin fluoride were procured from TCI America and Alfa Aesar, respectively and used as received.

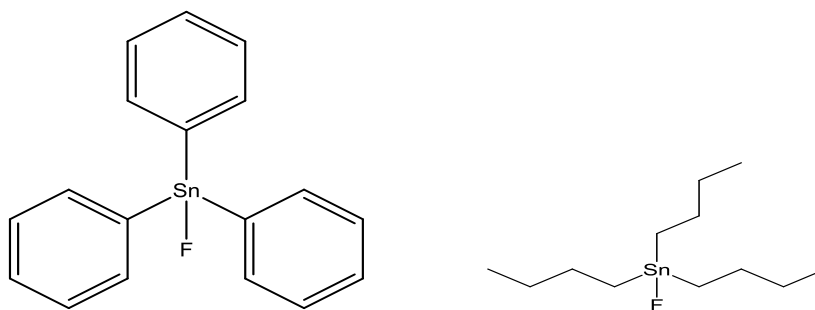


Figure 24. Structure of triphenyltin fluoride and tributyltin fluoride

Synthesis: Owing to insolubility of triphenyltin fluoride and remarkable solubility of tributyltin fluoride in pentane and hexane at ambient pressure, we decided to synthesize dimethylphenyltin fluoride and assess its thickening capabilities in NGLs. As this molecule reported to be thickener for some hydrocarbon liquids such as toluene and hexane at lower temperatures. (Beckmann et al., 2003)

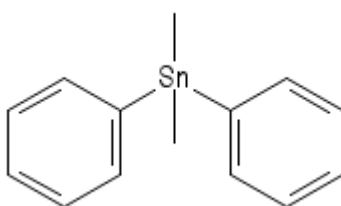


Figure 25. Dimethyldiphenyltin, purchased from Alfa Aesar

Dimethylphenyltin Iodide: Dimethyldiphenyltin (5g, Figure 25) was dissolved anhydrously under nitrogen atmosphere, in dichloromethane (100 ml) and the solution chilled to 0°C, the solution was then magnetically stirred, and iodine (2.4 g) was added in small portions to the ice

cooled solution. The reaction was then stirred at 0°C for 2.5 hours, before the solvent and iodobenzene were removed by rotary evaporation. This gave a clear, light yellow, slightly viscous oil (6 g), dimethylphenyltin iodide (Figure 26).

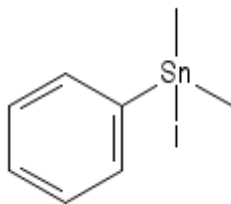


Figure 26. Dimethylphenyltin iodide, produced by iodination of Dimethyldiphenyltin

Dimethylphenyltin Fluoride: A solution of potassium fluoride (3.76 g) dissolved in 60 ml of water was added to a solution of Dimethylphenyltin iodide (5.72 g) dissolved in 60 ml of diethyl ether. The resulting mixture was stirred at room temperature for 24 hours. After completion the mixture was allowed to stand for a few hours, before all the solvent and water was removed (azeotropically with hexane), and the resulting solid product was dissolved in dry diethyl ether (potassium iodide and excess potassium fluoride do not dissolve). The insoluble inorganic salts are then filtered off and the solvent removed under vacuum to give slightly yellow crystals, (melting point 120°C, 2.8 g), dimethylphenyltin fluoride.

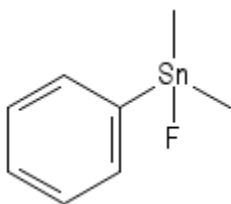


Figure 27. Dimethylphenyltin fluoride, produced by halogen exchange of Dimethylphenyltin iodide with potassium fluoride.

5.1.1 Ambient pressure testing

The solubility and thickening ability of trialkyltin fluoride compounds in pentane and hexane are illustrated in below figures 28-29. The viscosity of the resultant solutions was determined over the shear rate range of 15-350 s^{-1} at 23°C and 1 atm. In case of tributyltin fluoride for concentration greater than 0.4 wt%, viscosity of pentane as well as hexane solution were too high to be measured by the instrument.

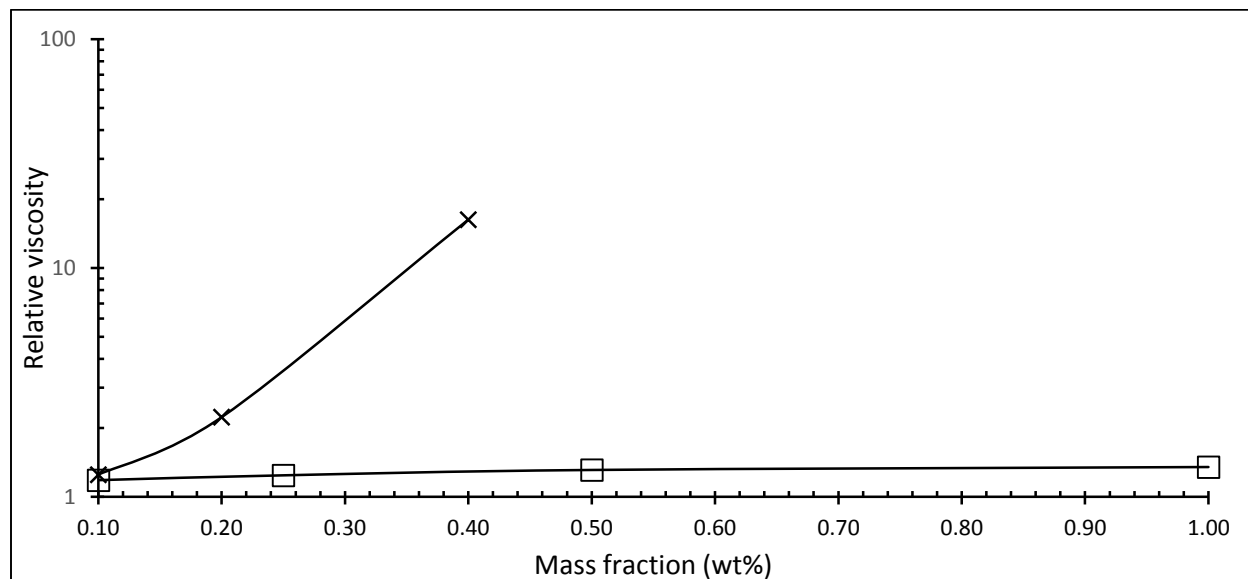


Figure 28. Relative viscosity (viscosity of pentane solution/viscosity of pentane) x tributyltin fluoride ; □ dimethylphenyltin fluoride at 23°C.

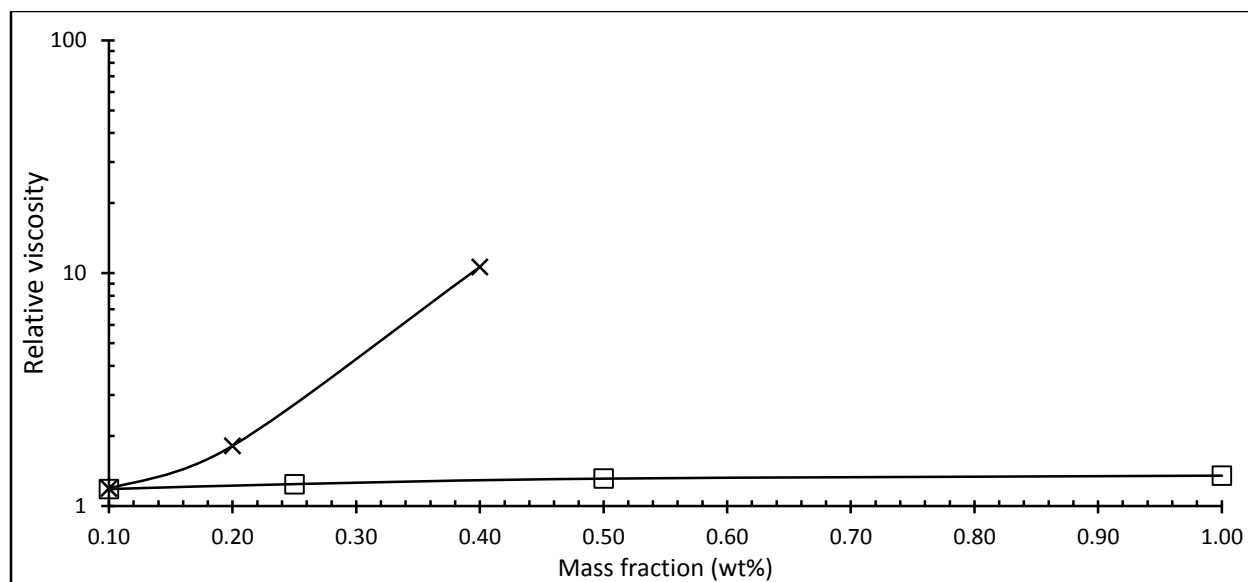


Figure 29. Relative viscosity (viscosity of hexane solution/viscosity of pentane) x tributyltin fluoride ; □ dimethylphenyltin fluoride at 23oC

5.1.2 High pressure testing

Tributyltin fluoride dissolves quickly up to 1 wt% in ethane, propane and n-butane at pressures above the cloud point pressure values listed in Table 7. TBTF was soluble in propane and n-butane at pressure slightly above the vapor pressure of respective component. Dissolution in ethane, however, requires pressures much greater than the ethane vapor pressure. This is not surprising because ethane is a weaker solvent for organometallic compounds than propane and butane. This is reflected by the very low value of the solubility parameter for liquid ethane, $5.80(\text{cal}/\text{cm}^3)^{0.5}$, relative to that of liquid propane, $6.55(\text{cal}/\text{cm}^3)^{0.5}$, and liquid *n*-butane, $6.89(\text{cal}/\text{cm}^3)^{0.5}$ (Hansen, 2007). Note that all of the cloud point pressures listed for ethane in Table 7 exceed 3000 psi, which was the pressure limit of the viscometer used by Heller and co-workers when they reported that TBTF was essentially ethane-insoluble.

Table 7. Cloud point pressure of TBTF in NGL

Solvent	TBTF concentrations (wt%)	Cloud point (psi)				
		25C	40C	60C	80C	100C
Ethane	0.2	4835	5120	5795	6135	6470
	0.5	5535	5915	6450	6695	6915
	0.75	5645	5995	6520	6820	7025
	1.0	5865	6215	6850	7010	7350
Propane	0.5	153	231	355		
	1.0	155	238	370		
n-Butane	0.5	45	61	112		
	1.0	52	62	115		

The relative viscosity of the high pressure solutions of TBTF in ethane, propane and n-butane are provided in the Figures 30-40. There is only a very slight increase in relative viscosity with increasing pressure at any temperature and TBTF concentration. This is in stark contrast to the significant increases in relative viscosity that are observed when polymers are used to thicken these light alkanes (Dhuwe et al., 2015) Increasing the pressure of the light alkanes increases fluid density and solvent strength for not only dissolving the polymer but also swelling polymer coils and enhancing viscosity. TBTF, on the other hand, is a small molecule that self-assembles into a linear supramolecular structure. Therefore as long as the TBTF is dissolved, further increases in pressure-induced solvent strength should not have a significant effect on solution viscosity.

Increasing temperature above 40°C diminishes the intermolecular associations between the adjacent tin fluoride molecules, resulting in significant decreases in relative viscosity for all of the light alkanes. For example, at 25°C, 1% TBTF in ethane and 9000 psi, the relative viscosity is 90. At 40°C, the relative viscosity is 75. However, at 60°C, 80°C and 100°C, the relative viscosity drops to 20, 6 and 2, respectively.

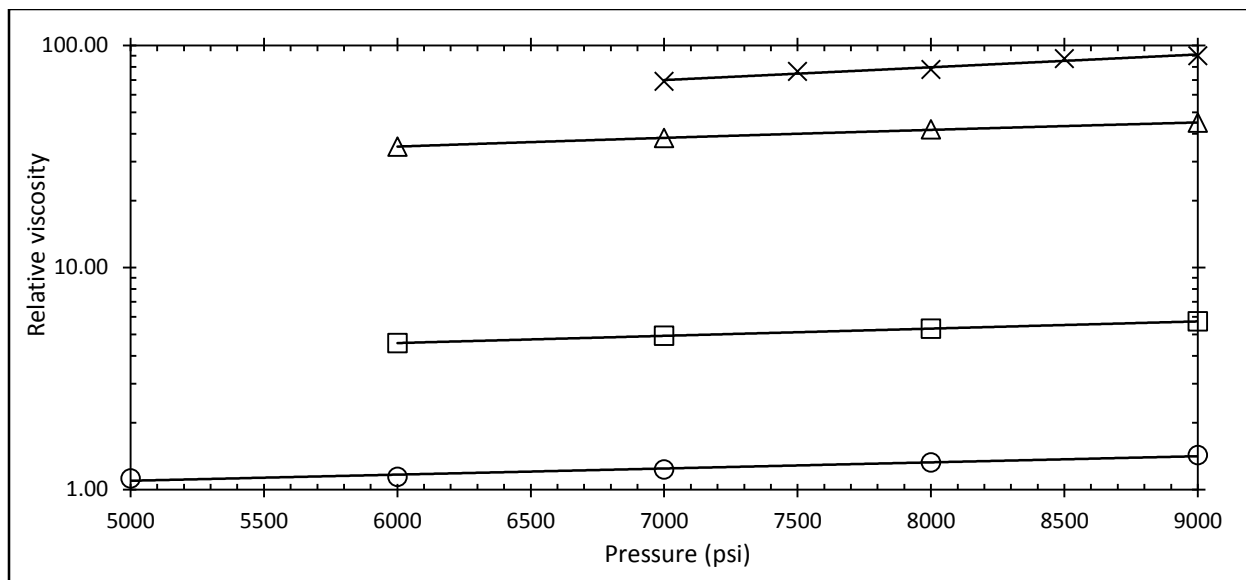


Figure 30. Viscosity change in ethane by TBTF at 25°C and average shear rate of 100-7100 s⁻¹ (Logarithmic Y-axis). x TBTF at 1 wt%; Δ TBTF at 0.75 wt%; □ TBTF 0.5 wt%; ○ TBTF 0.2 wt%.

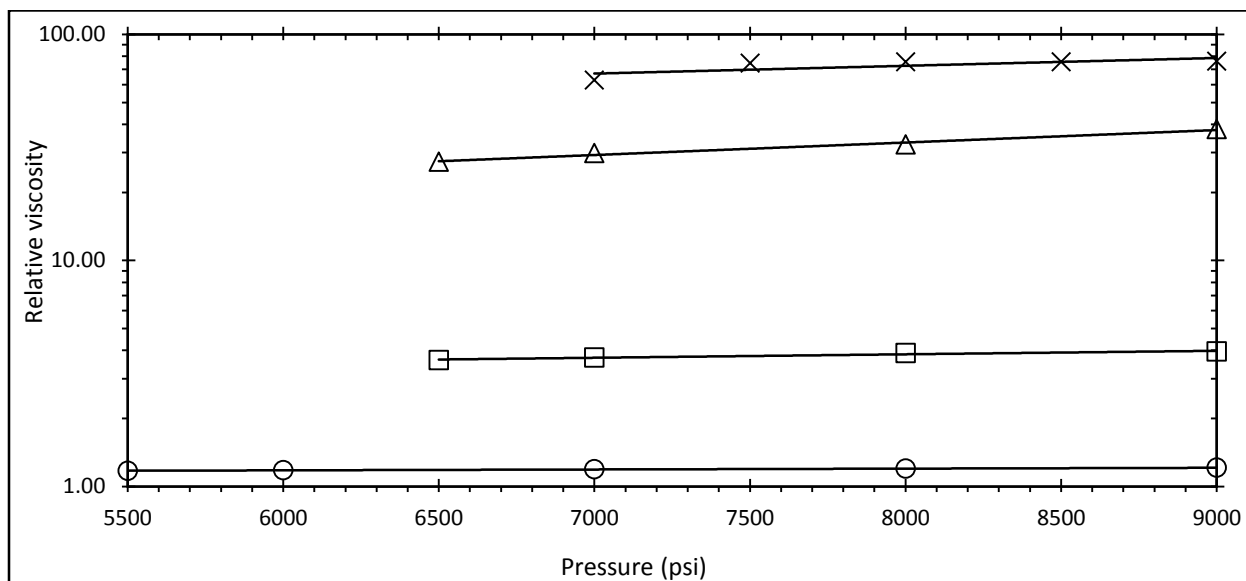


Figure 31. Viscosity change in ethane by TBTF at 40°C and average shear rate of 100-7100 s⁻¹ (Logarithmic Y-axis). x TBTF at 1 wt%; Δ TBTF at 0.75 wt%; □ TBTF 0.5 wt%; ○ TBTF 0.2 wt%.

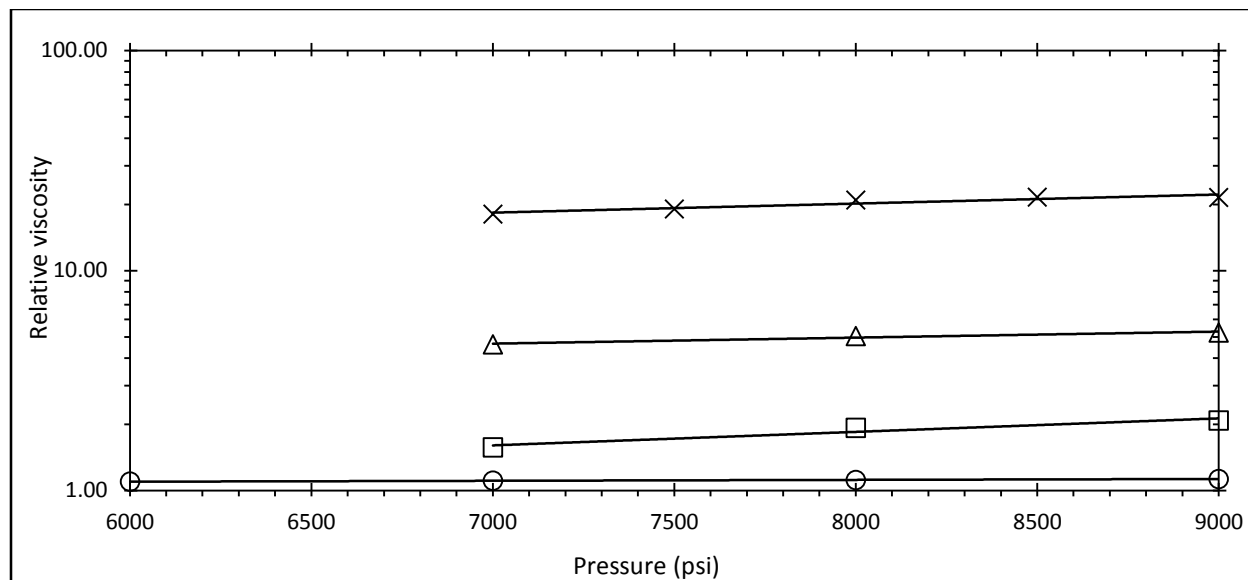


Figure 32. Viscosity change in ethane by TBTF at 60°C and average shear rate of 350-7100 s⁻¹ (Logarithmic Y-axis). x TBTF at 1 wt%; Δ TBTF at 0.75 wt%; □ TBTF 0.5 wt%; ○ TBTF 0.2 wt%.

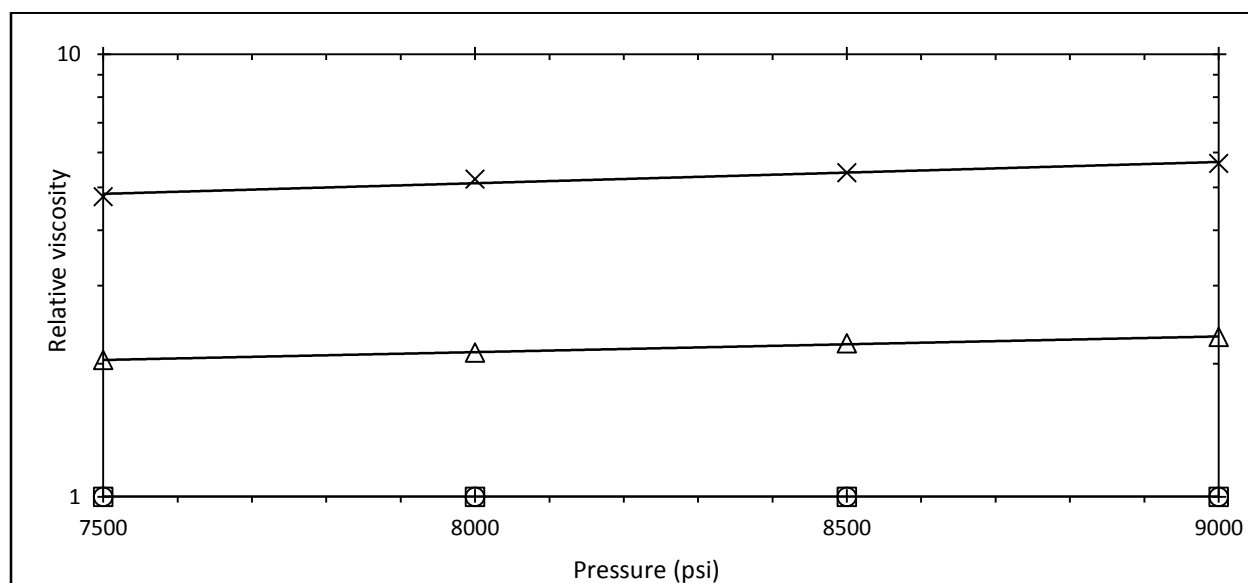


Figure 33. Viscosity change in ethane by TBTF at 80°C and average shear rate of 1500-7100 s⁻¹ (Logarithmic Y-axis). x TBTF at 1 wt%; Δ TBTF at 0.75 wt%; □ TBTF 0.5 wt%; ○ TBTF 0.2 wt%.

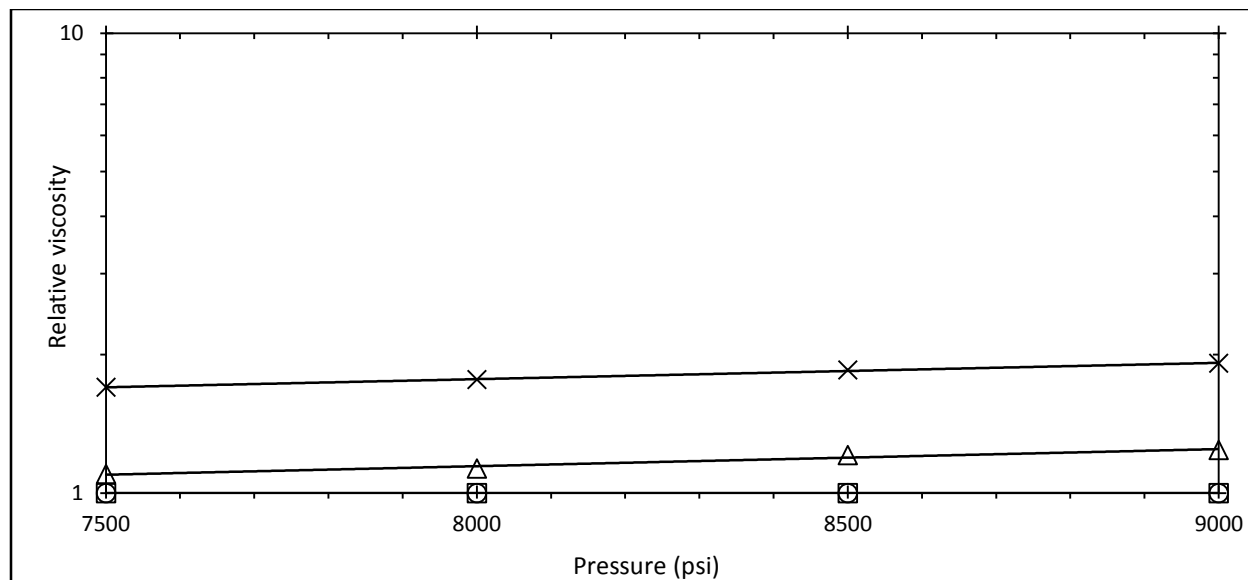


Figure 34. Viscosity change in ethane by TBTF at 100°C and average shear rate of 3500-7100 s^{-1} (Logarithmic Y-axis). x TBTF at 1 wt%; Δ TBTF at 0.75 wt%; □ TBTF 0.5 wt%; ○ TBTF 0.2 wt%.

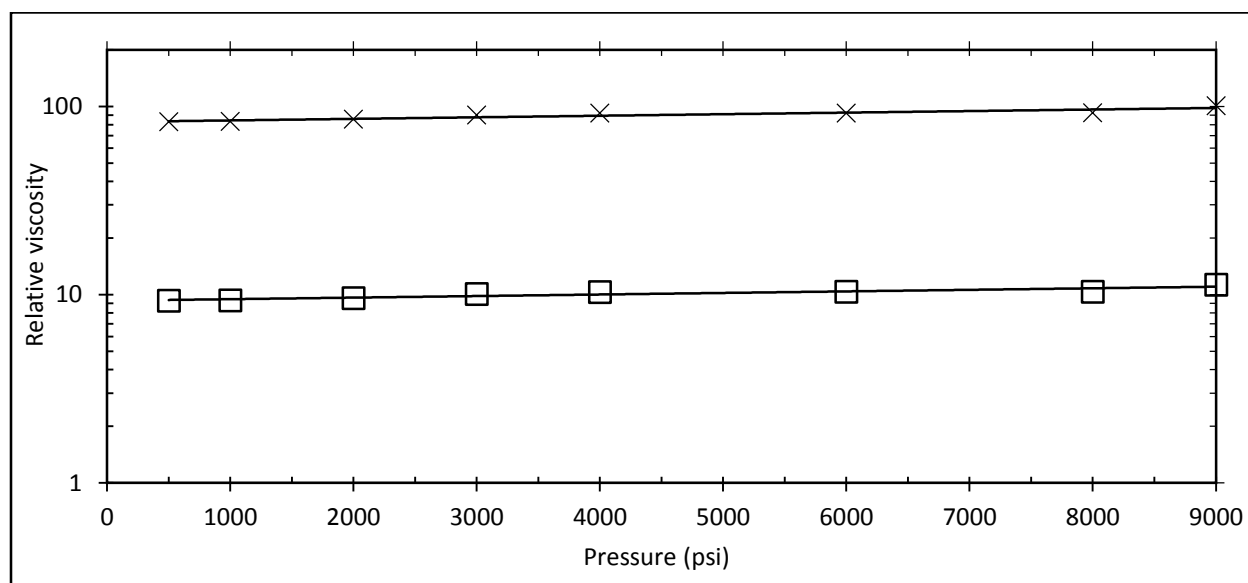


Figure 35. Viscosity change in propane by TBTF at 25°C and average shear rate of 70-710 s^{-1} (Logarithmic Y-axis). x TBTF at 1 wt%; □ TBTF 0.5 wt%.

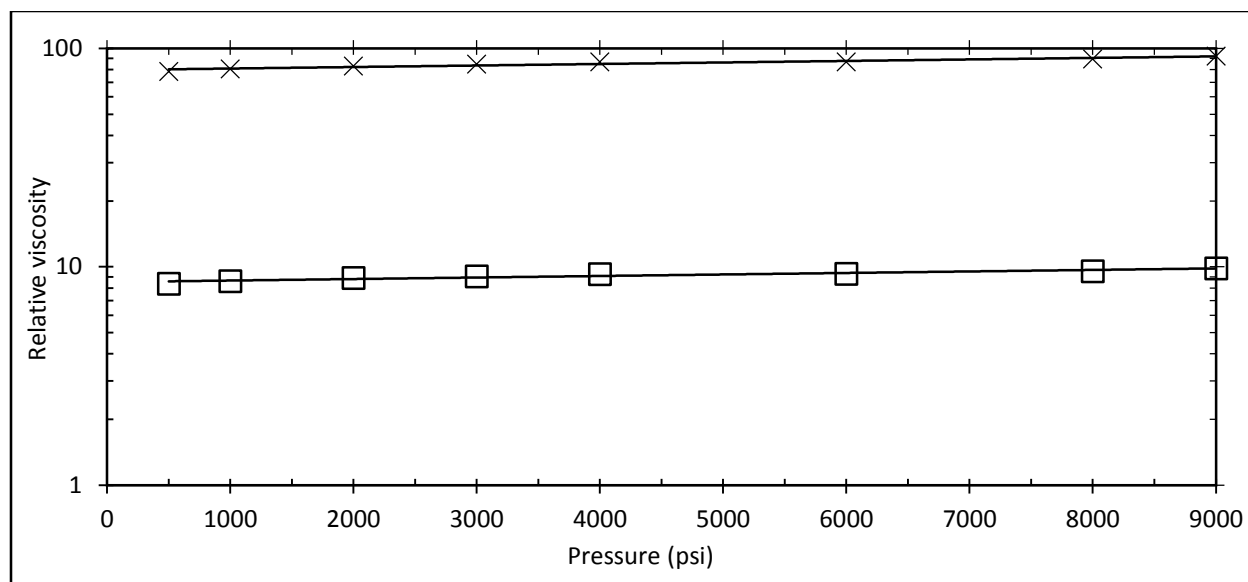


Figure 36. Viscosity change in propane by TBTF at 40°C and average shear rate of 70-710 s⁻¹ (Logarithmic Y-axis). x TBTF at 1 wt%; □ TBTF 0.5 wt%.

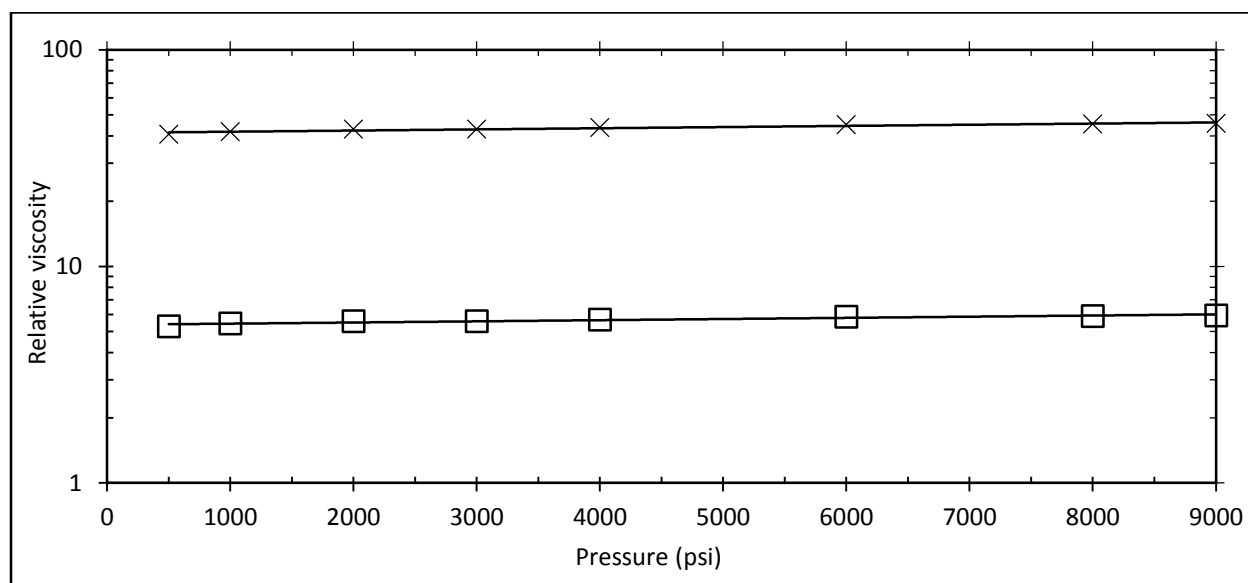


Figure 37. Viscosity change in propane by TBTF at 60°C and average shear rate of 100-1000 s⁻¹ (Logarithmic Y-axis). x TBTF at 1 wt%; □ TBTF 0.5 wt%.

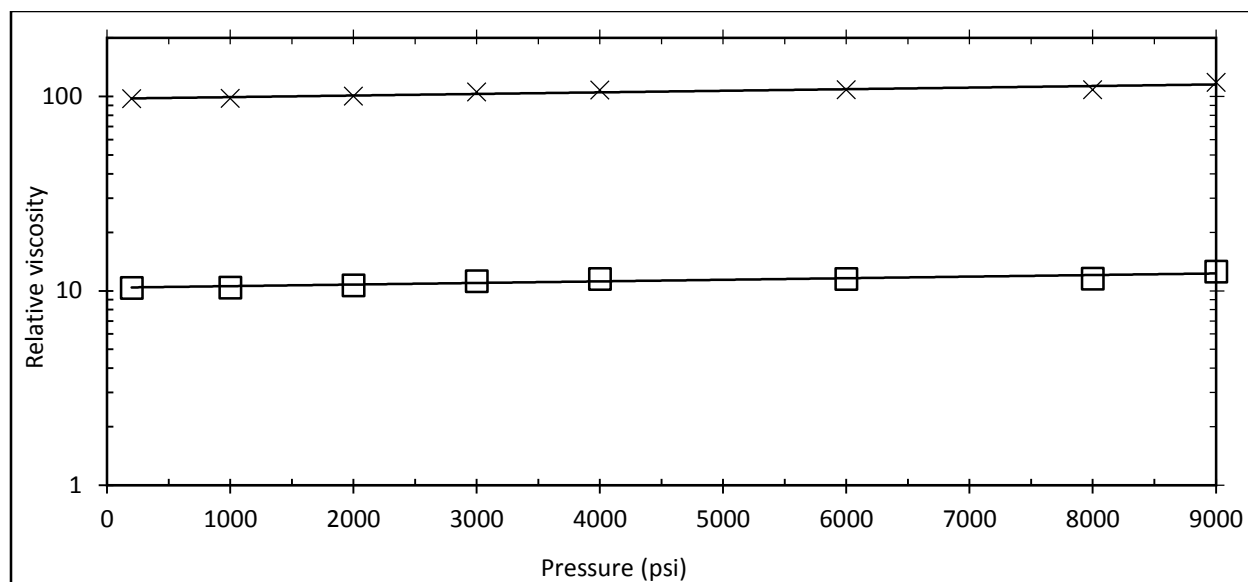


Figure 38. Viscosity change in n-butane by TBTF at 25°C and average shear rate of 70-710 s⁻¹ (Logarithmic Y-axis). x TBTF at 1 wt%; □ TBTF 0.5 wt%.

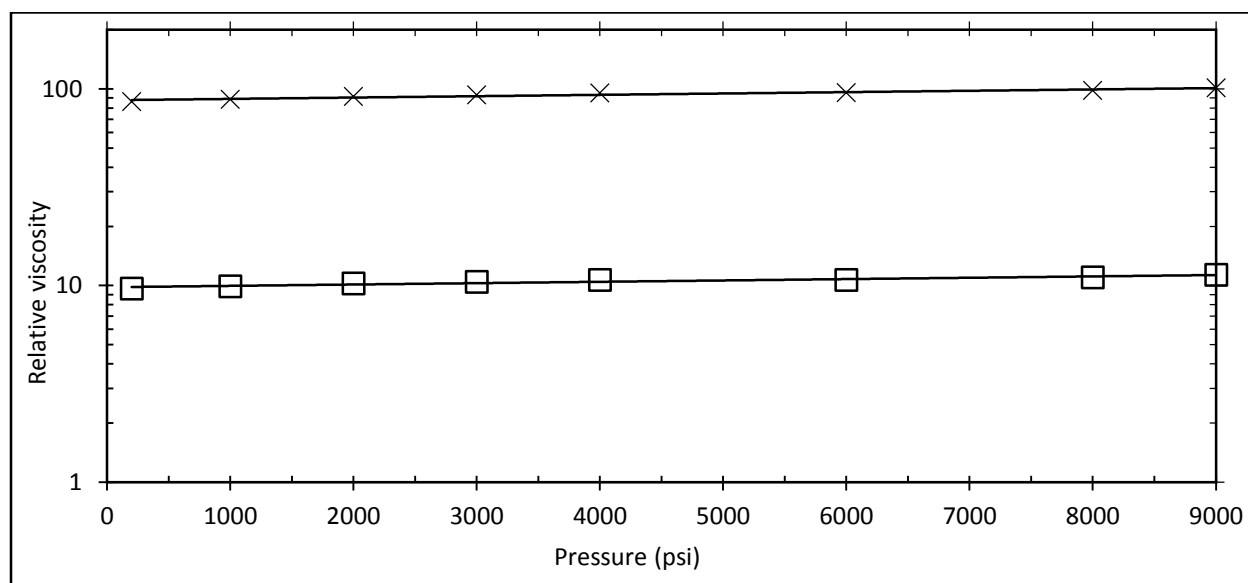


Figure 39. Viscosity change in n-butane by TBTF at 40°C and average shear rate of 70-710 s⁻¹ (Logarithmic Y-axis). x TBTF at 1 wt%; □ TBTF 0.5 wt%.

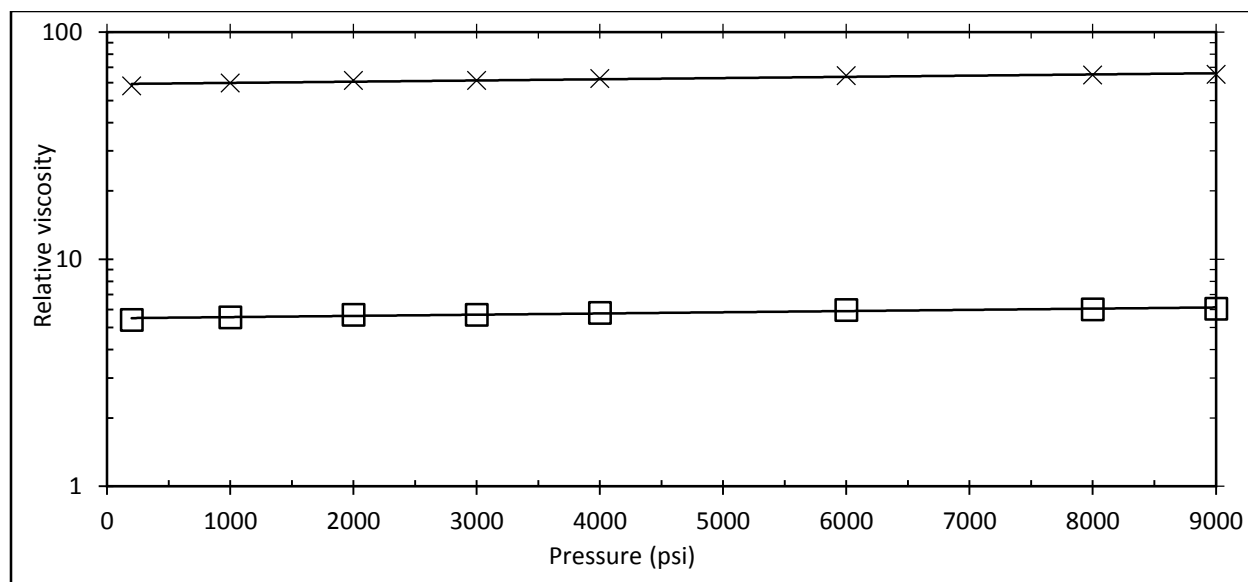


Figure 40. Viscosity change in n-butane by TBTF at 60°C and average shear rate of 100-1000 s⁻¹ (Logarithmic Y-axis). x TBTF at 1 wt%; □ TBTF 0.5 wt%.

5.2 ALUMINUM SOAPS

These thickeners are aluminum salts of saturated or unsaturated soap forming-forming fatty acids. A mixture of aluminum salts of naphthenic and palmitic acids, deemed “Napalm”, was invented to gel gasoline during World War II in order to weaponized this flammable liquid (Fieser et al., 1946; Hughes, 2014; Mysels, 1949). Typically, the mixture of the powdered aluminum disoap and the organic liquid is heated to a temperature high enough to disrupt the intermolecular associations between aluminum disoaps thereby promoting dissolution, and then cooled to allow the disoap molecules to self-assemble into a viscosity-enhancing supramolecular structure, Figure 41. Various aluminum based soaps were investigated during that time and interestingly first attempt was made using aluminum stearate. (Rueggeberg, 1948). The exceptional thickening ability of

aluminum based thickener in hydrocarbon fuel persuade us to consider them to be thickener candidates for NGLs

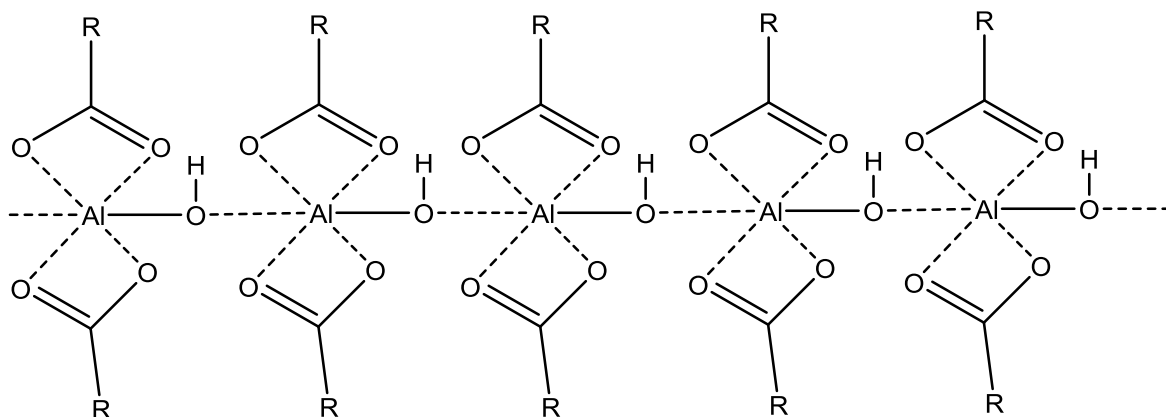
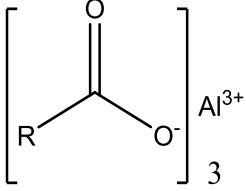
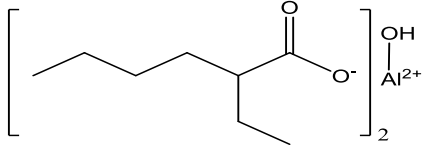
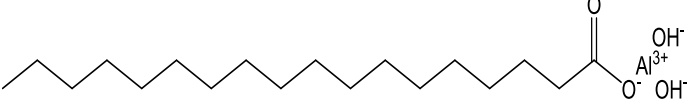
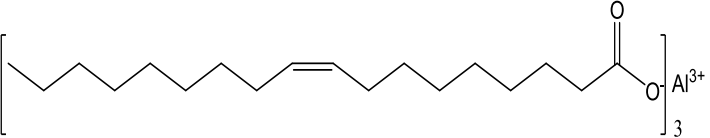
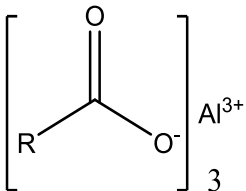
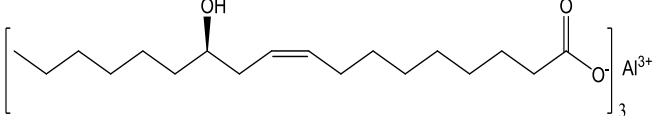


Figure 41. Possible association of HAD2EH molecules (Pilpel, 1963)

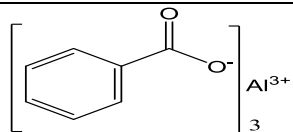
A single aluminum salt, hydroxyaluminum di-2-ethylhexanoate (HAD2EH), which is a powder with a melting point of 276°C, also exhibits remarkable liquid hydrocarbon thickening abilities. HAD2EH was also reported to be effective thickener for compressed liquid propane and butane. At 20°C and dilute HAD2EH concentrations of 0.2-1.0 wt%, 10-100 fold viscosity increases were detected with a high pressure close-clearance falling cylinder viscometer after several hours of mixing (Enick, 1991b). However, these HAD2EH-propane and HAD2EH-butane solutions were not transparent. Rather they were translucent and hazy, which was indicative of the HAD2EH forming a network of solid interlocking fibers in the high pressure liquid propane.

Materials: Numerous aluminum based compounds (listed in beneath table 8) were purchased from commercial source such as Sigma Aldrich, Alfa Aesar and BOC Science and used as received.

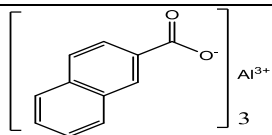
Table 8. Aluminum soaps

Structure	Soluble in hexane and pentane (after heating) at 0.1-1 wt% ?
 <p style="text-align: center;"> $R = n\text{-C}_{17}\text{H}_{36}$ Name: Aluminum tri-stearate White powder </p>	Yes
 <p style="text-align: center;"> Name: Bis-hydroxyaluminum ethyl-2hexanoate (HADEH) White powder </p>	Yes
 <p style="text-align: center;"> Name: Aluminum Monostearate White powder </p>	Yes
 <p style="text-align: center;"> Name: Aluminum Oleate White powder </p>	No
 <p style="text-align: center;"> $R = n\text{-C}_{14}\text{H}_{30}$ Name: Aluminum Palmitate White powder </p>	No
	No

Name: Aluminum Ricinoleate
White powder



Name: Aluminum Benzoate
Blackish wax



Name: Aluminum Naphthenate
Blackish wax

No

No

5.2.1 Ambient pressure testing

The solubility and thickening results obtained with these soluble aluminum soap thickeners, namely, HADEH, aluminum mono-stearate and aluminum tri-stearate are shown in figures 42-43. The viscosity of the resultant solutions was determined over the shear rate range of 150-450 s⁻¹ and 1 atm and results obtained at 375 s⁻¹ are represented in beneath figures. The viscosity values for all solution correspond to data obtained at some elevated temperatures (rather than 23°C) because dissolution of aluminum soaps : HADEH and aluminum stearates require heating close to boiling point solvents in case of hexane and pentane followed by cooling to temperatures; at lower temperatures the aluminum soaps comes out of solution.

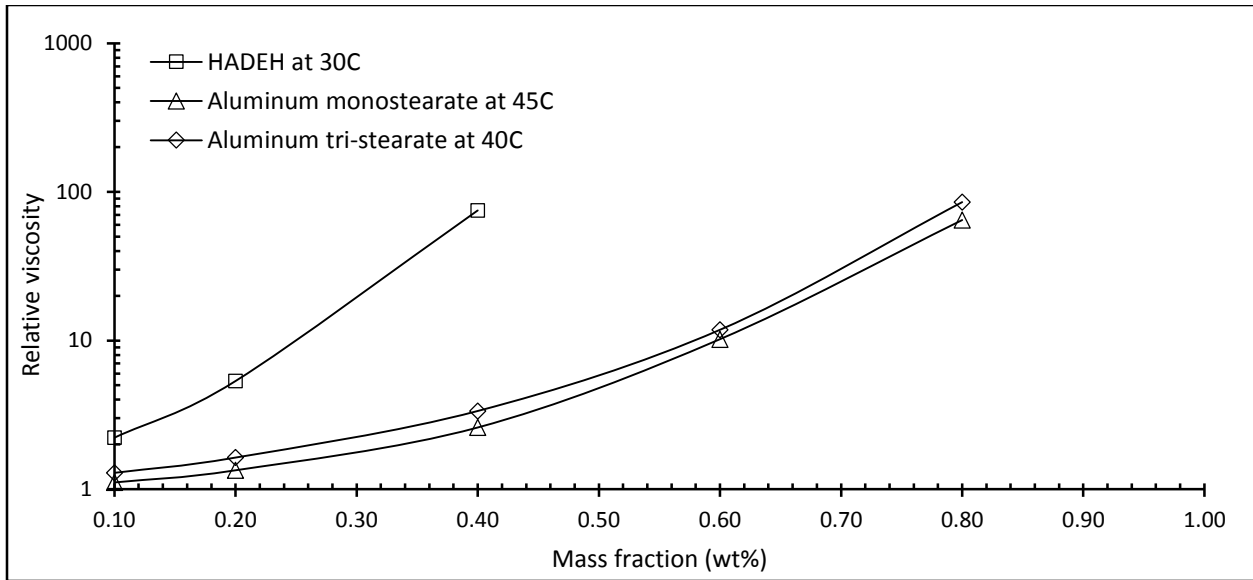


Figure 42. Viscosity change in pentane

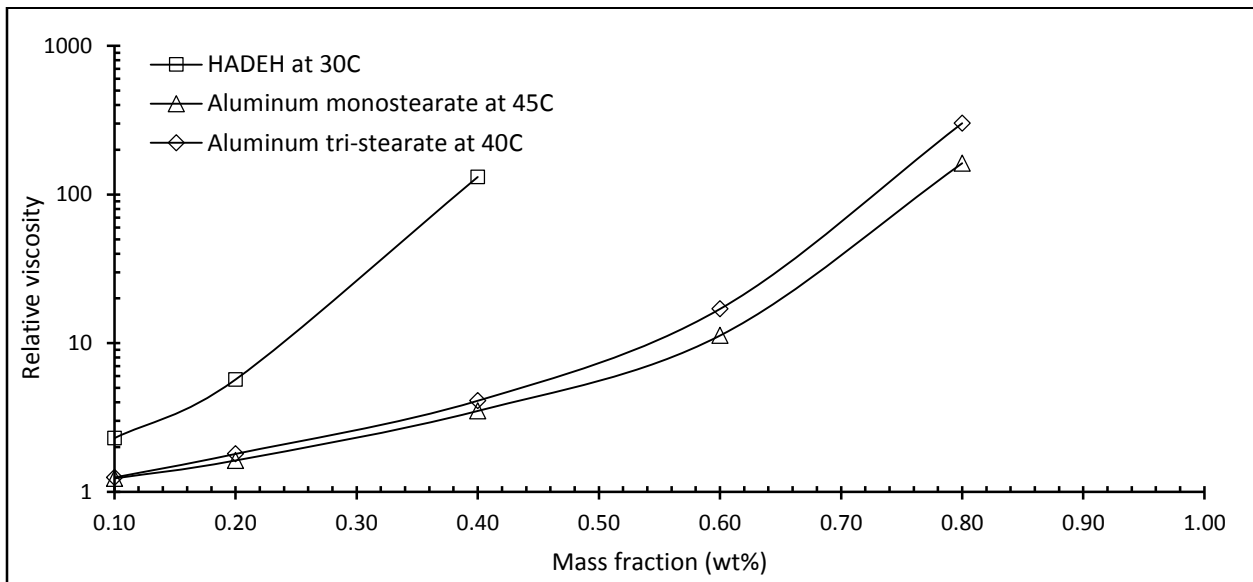


Figure 43. Viscosity change in hexane

Clearly the HADEH outperforms the other aluminum soap thickeners and hence was selected for high pressure testing in NGLs.

5.2.2 High pressure testing

HAD2EH is ethane-insoluble. The solubility of the HAD2EH in propane and butane at 25°C, 40°C, 60°C, 80°C and 100°C is provided in Table 9. Unlike TBTF, the dissolution of HAD2EH in light alkanes requires heating the high pressure mixture to a temperature of ~ 100°C while being mixed, attaining a clear solution, and cooling the solution to the targeted temperature. The HAD2EH remained in solution to temperatures of 40°C, but precipitated at 25°C in both propane and butane.

Table 9. Cloud point data for HADEH. In all cases the HAD2EH-alkane mixture was heated to 100°C at high pressure while being mixed, followed by cooling to the temperature listed in table.

Solvent	HADEH concentrations (wt%)	Cloud point (psi)				
		25C	40C	60C	80C	100C
Ethane	0.5	Insoluble	Insoluble	Insoluble	Insoluble	Insoluble
	1.0	Insoluble	Insoluble	Insoluble	Insoluble	Insoluble
Propane	0.5	Insoluble	231	355	512	780
	1.0	Insoluble	238	370	525	815
n-Butane	0.5	Insoluble	61	112	162	254
	1.0	Insoluble	62	115	165	255

The relative viscosity of HAD2EH-thickened solutions of propane and butane are shown in Figures 44-51. Increasing pressure has little effect on relative viscosity. Surprisingly, temperature also had little effect on the thickening ability of the HAD2EH; only very slight decreases in viscosity were observed with increasing temperature. HAD2EH is a much more effective thickener in butane than in propane. For example, at a concentration of 1 wt% HADEH in butane, the transparent solution is so viscous that the Pyrex ball does not fall, while the viscosity of propane increases by a factor of 10-20. At 0.5 wt% HAD2EH, butane is thickened by a factor of 13-28, while propane viscosity increases by a factor of 2-5.

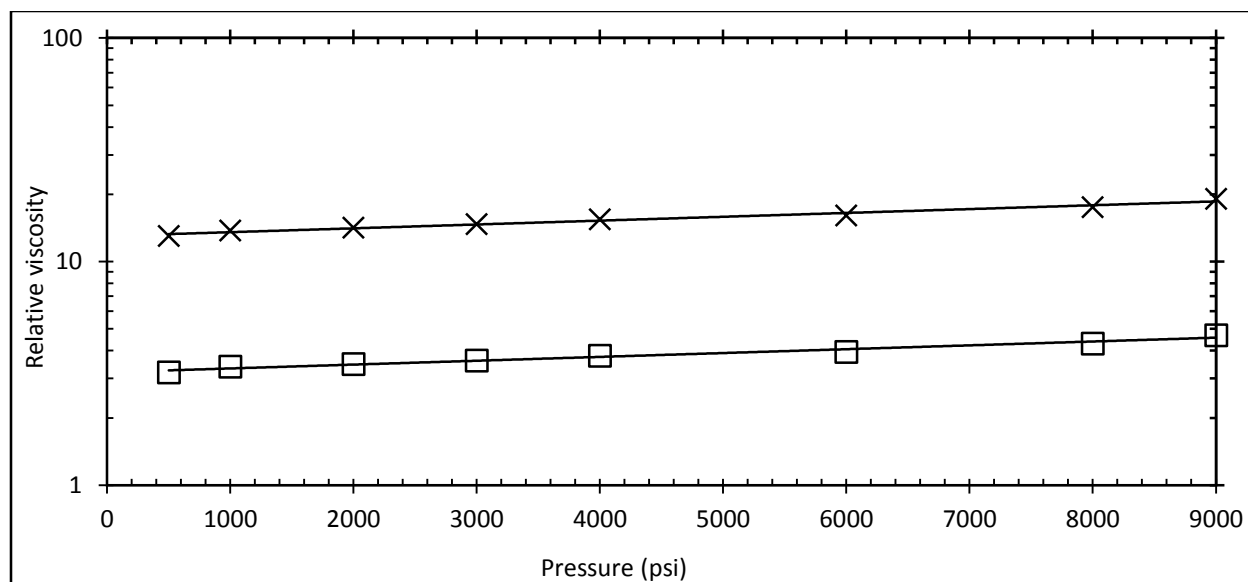


Figure 44. Viscosity change in propane by HADEH at 40°C and average shear rate of 350-2500 s⁻¹ (Logarithmic Y-axis). x HAD2EH at 1 wt%; □ HADEH 0.5 wt%.

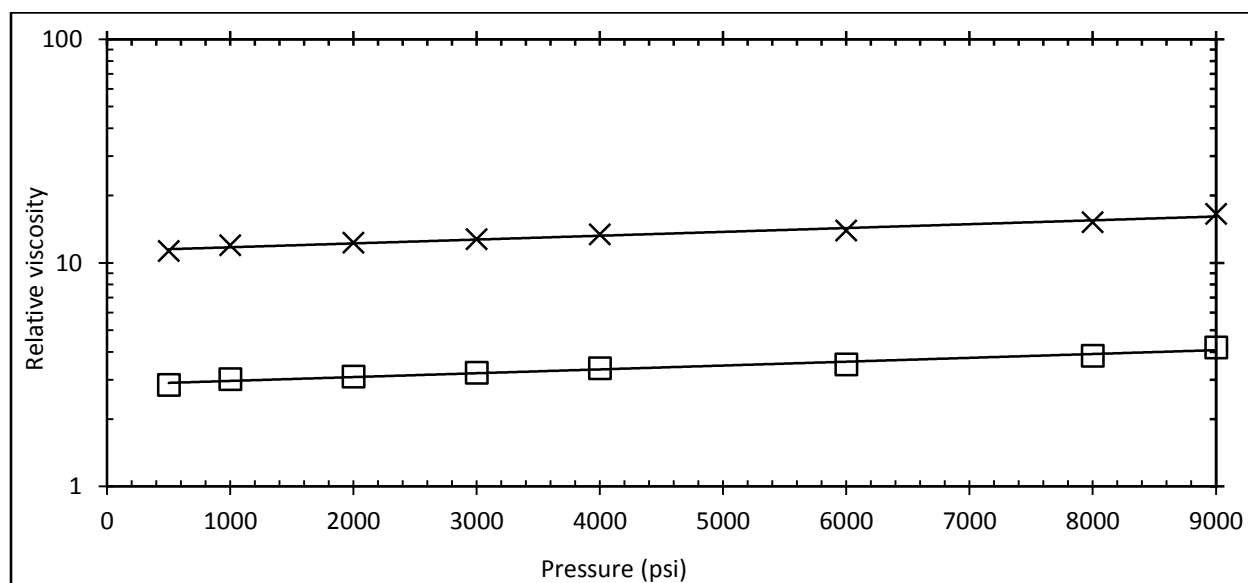


Figure 45. Viscosity change in propane by HADEH at 60°C and average shear rate of 450-2500 s⁻¹ (Logarithmic Y-axis). x HADEH at 1 wt%; □ HADEH 0.5 wt%.

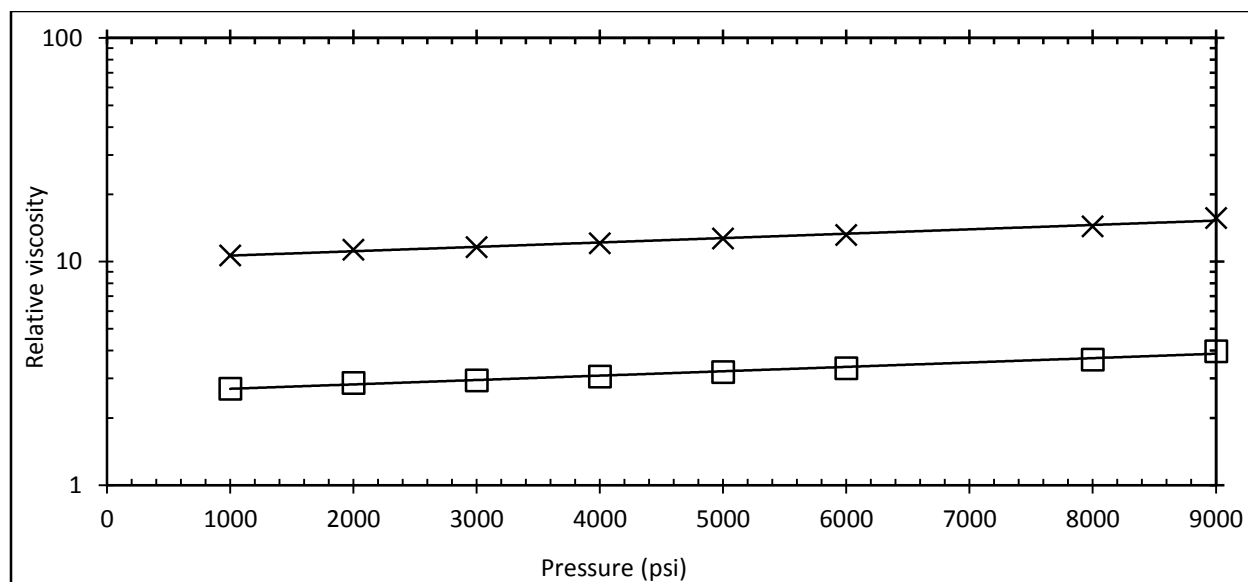


Figure 46. Viscosity change in propane by HADEH at 80°C and average shear rate of 450-2800 s⁻¹ (Logarithmic Y-axis). x HADEH at 1 wt%; □ HADEH 0.5 wt%.

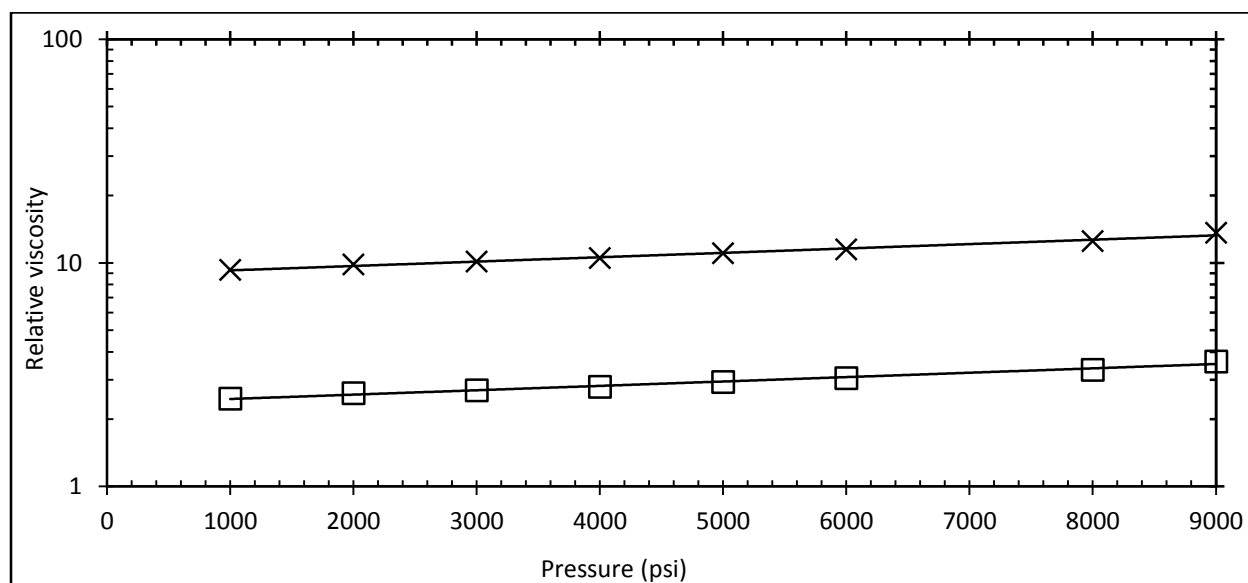


Figure 47. Viscosity change in propane by HADEH at 100°C and average shear rate of 500-2800 s⁻¹ (Logarithmic Y-axis). x HADEH at 1 wt%; □ HADEH 0.5 wt%.

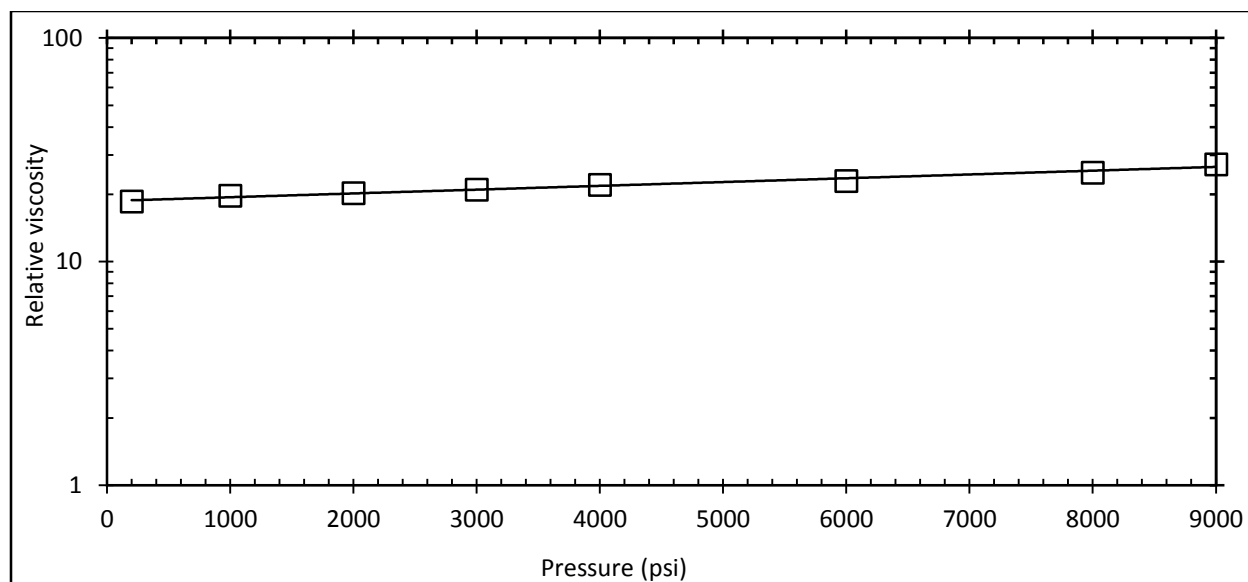


Figure 48. Viscosity change in n-butane by HADEH at 40°C and average shear rate of 250-400 s⁻¹ (Logarithmic Y-axis). □ HADEH 0.5 wt%.

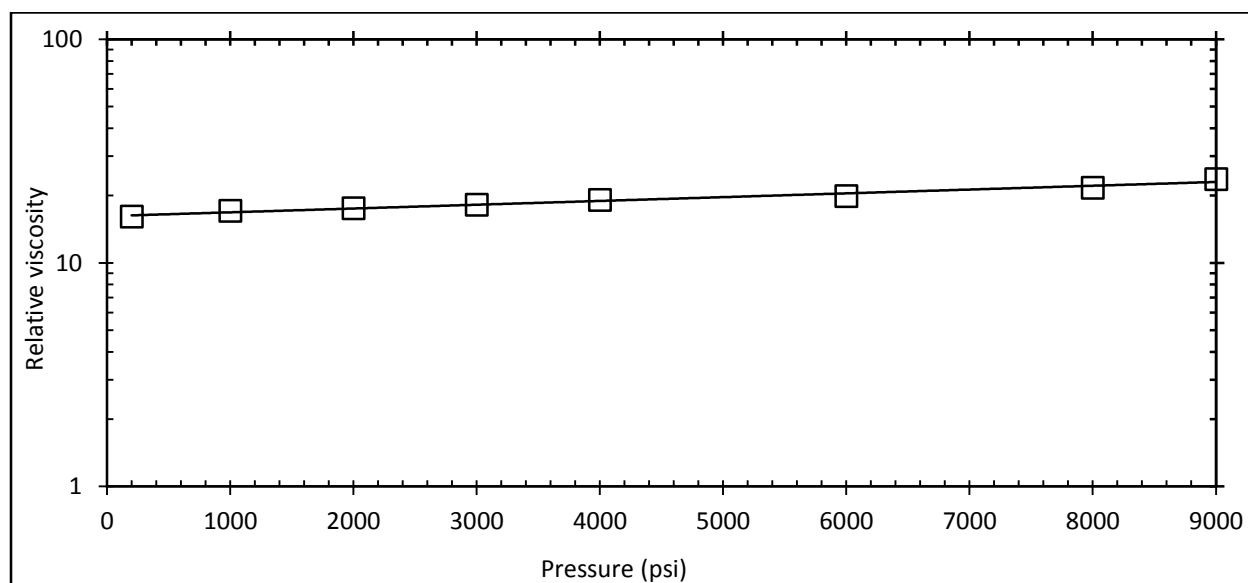


Figure 49. Viscosity change in n-butane by HADEH at 60°C and average shear rate of 280-450 s⁻¹ (Logarithmic Y-axis). □ HADEH 0.5 wt%.

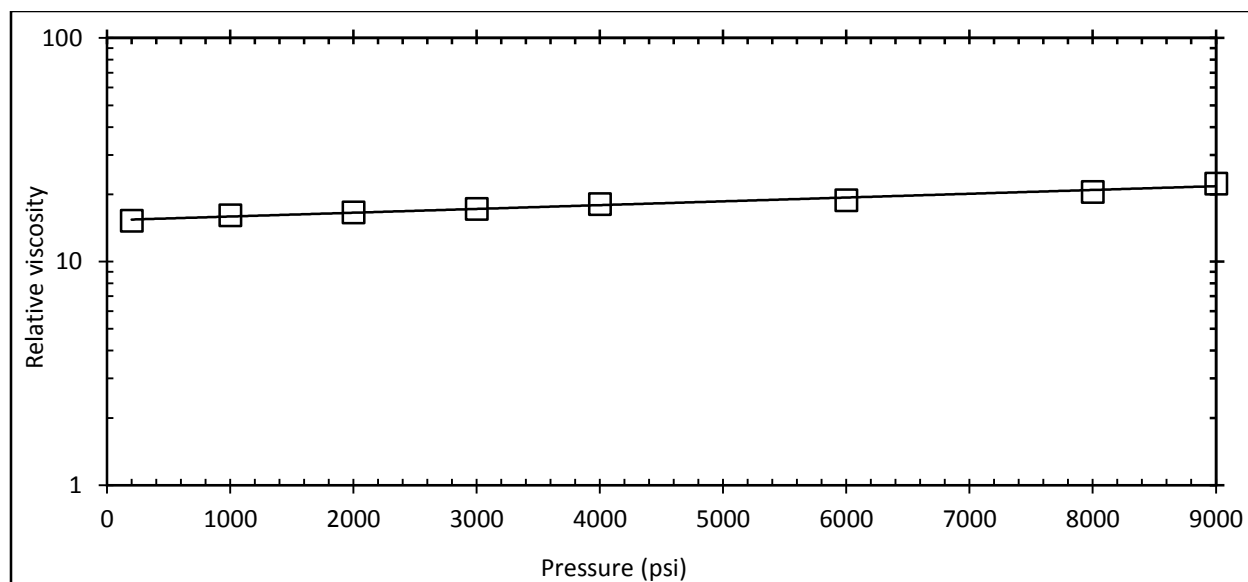


Figure 50. Viscosity change in n-butane by HAD2EH at 80°C and average shear rate of 300-450 s⁻¹ (Logarithmic Y-axis). □ HADEH 0.5 wt%.

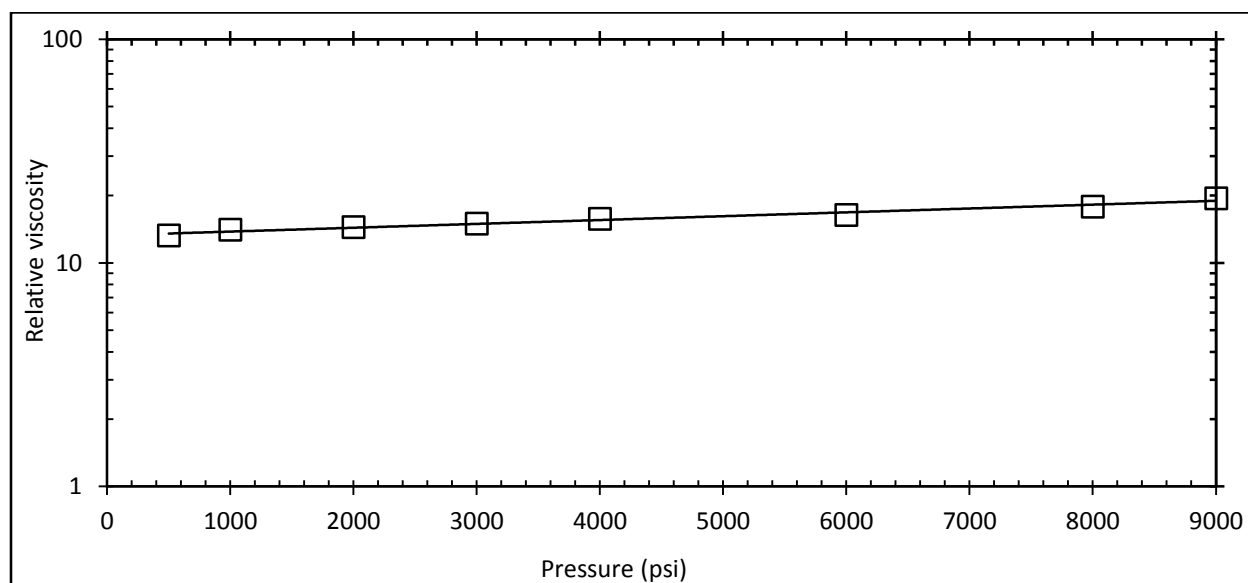


Figure 51. Viscosity change in n-butane by HAD2EH at 100°C and average shear rate of 350-550 s⁻¹ (Logarithmic Y-axis). □ HADEH 0.5 wt%.

5.3 CROSS LINKED PHOSPHATE ESTERS (CPE)

Many companies such as Halliburton, Ethox Chemicals, and Clearwater Inc. have patented techniques for “gelling” LPG with phosphorous based esters shown in Figure 52, which are crosslinked with polyvalent metal ions to enhance LPG performance during the “fracking” process. (Smith and Persinski, 1995, 1996, 1997; Taylor and Funkhouser, 2003, 2008; Taylor et al., 2008). Phosphate (mono, di or the mixture of mono & di) esters with alkyl tails are used commonly.

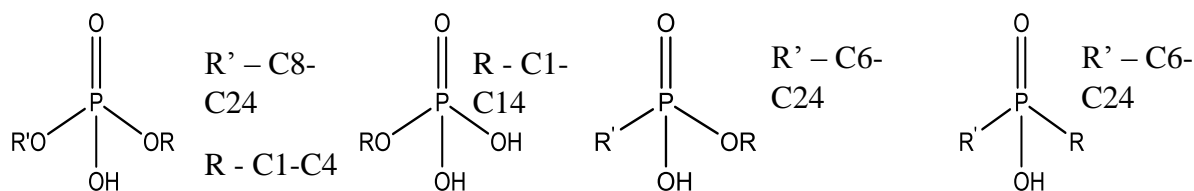


Figure 52. Phosphate di-ester, Phosphate mono-ester, Phosphonic acid ester and dialkyl phosphinic acid

Typically, two low viscosity liquids, the phosphate ester and a solution containing an organometallic compound. These two reactants are added to the liquid that is targeted for thickening. If the polyvalent metal ion can be bound more tightly by the phosphate ester than the ligand that it was originally formulated with in the crosslinker solution, then the phosphate esters will rapidly chelate the metal ions and form a linear, supramolecular, micellar structure shown in Figure 53. If this long micelle remains soluble in the liquid, it can quickly and dramatically enhance viscosity without the need for a heating/cooling cycle.

For example, oil-soluble phosphate mono/di-esters, alkyl phosphonic acid ester or dialkyl phosphinic acids can be crosslinked with polyvalent metal ions such as Fe^{3+} , Al^{3+} , Mg^{2+} , Ti^{4+} and Zn^{2+} to induce significant viscosity changes (2-100 fold) in hydrocarbon liquids such as kerosene

and diesel oil at combined concentration of 0.2-2.5 wt%. (Delgado and Keown, 2013; Taylor and Funkhouser, 2003, 2008). It has also been reported that hydrocarbon liquid gelling agents, based on phosphate esters could be used to gel mixtures of CO₂ and hydrocarbon liquids (Taylor et al., 2002, 2005b).

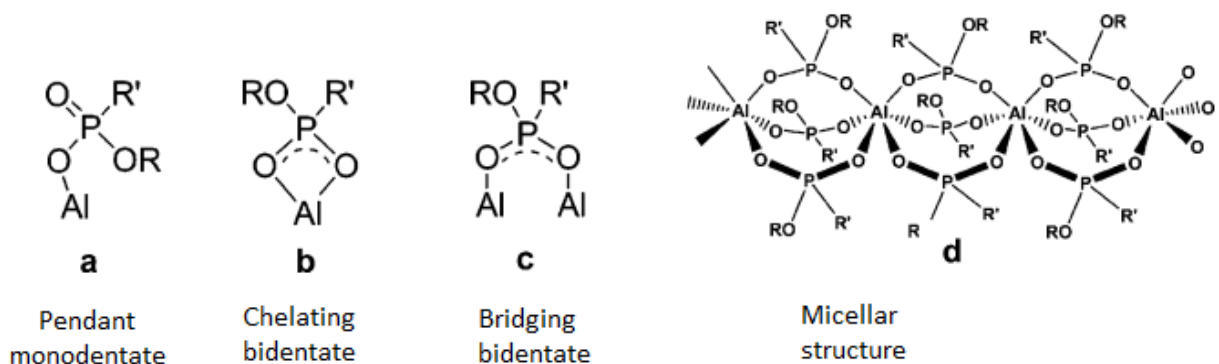


Figure 53. Mechanism of chelating complex (phosphate ester with metal ion cross linker) (Funkhouser et al., 2009; George et al., 2006, 2008; Page and Warr, 2009)

Hydrocarbon fluids have been used for fracturing purpose since the 1970's, sometimes with addition of CO₂ (Hurst, 1972; Smith, 1973). More recently (Taylor et al., 2006; Tudor et al., 2009) described the properties of gelled LPG for fracturing applications. Despite the numerous reports of “gelled” LPG found in many references (Hurst, 1972; Lestz et al., 2007; Smith, 1973; Taylor et al., 2006; Tudor et al., 2009), to the best of our knowledge a detailed analysis of the phase behavior of phosphate ester and crosslinker mixtures in ethane, propane, butane, NGL or LPG has not been published, nor has a detailed description of the viscosity of such mixtures in a viscometer or rheometer been presented. Rheological data for gelled LPG is very scarce in the literature (Taylor et al., 2005a). Moreover, phosphate compositions, crosslinker solution compositions, high pressure rheology results, and protocols for gelling and mixing often remain proprietary.

Materials: Six Lubrizol Oilfield Solutions (LZOS) phosphate ester products (HGA 70, HGA 70-C6, HGA 37, HGA 37D, HGA 715LP and HGA 702) and LZOS three LZOS crosslinking solutions (HGA 65, HGA 48, and HGA 44) were provided by LZOS and used as received. For all 18 combinations of phosphate ester and crosslinker, the LZOS products are designed to be used in equal mass concentrations in order to have the appropriate stoichiometric amounts of phosphate ester and polyvalent crosslinker.

5.3.1 Ambient pressure testing

In case of the CPE, the use of the HGA 70C6 phosphate ester and HGA 65 crosslinker was found to be the most effective pairing of the 18 possible combinations of three phosphate esters and six crosslinkers. In order to put the approximate length of the long, linear transient polymers or micelles formed by these small associating compounds, the viscosity increase associated with a poly- α -olefin drag reducing agent (DRA) with a molecular weight greater than 20,000,000 is also shown in Figures 54 and 55. (Dhuwe et al., 2015). Further, Figures 54 and 55 indicate that, in general, several tenths of a wt% of these thickeners may be required for order-of-magnitude changes in solution viscosity.

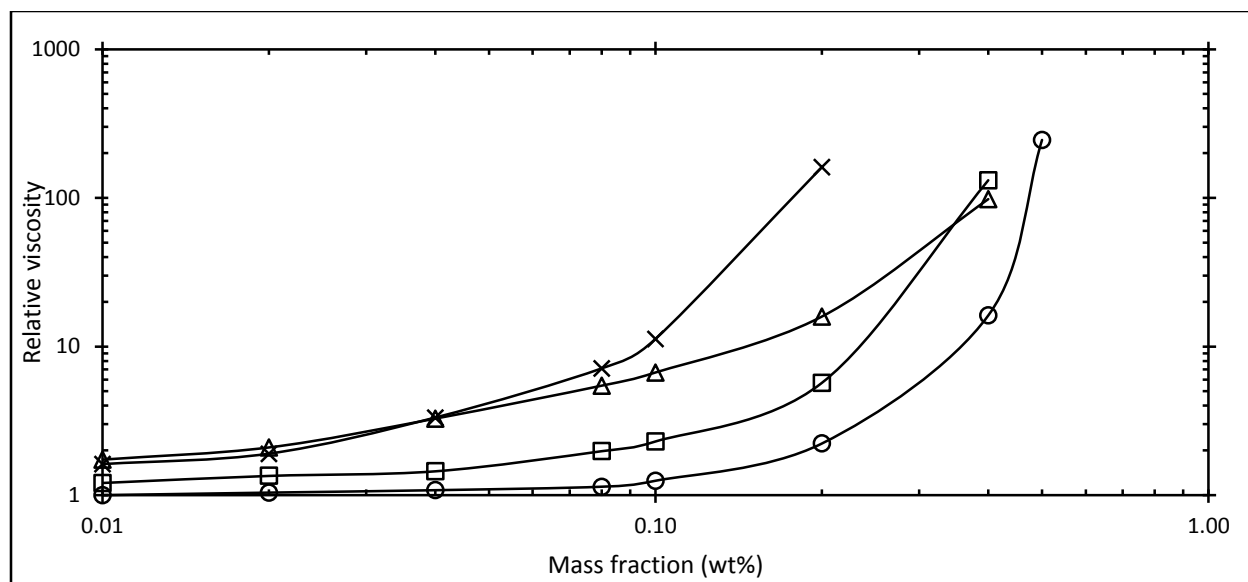


Figure 54. Relative viscosity (viscosity of pentane solution/viscosity of pentane) x HGA70C6 + HGA65 at 23°C; Δ DRA at 23°C; \square HAD2EH at 30°C; \circ TBTF at 23°C.

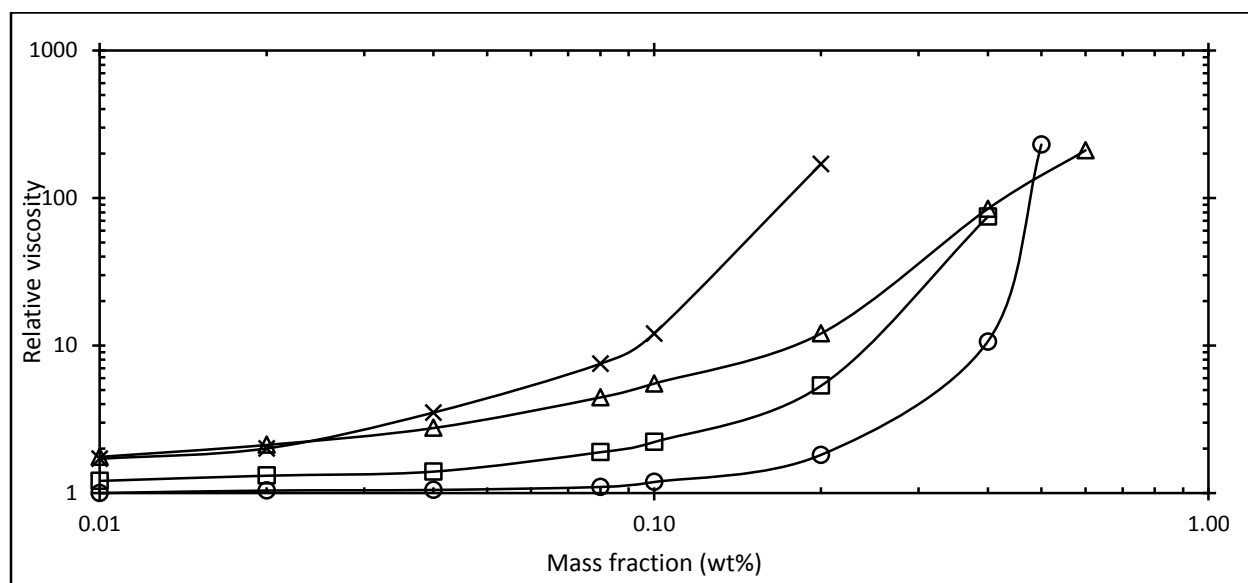


Figure 55. Relative viscosity (viscosity of hexane solution/viscosity of hexane) x HGA70C6 + HGA65 at 23°C; Δ DRA at 23°C; \square HADEH at 30°C; \circ TBTF at 23°C.

5.3.2 High pressure testing

Both the phosphate ester and the crosslinker solution are soluble to at least 1wt% in light alkanes such as pentane and hexane, and also in high pressure liquid ethane, propane and butane. However (unlike the TBTF and HAD2EH solutions), a transparent single phase cannot be realized with the phosphate ester + crosslinker solutions in the NGL constituents. These high pressure mixtures appear as a slightly hazy, translucent fluid that contains a very small amount of suspended, sub-millimeter droplets that form when the components are mixed in the light alkane. As this mixture is expanded, a pressure is reached where a significant precipitate becomes to come out of solution, rendering the mixture completely opaque. The pressure at which this occurs is designated as the “cloud point” of the translucent phase.

Table 10. Cloud point data for Phosphate ester (HGA-70 C6) and cross linker (HGA65). Unlike the other systems that formed transparent single phases, these CPE cloud point values correspond to the transition from a translucent phase with small suspended droplets to a completely opaque mixture

Solvent	Combined concentrations (wt%)	Cloud point* (psi)		
		25°C	40°C	60°C
Ethane	0.25	1550	1525	1510
	0.50	1708	1650	1610
	1.00	2615	2465	2305
Propane	0.25	155	221	332
	0.50	155	220	328
	1.00	154	215	325
n-Butane	0.50	41	61	108
	1.0	42	61	110

The relative viscosity of ethane, propane and butane at pressures above the cloud point pressure of the mixture is illustrated in Figures 56-64. In all cases, the small droplets suspended in

the thickened alkane have no difficulty flowing around the falling ball. The ability of the (phosphate ester + crosslinker) mixture to thicken the light alkanes increased slightly with increasing pressure and decreased with increasing temperature.

A very modest viscosity enhancement occurs with the addition of the (phosphate ester + crosslinker) mixture to ethane. For example, at a combined concentration of 1wt% at 25°C and 9000 psi, the viscosity increased by a factor of only 2.5. Greater increases were observed in propane, and the largest viscosity increases occur when butane is thickened. For example, at a combined concentration of 1wt% at 25°C and 9000 psi, the viscosity of butane increased by a factor of 6.4.

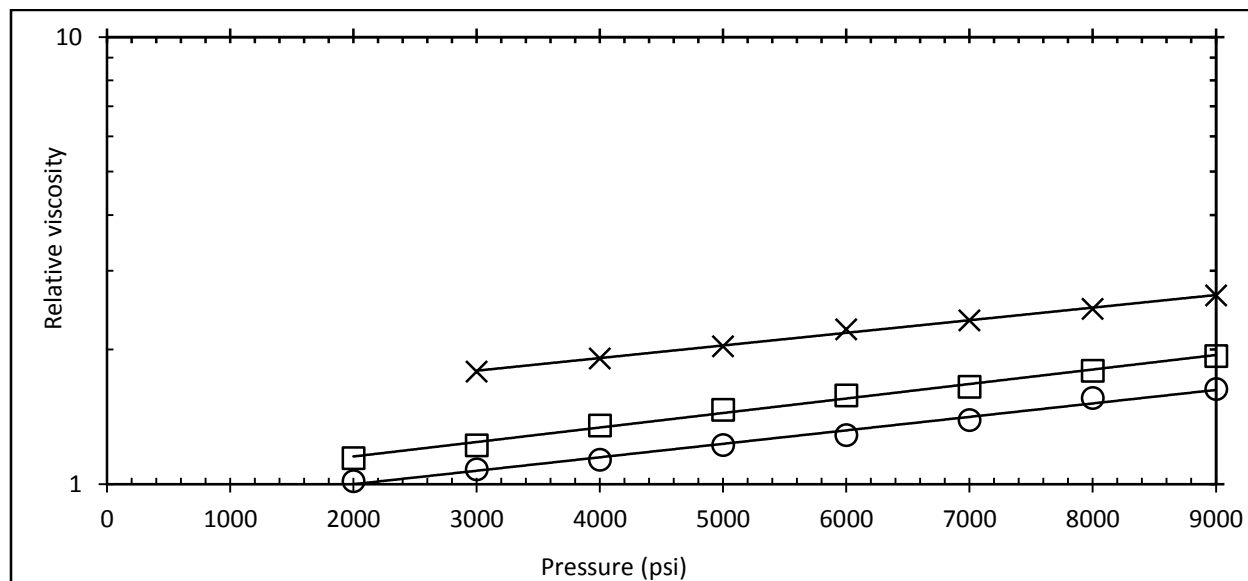


Figure 56. Viscosity change in ethane by HGA70 C6+ HGA 65 at 25°C and average shear rate of 3500-7100 s⁻¹ (Logarithmic Y-axis). x 1 wt% ; □ 0.5 wt% ; ○ 0.25 wt%.

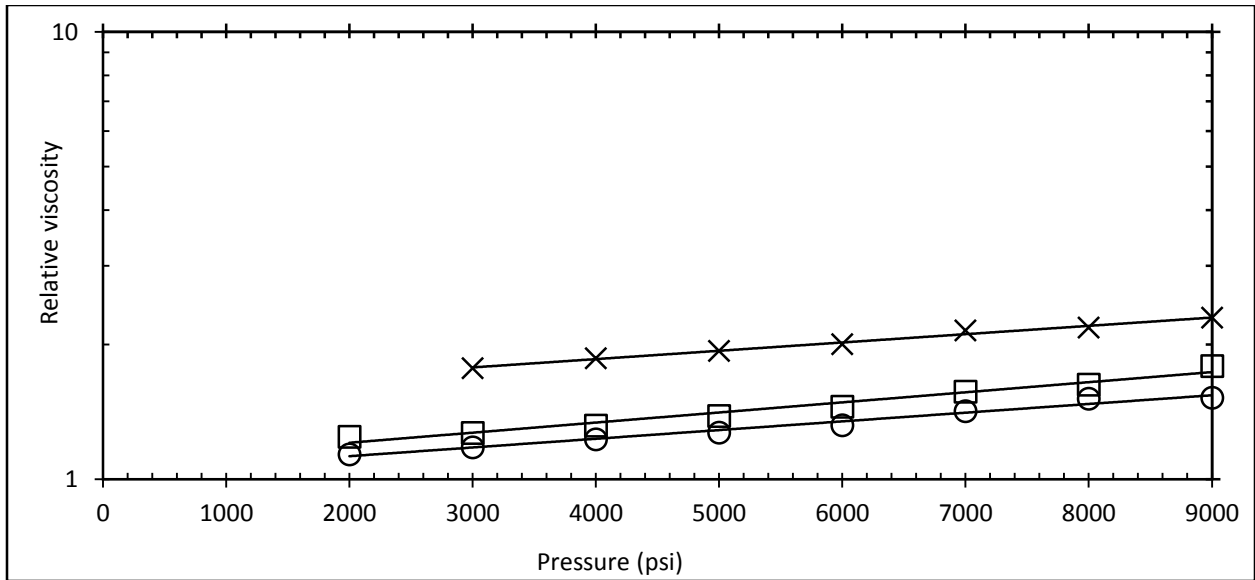


Figure 57. Viscosity change in ethane by HGA70 C6+ HGA 65 at 40°C and average shear rate of 3500-7100 s⁻¹ (Logarithmic Y-axis). x 1 wt% ; □ 0.5 wt% ; ○ 0.25 wt%.

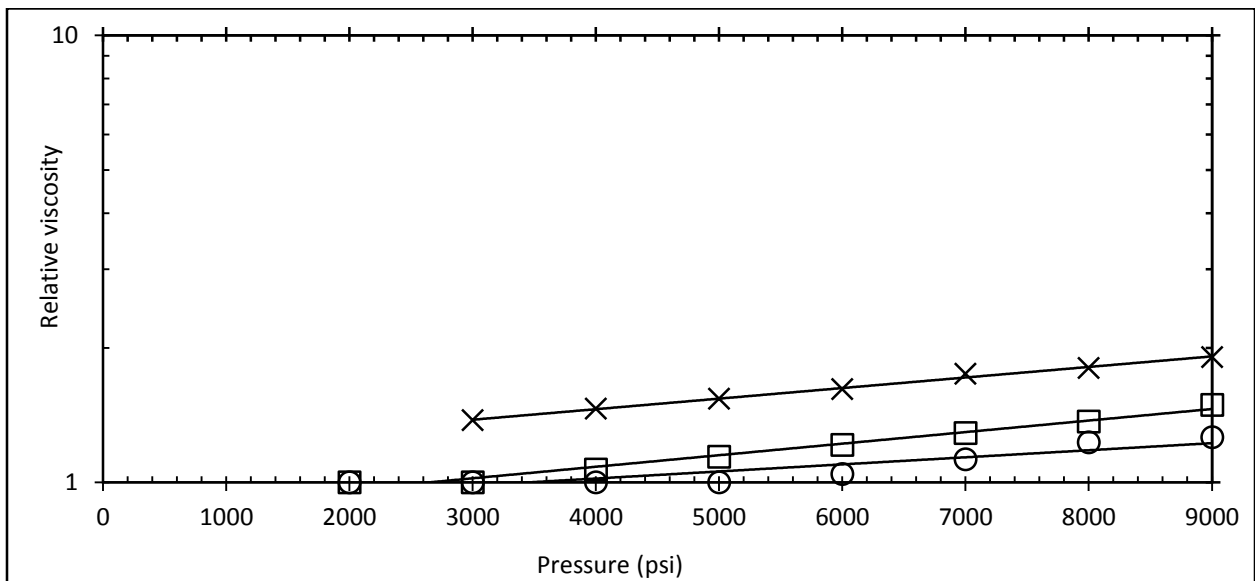


Figure 58. Viscosity change in ethane by HGA70 C6+ HGA 65 at 60°C and average shear rate of 3500-7100 s⁻¹ (Logarithmic Y-axis). x 1 wt% ; □ 0.5 wt% ; ○ 0.25 wt%.

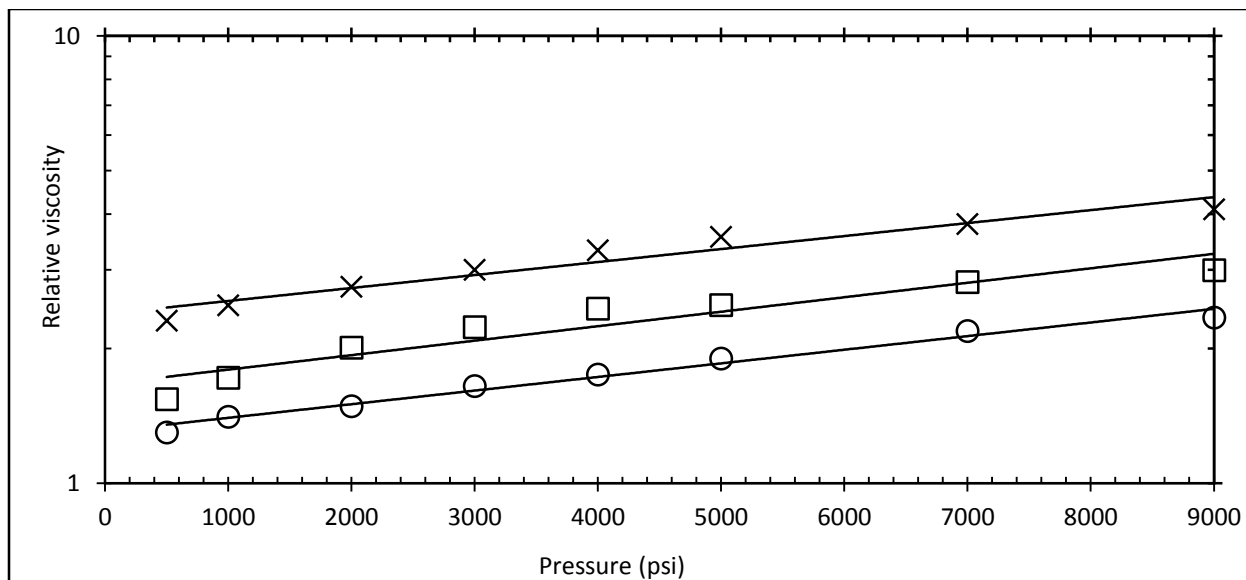


Figure 59. Viscosity change in propane by HGA70 C6+ HGA 65 at 25°C and average shear rate of 2000-7100 s⁻¹ (Logarithmic Y-axis). x 1 wt% ; □ 0.5 wt%; ○ 0.25 wt%.

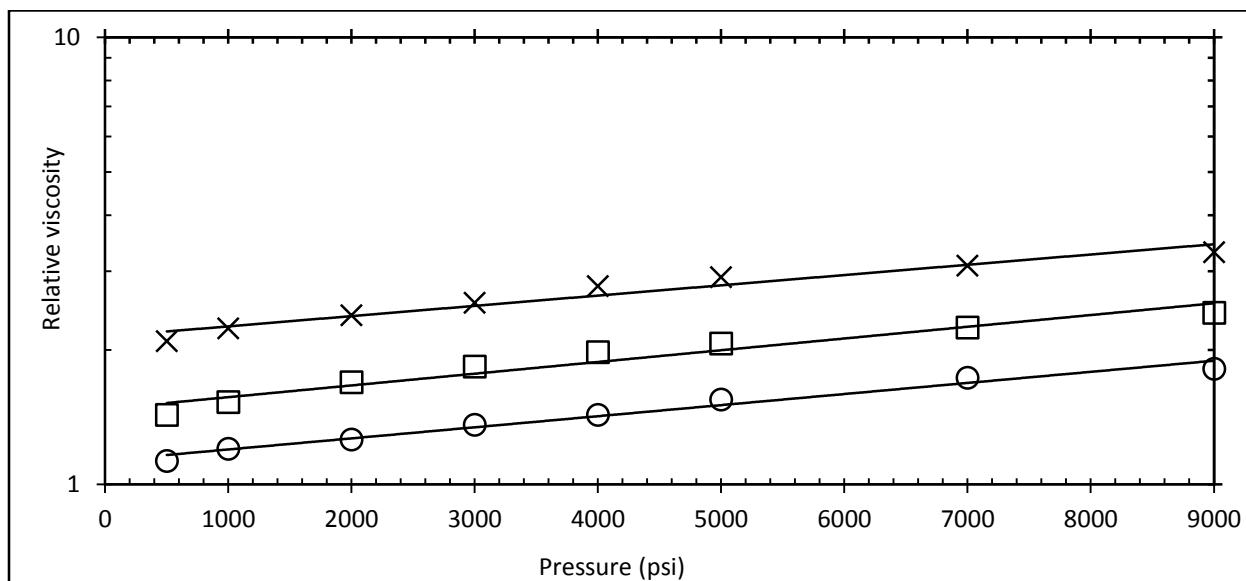


Figure 60. Viscosity change in propane by HGA70 C6+ HGA 65 at 40°C and average shear rate of 2200-7100 s⁻¹ (Logarithmic Y-axis). x 1 wt% ; □ 0.5 wt%; ○ 0.25 wt%.

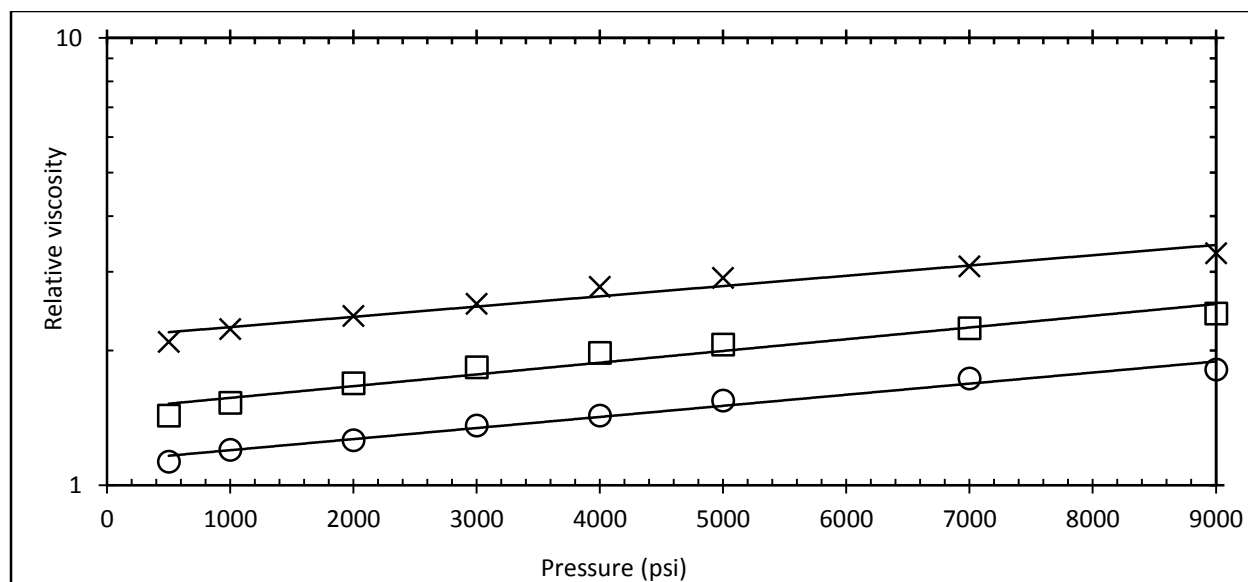


Figure 61. Viscosity change in propane by HGA70 C6+ HGA 65 at 60°C and average shear rate of 2500-7100 s⁻¹ (Logarithmic Y-axis). x 1 wt% ; □ 0.5 wt% ; ○ 0.25 wt%.

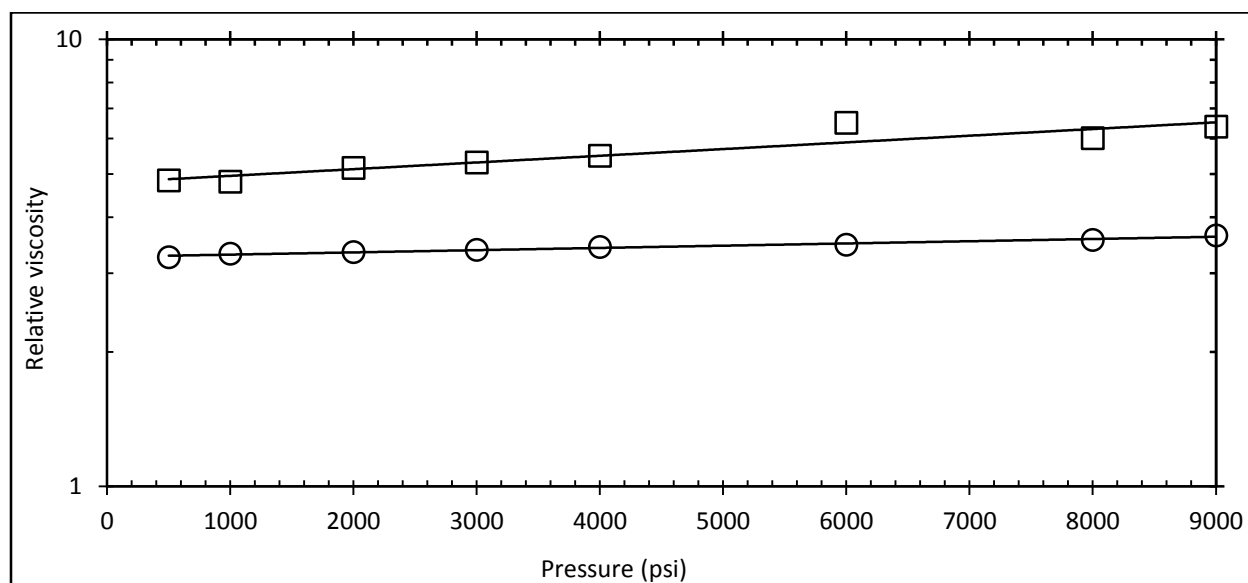


Figure 62. Viscosity change in butane by HGA70 C6+ HGA 65 at 25°C and average shear rate of 1500-3500 s⁻¹ (Logarithmic Y-axis). □ 1.0 wt% ; ○ 0.5 wt%.

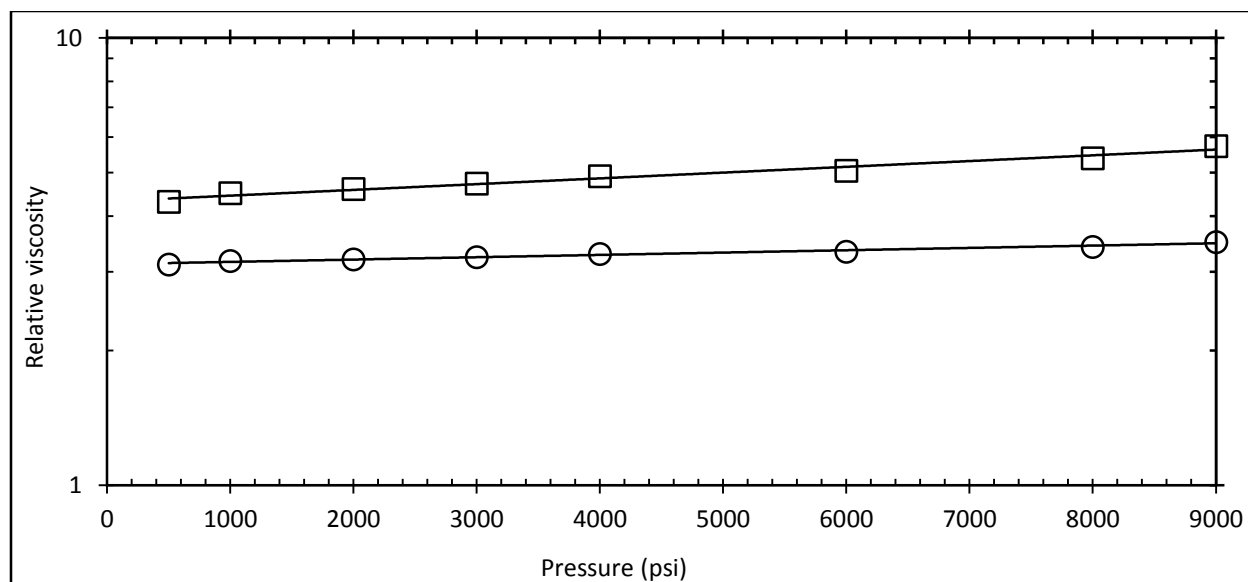


Figure 63. Viscosity change in butane by HGA70 C6+ HGA 65 at 40°C and average shear rate of 1500-3500 s⁻¹ (Logarithmic Y-axis). □ 1.0 wt%; ○ 0.5 wt%.

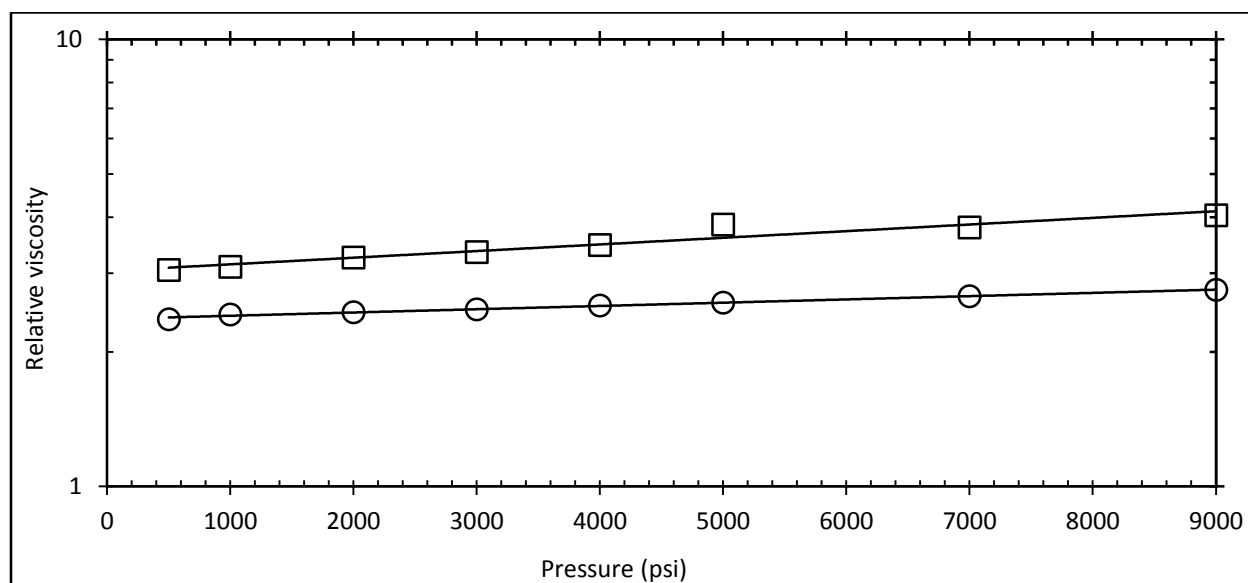


Figure 64. Viscosity change in butane by HGA70 C6+ HGA 65 at 60°C and average shear rate of 1500-3500 s⁻¹ (Logarithmic Y-axis). □ 1.0 wt%; ○ 0.5 wt%.

6.0 CONCLUSIONS

6.1 POLYMERIC THICKENERS

A high molecular weight (20,000,000+) poly- α -olefin drag reducing agent (DRA) polymer was found to be the most effective polymeric thickener for pentane and hexane, followed by a high molecular weight polyisobutylene (PIB 10000000) and a hydroxyl-terminated high molecular weight polydimethyl siloxane (Silanol). Therefore these high molecular weight polymers were assessed as thickeners for high pressure ethane, propane and butane at 25°C, 40°C and 60°C and pressures above the cloud point pressure up to 9000 psi.

Polyisobutylene (PIB 10000000) fails to dissolve in the light alkanes even when 100 times as much hexane as PIB is added to the high pressure mixture.

Silanol is soluble in ethane, propane and butane at concentrations of at least 2 wt%. In all cases an increase in pressure leads to a slight increase in the ability of the Silanol to thicken the solution, probably due to the increased ability of the denser alkane to not only dissolve but also swell the polymer. However, the viscosity enhancement is modest even at a very high pressure of 9000 psi (3.8-fold for butane, 2.0-fold for propane, and 1.2-fold for ethane). At a specified wt% concentration in the high pressure solution, Silanol 980000 is most effective as a thickener for butane, and least effective for ethane. This indicates that butane is the best solvent for not only dissolving the polymer, but swelling the polymer in solution such that viscosity enhancement is more readily achieved.

The DRA polymer was clearly the most effective thickener for ethane, propane and butane and an increase in pressure leads to a slight increase in the ability of the DRA to thicken the solution. At 0.5wt% of the DRA, 3-9-fold increases in ethane and propane viscosity occur, while 23-30 fold increases occur in butane. These results again indicate that butane is a significantly stronger solvent for the dissolution and swelling of ultrahigh molecular weight polymers than either ethane or propane.

6.2 SMALL ASSOCIATIVE MOLECULE THICKENERS

In small molecule associative thickeners, mainly, three types of small molecule thickeners were assessed for their ability to dissolve in high pressure ethane, propane and butane and induce significant viscosity changes at temperatures of 25 to 100°C. All viscosity measurements were conducted with a close-clearance falling ball viscometer at pressures above the mixture cloud point. In general, increasing pressure resulted in slight increases in viscosity, while increasing temperature led to decreases in viscosity due to disruption of intermolecular associations.

Tributyltin fluoride (TBTF) is remarkably effective in that it does not require a heating/cooling cycle to attain dissolution. TBTF dissolves readily in these fluids with several minutes of mixing and, at a concentration of 1wt%, induces nearly 100-fold viscosity increases at a concentration of 1wt% at 25°C. Although much higher pressures were required to dissolve the TBTF in ethane, TBTF induces viscosity changes in ethane that are comparable to those observed for propane and butane. To the best of our knowledge, this is the first time that a small molecule thickener has ever been reported for ethane.

Hydroxyaluminum di-2-ethylhexanoate (HAD2EH) is completely insoluble in ethane. HAD2EH does not dissolve in propane or butane unless the high pressure mixture of the alkane and HAD2EH are first mixed at roughly 100°C and then cooled to the temperature of interest. The solution of HAD2EH in propane or butane remains transparent when the system is cooled to temperature as low as 40°C; but at 25°C the HAD2EH falls out of solution. Relative to the other TBTF, HAD2EH induces larger viscosity if it remains in solution. For example, HAD2EH increases the viscosity of liquid propane by a factor of ~10 at a concentration of 1.0wt% at 100°C, while TBTF at 1wt% and a lower temperature of 60°C increases the viscosity of propane by a factor of only 6.

A (phosphate ester + crosslinker) combination exhibits highly desirable attributes for practical application (e.g. low viscosity pump-able liquid components, very fast crosslinking kinetics) and yields incredible viscosity increases for pentane and hexane via the formation of a crosslinked phosphate ester (CPE). However, this two-component mixture did not form a clear or faintly hazy solution in ethane, propane and butane. Rather, a white, translucent fluid formed that contained very fine droplets of a second liquid phase (probably derived from the solvent for the crosslinker solution). The “cloud point” for this system is reported as the pressure at which the solution becomes completely opaque upon expansion. Because the ball is able to fall at a terminal velocity through this fluid mixture above the cloud point in a close-clearance falling ball viscometer, relative viscosity can be measured (even though the system is not a transparent single phase). At a combined concentration of 1wt% (HGA 70C6 phosphate ester + HGA 65 crosslinker), 25°C and 3000 psi, the viscosity of ethane, propane and butane increase by factors of only 1.9, 3.0 and 5.3 at pressures above the cloud point.

BIBLIOGRAPHY

- Advanced Resources International (ARI) (2010). U.S. Oil Production Potential from Accelerated Deployment of Carbon Capture and Storage.
- Barrage, T.C. (1987). A High Pressure Visual Viscometer Used in the Evaluation of the Direct Viscosity Enhancement of High Pressure Carbon Dioxide (University of Pittsburgh).
- Beckmann, J., Horn, D., Jurkschat, K., Rosche, F., Schürmann, M., Zachwieja, U., Dakternieks, D., Duthie, A., and Lim, A.E.K. (2003). Triorganotin Fluoride Structures: A Ligand Close-Packing Model with Predominantly Ionic Sn–F Bonds. *Eur. J. Inorg. Chem.* 2003, 164–174.
- Burger, E.D., Chorn, L.G., and Perkins, T.K. (1980). Studies of Drag Reduction Conducted over a Broad Range of Pipeline Conditions when Flowing Prudhoe Bay Crude Oil. *J. Rheol.* 1978-Present 24, 603–626.
- Canevari, G.P., and Peruyero, J.M. (1970). US3493000 A: Method for reducing the frictional drag of flowing fluids.
- Clark, H.C., O'Brien, R.J., and Trotter, J. (1964). The structure of trimethyltin fluoride. *J. Chem. Soc. Resumed* 2332.
- Dandge, D.K., and Heller, J.P. (1987). Polymers for Mobility Control in CO₂ Floods. (Society of Petroleum Engineers),.
- Dandge, D.K., Taylor, C., Heller, J.P., Wilson, K.V., and Brumley, N. (1989). Associative Organotin Polymers. 2. Solution Properties of Symmetric Trialkyltin Fluorides. *J. Macromol. Sci. Part A* 26, 1451–1464.
- Dauben, D.L., Reed, J., Shelton, J., and Lyman, Y. (1971). US3570601 A: Recovery of oil with viscous propane.
- Delgado, E., and Keown, B. (2013). Low volatile phosphorous gelling agent.
- Dhuwe, A., Sullivan, J., Lee, J., Cummings, S., Enick, R., Beckman, E., and Perry, R. (2015). Close-clearance high pressure falling ball viscometer assessment of ultra-high molecular weight polymeric thickeners for ethane, propane and butane. *J. Supercrit. Fluids* in press.

- Doffin, J., Perrault, R., and Garnaud, G. (1984). Blood viscosity measurements in both extensional and shear flow by a falling ball viscometer. *Biorheol. Suppl. Off. J. Int. Soc. Biorheol.* 1, 89–93.
- Dunn, P., and Oldfield, D. (1970). Tri-Normal-Butyltin Fluoride - a Novel Coordination Polymer in Solution. *J. Macromol. Sci.-Chem. A* 4, 1157 – &.
- Enick, R.M. (1991a). The Effect of Hydroxy Aluminum Disoaps on the Viscosity of Light Alkanes and Carbon Dioxide. (Society of Petroleum Engineers),.
- Enick, R.M. (1991b). The Effect of Hydroxy Aluminum Disoaps on the Viscosity of Light Alkanes and Carbon Dioxide. (Society of Petroleum Engineers),.
- Evans, A.P. (1974). A new drag-reducing polymer with improved shear stability for nonaqueous systems. *J. Appl. Polym. Sci.* 18, 1919–1925.
- Fieser, L., Harris, G., Hershberg, E., Morgana, M., Novello, F., and Putnam, S. (1946). Napalm. *Ind. Eng. Chem.* 38, 768–773.
- Fons, C., Brun, J., Supparo, I., Mallard, C., Bardet, L., and Orsetti, A. (1993). Evaluation of Blood-Viscosity at High-Shear Rate with a Falling Ball Viscometer. *Clin. Hemorheol.* 13, 651–659.
- Frazier, G.D., and Todd, M.R. (1984). Alvord [3000 ft Strawn] LPG Flood Design and Performance Evaluation. *J. Pet. Technol.* 36, 119–131.
- Friend, D.G., Ingham, H., and Fly, J.F. (1991). Thermophysical Properties of Ethane. *J. Phys. Chem. Ref. Data* 20, 275–347.
- Funkhouser, G.P., Tonmukayakul, N., and Liang, F. (2009). Rheological comparison of organogelators based on iron and aluminum complexes of dodecylmethylphosphinic acid and methyl dodecanephosphonic acid. *Langmuir ACS J. Surf. Colloids* 25, 8672–8677.
- George, M., Funkhouser, G.P., Terech, P., and Weiss, R.G. (2006). Organogels with Fe(III) complexes of phosphorus-containing amphiphiles as two-component isothermal gelators. *Langmuir ACS J. Surf. Colloids* 22, 7885–7893.
- George, M., Funkhouser, G.P., and Weiss, R.G. (2008). Organogels with complexes of ions and phosphorus-containing amphiphiles as gelators. Spontaneous gelation by in situ complexation. *Langmuir ACS J. Surf. Colloids* 24, 3537–3544.
- Habermann, B. (1960). The Efficiency of Miscible Displacement as a Function of Mobility Ratio. SPE-1540-G.
- Hansen, C.M. (2007). Hansen solubility parameters: a user's handbook (Boca Raton: CRC Press).
- Heller, J.P., and Taber, J.J. (1982). Development of Mobility Control Methods to Improve Oil Recovery by Co/Sub 2/. Second Annual Report, October 1, 1980-September 30, 1981

- (New Mexico Inst. of Mining and Technology, Socorro (USA). New Mexico Petroleum Recovery Research Center).
- Henderson, J., Meyer, W., and Taber, J. (1967). US3330345 A: Miscible drive secondary oil recovery process.
- Holm, L.W. (1976). Status of CO₂ and Hydrocarbon Miscible Oil Recovery Methods. *J. Pet. Technol.* 28, 76–84.
- Hong, L., Fidler, E., Enick, R., and Marentis, R. (2008). Tri-tert-butylphenol: A highly CO₂-soluble sand binder. *J. Supercrit. Fluids* 44, 1–7.
- Huang, Z.H., Shi, C.M., Xu, J.H., Kilic, S., Enick, R.M., and Beckman, E.J. (2000). Enhancement of the viscosity of carbon dioxide using styrene/fluoroacrylate copolymers. *Macromolecules* 33, 5437–5442.
- Hughes, M. (2014). Napalm: An American Biography. *War Hist.* 21, 560–562.
- Hurst, R.E. (1972). Use Of Liquefied Gases As Fracture Fluids For Dry Gas Reservoirs. (Society of Petroleum Engineers),.
- Iezzi, A., Enick, R., and Brandy, J. (1989). The direct viscosity enhancement of carbon dioxide.
- Kilic, S., Michalik, S., Wang, Y., Johnson, J.K., Enick, R.M., and Beckman, E.J. (2003). Effect of Grafted Lewis Base Groups on the Phase Behavior of Model Poly(dimethyl siloxanes) in CO₂. *Ind. Eng. Chem. Res.* 42, 6415–6424.
- Kirby, C.F., and McHugh, M.A. (1999). Phase Behavior of Polymers in Supercritical Fluid Solvents. *Chem. Rev.* 99, 565–602.
- Lestz, R.S., Wilson, L., Taylor, R.S., Funkhouser, G.P., Watkins, H., and Attaway, D. (2007). Liquid Petroleum Gas Fracturing Fluids for Unconventional Gas Reservoirs. *J. Can. Pet. Technol.* 46.
- Liaw, G. (1968). The effect of polymer structure on drag reduction in nonpolar solvents. In *Doctoral Dissertations*,.
- Ma, Y., Zheng, X., Shi, F., Li, Y., and Sun, S. (2003). Synthesis of poly(dodecyl methacrylate)s and their drag-reducing properties. *J. Appl. Polym. Sci.* 88, 1622–1626.
- Miller, M.B., Chen, D.-L., Xie, H.-B., Luebke, D.R., Karl Johnson, J., and Enick, R.M. (2009). Solubility of CO₂ in CO₂-philic oligomers; COSMOtherm predictions and experimental results. *Fluid Phase Equilibria* 287, 26–32.
- Milligan, S.N., Harris, W.F., and Burden, T.L. (2009). US20090107554 A1: High polymer content hybrid drag reducers.
- Miyamoto, H., and Watanabe, K. (2000). A Thermodynamic Property Model for Fluid-Phase Propane. *Int. J. Thermophys.* 21, 1045–1072.

- Miyamoto, H., and Watanabe, K. (2001). Thermodynamic Property Model for Fluid-Phase n-Butane. *Int. J. Thermophys.* 22, 459–475.
- Mysels, K. (1949). Napalm - Mixture of Aluminum Disoaps. *Ind. Eng. Chem.* 41, 1435–1438.
- Page, M.G., and Warr, G.G. (2009). Influence of the structure and composition of mono- and dialkyl phosphate mixtures on aluminum complex organogels. *Langmuir ACS J. Surf. Colloids* 25, 8810–8816.
- Pilpel, N. (1963). Properties of Organic Solutions of Heavy Metal Soaps. *Chem. Rev.* 63, 221–234.
- Roberts, A.C., Claude, C.E., and Robert, W. (1969). US3444930 A: Oil recovery process by miscible displacement.
- Rueggeberg, W.H.C. (1948). Use of Aluminum Soaps and Other Fuel Thickeners in Gelling Gasolines. *J. Phys. Colloid Chem.* 52, 1444–1460.
- Smith, C.F. (1973). Gas Well Fracturing Using Gelled Non-Aqueous Fluids. (Society of Petroleum Engineers),.
- Smith, K.W., and Persinski, L.J. (1995). Hydrocarbon gels useful in formation fracturing.
- Smith, K.W., and Persinski, L.J. (1996). Hydrocarbon gels useful in formation fracturing.
- Smith, K.W., and Persinski, L.J. (1997). Hydrocarbon gels useful in formation fracturing.
- Taber, J.J. (1983). Technical Screening Guides for the Enhanced Recovery of Oil. In Society of Petroleum Engineers,.
- Taylor, R.S., and Funkhouser, G.P. (2003). Methods and compositions for treating subterranean formations with gelled hydrocarbon fluids.
- Taylor, R.S., and Funkhouser, G.P. (2008). Methods and compositions for treating subterranean formations with gelled hydrocarbon fluids.
- Taylor, R., Khallad, A., Cheng, A., Barree, B., Byrnes, J., Kelly, K., Conway, M., Caufield, R., and Tourigny, S. (2002). Optimized Gas-Well Stimulating Using CO₂-Miscible, Viscosified Hydrocarbon Fracturing Fluids. (Society of Petroleum Engineers),.
- Taylor, R.S., Lestz, R.S., Bennion, D.B., Funkhouser, G.P., and Geddes, I.R. (2005a). Rheological Evaluations of CO Miscible Hydrocarbon Fracturing Fluids. *J. Can. Pet. Technol.* 44.
- Taylor, R.S., Funkhouser, G.P., Dusterhoft, R.G., and Lestz, R.S. (2005b). Co₂ miscible optimized hydrocarbon blends and methods of using co₂ miscible optimized hydrocarbon blends.
- Taylor, R.S., Lestz, R.S., Wilson, L., Funkhouser, G.P., Watkins, H., and Attaway, D. (2006). Liquid Petroleum Gas Fracturing Fluids for Unconventional Gas Reservoirs. (Petroleum Society of Canada),.

- Taylor, R.S., Funkhouser, G.P., Dusterhoft, R.G., Lestz, R.S., and Byrd, A. (2008). Compositions and methods for treating subterranean formations with liquefied petroleum gas.
- The National Enhanced Oil Recovery Initiative (NEORI) (2012). Carbon Dioxide Enhanced Oil Recovery: A Critical Domestic Energy, Economic, And Environmental Opportunity.
- Tudor, E.H., Nevison, G.W., Allen, S., and Pike, B. (2009). 100% Gelled LPG Fracturing Process: An Alternative to Conventional Water-Based Fracturing Techniques. (Society of Petroleum Engineers),.
- Van Den Berghe, E.V., and Van Der Kelen, G.P. (1971). A study of the chemical bond in $(\text{CH}_3)_n\text{Sn}(\text{SCH}_3)_{4-n}$ ($n=0, 1, 2, 3$) by nmr (^1H , ^{119}Sn , ^{13}C) spectroscopy. *J. Organomet. Chem.* 26, 207–213.
- Xu, J., Wlaschin, A., and Enick, R.M. (2003). Thickening Carbon Dioxide With the Fluoroacrylate-Styrene Copolymer. *SPE J.* 8, 85–91.
- Zeman, L., Delmas, G., Biros, J., and Patterso, D. (1972). Pressure Effects in Polymer-Solution Phase Equilibria .1. Lower Critical Solution Temperature of Polyisobutylene and Polydimethylsiloxane or Lower Alkanes. *J. Phys. Chem.* 76, 1206 – &.